WILEY-VCH

Article type: Review

Device Performance of Emerging Photovoltaic Materials (Version 4)

Osbel Almora*, Carlos I. Cabrera, Sule Erten-Ela, Karen Forberich, Kenjiro Fukuda, Fei Guo, Jens Hauch, Anita W.Y. Ho-Baillie, T. Jesper Jacobsson, Rene A.J. Janssen, Thomas Kirchartz, Maria A. Loi, Xavier Mathew, David B. Mitzi, Mohammad K. Nazeeruddin, Ulrich W. Paetzold, Barry P. Rand, Uwe Rau, Takao Someya, Eva Unger, Lídice Vaillant-Roca, and Christoph J. Brabec*

Dr. O. Almora
Universitat Rovira i Virgili, 43007 Tarragona, Spain
Dr. O. Almora, Prof. C. J. Brabec
Erlangen Graduate School of Advanced Optical Technologies (SAOT), 91052 Erlangen, Germany.
Prof. C. J. Brabec
Zernike Institute for Advanced Materials University of Groningen Groningen 9747, The Netherlands
Prof. C. I. Cabrera
Unidad Académica de Ciencia y Tecnología de la Luz y la Materia, Universidad Autónoma de Zacatecas, Zacatecas, 98160, Mexico
Prof. S. Erten-Ela
Ege University, Solar Energy Institute, Bornova, 35100, Izmir, Turkey
K. Fukuda
Thin-Film Device Laboratory & Center for Emergent Matter Science, RIKEN, Saitama 351-0198, Japan
Prof. F. Guo
Institute of New Energy Technology, College of Information Science and Technology, Jinan University, Guangzhou 510632, China
Prof. C. J. Brabec, Dr. Karen Forberich, Dr. J. Hauch
Forschungszentrum Jülich GmbH, Helmholtz-Institut Erlangen-Nürnberg for Renewable Energy (HI ERN), 91058 Erlangen, Germany
Prof. A. W. Y. Ho-Baillie
School of Physics and The University of Sydney Nano Institute, The University of Sydney, NSW 2006, Australia
Prof. T. J. Jacobsson
Institute of Photoelectronic Thin Film Devices and Technology, Key Laboratory of Photoelectronic Thin Film Devices and Technology of Tianjin, College of Electronic Information and Optical Engineering, Nankai University, Tianjin 300350, China
Prof. R. A. J. Janssen
Molecular Materials and Nanosystems & Institute for Complex Molecular Systems, Eindhoven University of Technology, 5600 MB Eindhoven, The Netherlands; Dutch Institute for Fundamental Energy Research, De Zaale 20, Eindhoven, 5612 AJ, The Netherlands
Prof. T. Kirchartz, Prof. U. Rau,
IEK5-Photovoltaics, Forschungszentrum Jülich, 52425 Jülich, Germany
Prof. T. Kirchartz
Faculty of Engineering and CENIDE, University of Duisburg-Essen, 47057 Duisburg, Germany
Prof. M. A. Loi
Photophysics and OptoElectronics Group, Zernike Institute for Advanced Materials, University of Groningen, Nijenborgh 4, NL-9747 AG Groningen, The Netherlands
Prof. X. Mathew
Instituto de Energías Renovables, Universidad Nacional Autónoma de México, Temixco, Morelos 62580, México
Prof. D. B. Mitzi
Department of Mechanical Engineering and Material Science & Department of Chemistry, Duke University, Durham, North Carolina 27708, United States
Prof. M. K. Nazeeruddin
Group for Molecular Engineering and Functional Materials, Ecole Polytechnique Fédérale de Lausanne, Institut des Sciences et Ingénierie Chimiques, CH-1951 Sion, Switzerland
Prof. Dr. U. W. Paetzold
Institute of Microstructure Technology (IMT), Karlsruhe Institute of Technology (KIT), 76344, Eggenstein-Leopoldshafen, Germany; Light Technology Institute (LTI), Karlsruhe Institute of Technology (KIT), 76131, Karlsruhe, Germany
Prof. B. P. Rand
Department of Electrical Engineering and Andlinger Center for Energy and the Environment, Princeton University, Princeton, New Jersey 08544, United States
Prof. T. Someya
Electrical and Electronic Engineering and Information Systems, University of Tokyo, Tokyo 113-8656, Japan
Thin-Film Device Laboratory & Center for Emergent Matter Science, RIKEN, Saitama 351-0198, Japan
Prof. E. Unger
Helmholtz-Zentrum Berlin, Germany
Prof. L. Vaillant-Roca
Photovoltaic Research Laboratory, Institute of Materials Science and Technology – Physics Faculty, University of Havana, 10400, Havana, Cuba
Dr. C. Yang
Department of Chemical Engineering and Materials Science, Michigan State University, East Lansing, Michigan 48824, United States; Solaria Corporation, Fremont, California 94538, United States

*osbel.almora@urv.cat, christoph.brabec@fau.de

Keywords: multijunction solar cells; flexible photovoltaics; transparent and semitransparent solar cells; photovoltaic device operational stability

Abstract

Following the 3rd release of the *"Emerging PV reports"*, the best achievements in the performance of emerging photovoltaic (e-PV) devices in diverse e-PV research subjects are summarized, as reported in peer-reviewed articles in academic journals since August 2022. Updated graphs, tables and analyses are provided with several performance parameters, such as power conversion efficiency, open-circuit voltage, short-circuit current density, fill factor, light utilization efficiency, and stability test energy yield. These parameters are presented as a function of the photovoltaic bandgap energy and the average visible transmittance for each technology and application, and are put into perspective using, for example, the detailed balance efficiency limit. The 4th installment of the *"Emerging PV reports"* discusses the "PV emergence" classification with respect to the "PV technology generations" and "PV research waves" and highlights the latest device performance progress in multijunction and flexible photovoltaics. Additionally, Dale-Scarpulla's plots of efficiency-effort in terms of cumulative academic publication count are also introduced.

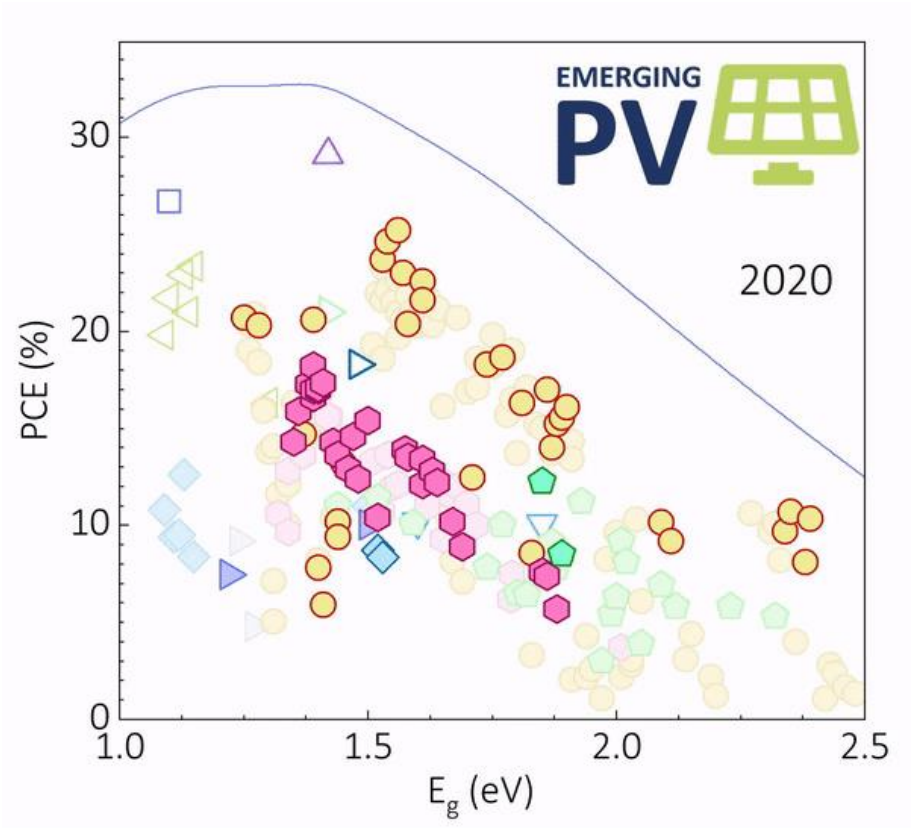

1. Introduction

The emerging photovoltaic (e-PV) devices (see **Table 1**)[1-3] show promise for providing cheaper, cleaner and more versatile scalable electricity generation, as an alternative and/or complement to traditional photovoltaics (PVs), such as silicon and thin film devices from first and second PV technology generations, respectively.[4] Among the e-PV devices, the heterostructure architecture has emerged as the most successful approach with absorber materials including, for instance, perovskites, polymers, dyes, kesterites or matildites. However, the optimizing these devices for higher power conversion efficiency (PCE), surface area and performance durability have been challenging; both because of the complexity of the device interfaces or the intrinsic properties of the e-PV materials. Therefore, it has not been until recently that e-PV research equaled, if not surpassed, the research attention of traditional PVs. A comparison of academic publication trends supports this shift: from a mere handful of publications in the 1980s to nearly ten thousand annually by 2010 (see **Figure 1**a). On the one hand, it is noticeably that the number of annual publications on perovskite and organic solar cells is twice more each than that of silicon solar cells. However, despite this momentum, these e-PV still face obstacles, particularly in terms of stability, and only ~10% of the research in the field addresses the instability challenge (see **Figure 1**b). Hence, questions arise regarding the time and cumulative efforts required to fully realize the potential of those e-PV technologies.

Versatility is one of the main attributes of e-PV, as the PCE increase for large-scale grid-connected electricity production is not the only research target. Interest in potential applications such as flexible, transparent and integrated photovoltaics has also been increasing during the last decade. This can similarly be illustrated by analyzing the percentage of annual publications that include. For instance, topics like flexibility and transparency are featured in approximately 4-8% of recent publications (see Figure S1). However, unlike PCE results, that can be certified by several international institutions, a standardized quantitative evaluation and certification of other relevant aspects of e-PV devices, for proper validation and comparison, is still a work in progress.

Digital data management is another challenge that is common in the modern science context in general. The increase in digital journals with faster publication rates has occurred in parallel, and arguably contributing, to the overall increase in academic publications in the e-PV field during the last decade. Consequently, while the benefits of broader data sharing coverage are acknowledged, the identification of state-of-the-art results without further and proportional assistance is time consuming and even ineffective, either during the investigation or throughout the peer-review process. For instance, one could argue that the greater the number of publications, the more likely it is to find published works claiming a new record efficiency, in some subcategory, which in fact does not beat previous results. Consequently, there is a growing awareness for better systems and routines for data dissemination. Additionally, the need for better antiplagiarism checks, reproducibility tests, and data coherency verifications is required not only by the faster rates of information production but also due to the newer modalities, such as the advent of the artificial intelligence algorithms. In this context, the emerging PV initiative,[5] with its accompanying website and database aspires to establish an international framework and benchmarking for systematic data collection, presentation, and analysis as a reference for best practices and state-of-the-art reports.

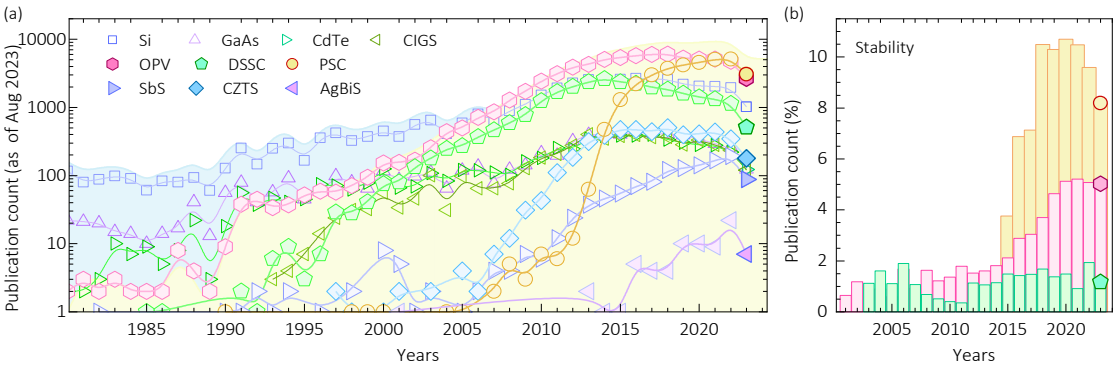

Figure 1. Annual academic research publications over time (a) in absolute count for several photovoltaic technologies, as indicated, and (b) corresponding percentage of those studies that include stability/degradation in the organic/hybrid material-based solar cells. In (a), the blue and yellow background regions indicate the total publication counts for traditional and emerging photovoltaics, respectively. The data corresponds to Clarivate's Web of Science as of August 2023 (see search terms in Table S1).

The state-of-the-art achievements in e-PV devices, as reflected in academic publications detailing top-performing devices in the research of e-PV devices have

been systematically parameterized and reported since 2020 through the annual emerging PV reports (e-PVr)[1-3], of which this is the fourth version. Herein, the performance data of the best e-PV devices are listed in comprehensible tables (e.g., see Green et al.).[6] Furthermore, the values are put into perspective by comparing the devices with respect to bandgap energy of the absorber material, number of device junctions, application class, and performance stability. Notably, we list and display the performance parameters for each technology and compare the experimental data to the corresponding theoretical limit in the detailed balance (DB)[7-9] model.

In this article, the updated graphs and tables of the best performing research photovoltaic cells are presented with the latest reports since August 2022. In the plot representations (sections 2-5), older and newer values are displayed with lighter and darker dot colors, respectively. Similarly, in the tables new entries are emphasized in bold (section 7). The following sections not only describe the updated plots and tables collected in our database but also highlight and discuss the most relevant and recent achievements in each category. Additionally, we provide comment on general trends and progress in the field during the last year.

1.1. Data inclusion criteria, definitions and emerging-pv.org

Consistent with previous e-PVr,[3] to be considered for these surveys, the data must meet a few specific criteria: the data should be published in a peer-reviewed academic journal and feature a proper "methods" section that allows experimental replication. Moreover, it should provide essential data for self-consistency checks. With respect to the *PCE* values, both the current density-voltage (*J*-*V*) curve measured under standard conditions and the external quantum efficiency (*EQE*) spectra should be presented and should be consistent, insofar that the short-circuit current density (J_{sc}) determined from both methods should not differ by more than 10%.[10] Reporting 5 minutes of maximum power point (MPP) tracking is encouraged, particularly for perovskite solar cells (PSCs).

For flexible and transparent/semitransparent devices, evidence of the bending radius and the explicit transmittance (*T*) spectra are required, respectively. In the case of operational stability test results, the published manuscript should clearly state both the initial and final efficiencies before and after 200 h or 1000 h are expected to be specified in the published manuscript. For multijunction devices,

only two-terminal (monolithic) devices with up to three junctions are considered in the current version of the reports. For those devices, analogous data/details on the devices should be provided with particular attention to the materials and *EQE* spectra of each sub-cell.

Articles lacking some of the mandatory requirements to be included in the e-PVr could still be considered, provided an extended or additional supporting information document be posted on the *emerging-pv.org* website.[5] A more in-depth discussion on the accuracy, performance parameters, exclusion criteria, and tiebreak rules is found in previous e-PVr[1-3] and within sections S1.5-S1.6 of the Supporting Information (SI).

The subject of emergence labeling and its relation with the PV technology generations and research are summarized in **Table 1**. While PV generations, as defined by M. Green,[11] have focus on the industry-oriented technological aspects, the herein introduced PV research waves are majorly concentrated on the research side of development. Somewhere in the middle, e-PVr's emergence[1-3] criteria attempt to balance both perspectives. For the established PVs, the main criterium relates to commercial availability. For emerging PVs, a distinction is made between "devices and technologies" and "materials and concepts". Devices and technologies are stand-alone structures with potential to become established technologies that can be characterized using the device-relevant concepts in **Table 2**. Different emerging PV technologies and devices, as listed in **Table 3**, are classified attending to the e-PV material, or material family, and/or fundamental device design (e.g., single junction or multijunction cells). The e-PV "materials and concepts" are research approaches designed as complementary strategies for optimizing the device performance of the e-PV devices, e.g., additives and optical managing structures. Notably, similar to the PV research waves, other definitions on PV research/technology generations have also been proposed.[12-18]

Table 1. Summary of approaches to classify PV technologies and concepts based on their age, technology readiness as well as cost and efficiency potential. Abbreviations can be found in **Table 2** and **Table 3**.

PV Research Waves	**1st Wave** Homojunction junction bulk devices Si	**2nd Wave** Thin film heterojunction devices fabricated via vacuum processes a-Si, CdTe, CCIGS	**3rd Wave** Devices and materials with low-cost/solution-based fabrication and/or PCE limits beyond single junction DB model with/without multijunction or concentration OPV, DSSC, PSCs, PSCs, OPV, DSSC, CZTS, SbS, AgBiS, quantum dots solar cells, multijunction cells, concentrated solar cells	**4th or next Wave** New devices, materials and/or concepts with potential for surpassing single junction DB PCE limit and low technology readiness level Down- and Up-Conversion (DwC, UpC) Singlet fission (SF) Multiple exciton generation (MEG) Plasmonic-enhanced cells (PeC) Rectenna solar conversion (RSC)
ePVr's Emergence	**Established PV** Mostly commercially available with ≳MW installation Si, a-Si, CdTe, CIGS		**Emerging PV** Exclusively or mostly in research stages with none or limited commercial availability and versatile applications including, but not limited to, large scale grid supply Tech. & Devices: PSCs, OPV, DSSC CZTS, SbS, AgBiS, multijunction cells, concentrated solar cells	Mater. & Concepts: QD, DwC, UpCm SF, MEG, PeC, RSC
PV Tech. Generations	**1st Generation** Silicon solar cells	**2nd Generation** Thin film solar cells: [a] a-Si, CdTe, CCIGS [b] PSC, OPV, DSSC, CZTS, SbS, AgBiS		**3rd Generation** Low-cost fabrication and/or PCE limit beyond single junction DB model: multijunction cells, concentrated cells

[a] 2nd generation PV technology considered in the original definition by M. Green[11] in the decade of 2000's, with fabrication methods based on vacuum processing as typical characteristic.

[b] The so-called solution-based thin film devices and/or emerging thin-film devices are here 2nd generation, prioritizing the thin-film criterium when adapting the 2020's decade reality[1-3] to the original 2000's concept.[11]

The equations, definitions and useful references already presented in the previous e-PVr[3] and updated in the current version are summarized in **Table 2**. Meanwhile, Table S2 reviews the minimal details to include in a research article to be considered in an e-PVr. Notably, we here emphasize the use of the definition of the photovoltaic bandgap energy as the inflection point of the absorption threshold of the *EQE* spectrum.[19, 20] This definition not only characterizes the operational response of the entire device (rather than an independent absorber layer or a combination of sub-layers), but also provides a framework for comparing different

emerging technologies, specially where a single optical bandgap energy is not directly defined,[1] such as in organic photovoltaics.

Table 2. Equations and definitions (updated after e-PVr version 3)[3]

No.	Equation	Definitions and comments	Ref.
(1)	$PCE = \frac{P_{out}}{P_{in}} = \frac{V_{oc} \cdot J_{sc} \cdot FF}{P_{in}}$	*PCE*, power conversion efficiency; P_{out}, output power density, P_{in}, incoming power density; V_{oc}, open-circuit voltage; J_{sc}, short-circuit current density; *FF*, fill factor	[1]
(2)	$EQE = \frac{A_m}{1 + \exp\left[\kappa \frac{\left(\lambda - \frac{hc}{E_g}\right)}{\lambda_s}\right]}$	Procedure to determine E_g from the *EQE(λ)* spectrum: *EQE*, external quantum efficiency; λ, wavelength; A_m, maximum EQE value just above the bandgap absorption threshold; h, Planck's constant; c, speed of light; E_g, photovoltaic bandgap energy; λ_s, sigmoid wavelength width parameter (*EQE* onset quality wavelength), $\kappa = \ln[7+4\sqrt{3}] \approx 2.63$, dimensionless coefficient related to the second derivative of the sigmoid.	[19]
(3)	$J_{sc,EQE} = \frac{q}{h\,c} \int EQE(\lambda) \lambda \Gamma_{AM1.5G}(\lambda)\, d\lambda$	$J_{sc,EQE}$, short-circuit current density as integrated from the EQE for the standard 1 sun illumination intensity AM1.5G spectrum $\Gamma_{AM1.5G}$ (typically in units of $W \cdot m^{-2} \cdot nm^{-1}$); q is the elementary charge.	
(4)	$EDBL = \frac{PCE^{real}}{PCE^{ideal}} = \frac{J_{sc}^{real}}{J_{sc}^{ideal}} \frac{V_{oc}^{real}}{V_{oc}^{ideal}} \frac{FF^{real}}{FF^{ideal}}$	*EDBL*, experiment-to-detailed-balance limit ratio, the "real" superscript refers to the experimental values; the "ideal" superscript refers to the theoretical limit of each performance parameter as in the detailed-balance models,[7, 8, 21] e.g., the highest efficiency for a single junction cell with absorber material of bandgap energy E_g at a temperature T_c under a spectral irradiance Γ. The proper application of a detailed- balance performance limit model on an experiment implies $EDBL \leq 1$.	[22]
(5)	$AVT = \frac{\int T(\lambda)\, P(\lambda)\, \Gamma_{AM1.5G}(\lambda)\, d\lambda}{\int P(\lambda)\, \Gamma_{AM1.5G}(\lambda)\, d\lambda}$	*AVT*, average visible transmittance; *T*, transmittance; *P*, photopic response of the human eye.	[23]
(6)	$LUE = AVT \cdot PCE$	*LUE*, light utilization efficiency	[24]
(7)	$PBCC = EQE(\lambda) + T(\lambda) + R(\lambda)$	The photon balance consistency check implies $PBCC \leq 1$	[23]
(8)	$E_{\Delta\tau} = \int_0^{\Delta\tau} P_{out}\, dt = \int_0^{\Delta\tau} P_{in}\, PCE\, dt$	Δτ, operational stability test time; $E_{\Delta\tau}$, operational stability test energy yield (STEY) for a test of duration Δτ; *t*, time; STEY is taken for 200 h and 1000 h of stability tests as E_{200h} and E_{1000h}, respectively.	[1]
(9)	$DR_{\Delta\tau} = \frac{PCE(\tau) - PCE(0)}{\Delta\tau}$	$DR_{\Delta\tau}$, effective overall degradation rate for an operational stability test of duration Δτ; DR_{200h} and DR_{1000h} are taken as the overall degradation rates for 200 h and 1000 h of stability tests, respectively.	[1]

Following the previous e-PVr,[3] each section showcases the best performing cells as reported in the literature, grouped by different technologies or material families. The corresponding abbreviations are listed in **Table 3**. Importantly, for multijunction PV cells we define the top sub-cell as the one that receives the total incident photon flux and generally has absorber material with the highest value of bandgap energy ($E_{g,top}$) compared to the other sub-cell(s). Similarly, the bottom sub-cell is the one receiving the residual and smaller fraction of the filtered incident photon flux, and generally has the absorber material with the smallest value of bandgap energy ($E_{g,bottom}$) in the stack. For two-junctions cells, or tandem devices, only the top and bottom sub-cells exist. That is in contrast to triple junction cells,

where a middle sub-cell is sandwiched between the top and bottom sub-cells, and which typically has an absorber material with a bandgap energy ($E_{g,mid}$) whose value is between those of $E_{g,bottom}$ and $E_{g,top}$.

Table 3. Abbreviations for PV technologies or material families (adapted from the e-PVr version 3)[3]

Abbreviation	Meaning and comments
AgBiS	$AgBiS_2$-based single junction photovoltaic cells, the so-called matildite solar cells.
a-Si:H	Amorphous silicon single junction photovoltaic cell; for representation purposes, a-SiGe:H-based single junction cells are exceptionally considered within this abbreviation.
CdTe	Cadmium telluride single junction photovoltaic cell
CIGS	$CuIn_xGa_{1-x}Se_2$-based single junction photovoltaic cell
CIGS/DSSC	Monolithic/2-terminal tandem photovoltaic cell: $CuIn_xGa_{1-x}Se_2$-based bottom sub-cell and dye sensitized top sub-cell
CIGS/perovskite	Monolithic/2-terminal tandem photovoltaic cell: $CuIn_xGa_{1-x}Se_2$-based bottom sub-cell and perovskite-based top sub-cell
CiGS/AlGaAs/GaInP	Monolithic/2-terminal triple junction photovoltaic cell: $CuIn_xGa_{1-x}Se_2$-based bottom sub-cell, AlGaAs-based middle sub-cell and GaInP-based top sub-cell
CZTS	$Cu_2ZnSn(S,Se)_4$-based single junction photovoltaic cell
DSSC	Dye sensitized single junction photovoltaic cell
DSSC/perovskite	Monolithic/2-terminal tandem photovoltaic cell: dye sensitized bottom sub-cell and perovskite-based top sub-cell
GaAs	Gallium arsenide single junction photovoltaic cell
GaAs/GaInP	Monolithic/2-terminal tandem photovoltaic cell: GaAs-based bottom sub-cell and GaInP-based top sub-cell
GaAs/perovskite	Monolithic/2-terminal tandem photovoltaic cell: GaAs-based bottom sub-cell and perovskite-based top sub-cell
GaAs(In,Bi,Al,P)	Monolithic/2-terminal triple junction photovoltaic cell including GaAs and no other material family specified in this table. For example: InGaAs- or GaAsBi-based bottom sub-cell, GaAs-based middle sub-cell and GaInP- or AlGaAs-based top sub-cell
nc-Si/a-Si	Monolithic/2-terminal tandem photovoltaic cell: nanocrystalline or microcrystalline Si bottom sub-cell and amorphous Si top sub-cell
nc-Si/nc-Si/a-Si	Monolithic/2-terminal triple junction photovoltaic cell: nanocrystalline silicon-based bottom and middle sub-cells, and amorphous silicon-based top sub-cell
OPV	Organic photovoltaic material-based single junction photovoltaic cell
OPV/a-Si	Monolithic/2-terminal tandem photovoltaic cell: organic-based bottom sub-cell and amorphous silicon-based top sub-cell
OPV/perovskite	Monolithic/2-terminal tandem photovoltaic cell: the bottom and top sub-cells are organic- and perovskite-based, respectively or vice versa.
PSC	Perovskite single junction photovoltaic cell
SbS	$Sb_2(S,Se)_3$-based single junction photovoltaic cell
Si	Monocrystalline or polycrystalline silicon single junction photovoltaic cell, including homo- or heterojunction structures.
Si/DSSC	Monolithic/2-terminal tandem photovoltaic cell: Si-based bottom sub-cell and dye sensitized top sub-cell
Si/GaAsP	Monolithic/2-terminal tandem photovoltaic cell: Si-based bottom sub-cell and $GaAs_{1-x}P_x$ -based top sub-cell
Si/GaInAsP/InGaP	Monolithic/2-terminal triple junction photovoltaic cell: silicon-based bottom sub-cell, GaInAsP-based middle sub-cell and GaInP-based top sub-cell
Si/perov/perov	Monolithic/2-terminal triple junction photovoltaic cell: Si-based bottom sub-cell and perovskite -based middle and top sub-cells
Si/perovskite	Monolithic/2-terminal tandem photovoltaic cell: Si-based bottom sub-cell and perovskite-based top sub-cell
TLSC	Transparent luminescent solar concentrator, including a lightguide, luminophore, and mounted solar cell(s).

The Emerging-PV website and database[5] has shown significant advancement during the last year, not only as the recommended data collection and visualization tool for the e-PV initiative, but also as an implementation framework for the definitions in **Table 2** and **Table 3**. The main progress since August 2022 includes the extension of data analysis from single to multi junction devices and the automatic calculation of *AVT* and *LUE* (see equations (5)-(6)) for transparent and semitransparent devices. These functionalities add to the already established calculation of PCE, E_g, $J_{sc,EQE}$ and *EDBL* (see equations (1)-(4)).

2. Highest efficiency photovoltaic cells

2.1. Single junction devices

The top efficiency single junction research cells are plotted in **Figure 2** as a function of the PV bandgap. This is presented alongside the detailed-balance theoretical efficiency limit,[7] which for a single junction assumes radiative emission from both the front and the rear side of the photovoltaic cell.[25] Notably, the new entries in the database are highlighted in more opaque colors.

Overall, most of the new record devices are either PSCs and OPVs, although a notable number of CZTSs has also emerged. In terms of material composition, and the consequent variation in the absorber bandgap energy value, most PSCs and OPVs with the highest efficiencies were reported with a cluster-like behavior in **Figure 2** around 1.5-1.6 eV and 1.35-1.45 eV, respectively.

For PSCs, this clustering may suggest a decrease of interest, breakthroughs, reproducibility issues and/or or fundamental physical problems for the development of some branches within the field, such as narrow bandgap lead-free (E_g<1.5 eV) and wide bandgap iodide-free (E_g>2.2 eV) devices. On the other hand, the consistent reproduction of PCE reports over 24% remains a trend for devices utilizing lead-based perovskites mostly composed of formamidinium, methylammonium and iodide. Those compositions often also include cesium and bromide around 5% of their respective cations and halide anions stoichiometries.

For OPVs, the polymer PBDB-T-2F (PM6) continues to be the most recurrent donor in both binary and ternary blends, including those with non-fullerene acceptors, in cells with PCE>19%. Similarly, we highlight the Y-series acceptor molecules as one of the most frequently employed among top efficiency devices.

Among the new PSCs entries, a new absolute certified record with an efficiency of 26.0% was reported in the tables published by Green et al.[6] However, this entry does only include the performance parameters and the *EQE* spectrum, without further information. Noteworthy is the work by Shi et al.[26] who achieved 25.4% (25% certified) with a formamidinium lead iodide ($FAPbI_3$)-based solar cell and, Zhang et al.[27] who reported a 25.2% efficient (25.1% certified) inverted device. In Shi et al.'s work,[26] in-situ monitoring of the $FAPbI_3$ crystallization process played a pivotal role to achieve oriented nucleation and crystal growth. This absorber-focused approach was found to favor the presence of black phases rather than the undesirable yellow phases, improving the optical properties of the perovskite films and the overall device performance. On the other hand, Zhang et al.'s inverted cell[27] optimization focused on improving the perovskite interface. This was achieved by introducing an amphiphilic molecular hole transporter equipped with a multifunctional cyanovinyl phosphonic acid group. This innovation lead to a superwetting underlayer which improved the perovskite deposition.

For OPVs, at least 14 (7 during the last year, 4 certified) reports present cells with efficiencies surpassing 19%. This validates the reproducibility of this milestone in the field. Among the latest top efficiency entries, we highlight the work by Wang et al.[28] who fabricated a 19.2% (19 % certified) efficient solar cell. They achieved this by using 3,5-dichlorobromobenzene (DCBB) – a high volatility and low cost solvent – to manipulate the morphological evolution of the PBQx-TF:eC9-2Cl blend. The addition of DCBB is suggested to effectively tune the aggregation of PBQx-TF:eC9-2Cl during film formation, resulting in a favorable phase separation and a reinforced molecular packing.

The latest record performance $Cu_2ZnSn(S,Se)_4$ cell has been featured in the records table by Green et al.[6] with a certified efficiency of 14.9%. In a related study, Zhou et al.[29] demonstrated control of the phase evolution of kesterite achieving 14.1% (13.8% certified) efficient devices. In their optimization strategy, the phase-evolution kinetics of Ag-alloyed kesterites was regulated by applying a positive pressure in the reaction chamber at the initial stage of the annealing process. This lowered the partial pressure of selenium, which reduced the collision probability between the selenium molecules and the kesterite precursor during the

initial formation of the crystals. Notably, an open-circuit voltage V_{oc}>550 mV was attained, which is a significant progress considering that reducing photovoltage losses is a major challenge in these devices.

Another new efficiency record has been established among $Sb_2(S,Se)_3$ solar cells reported by Chen et al.[30] with a PCE of 10.75%. In their study, a solvent-assisted hydrothermal deposition technique was implemented for direct deposition of high-quality antimony chalcogenide films. Particularly, they suggest that the addition of ethanol can regulate the reaction kinetics by regulating the concentration of the Sb source during the deposition procedure. This is believed to increase the grain size, smoothen the surface, and decrease the defect density of the prepared films by more than one order of magnitude, which benefits charge-carrier transport.

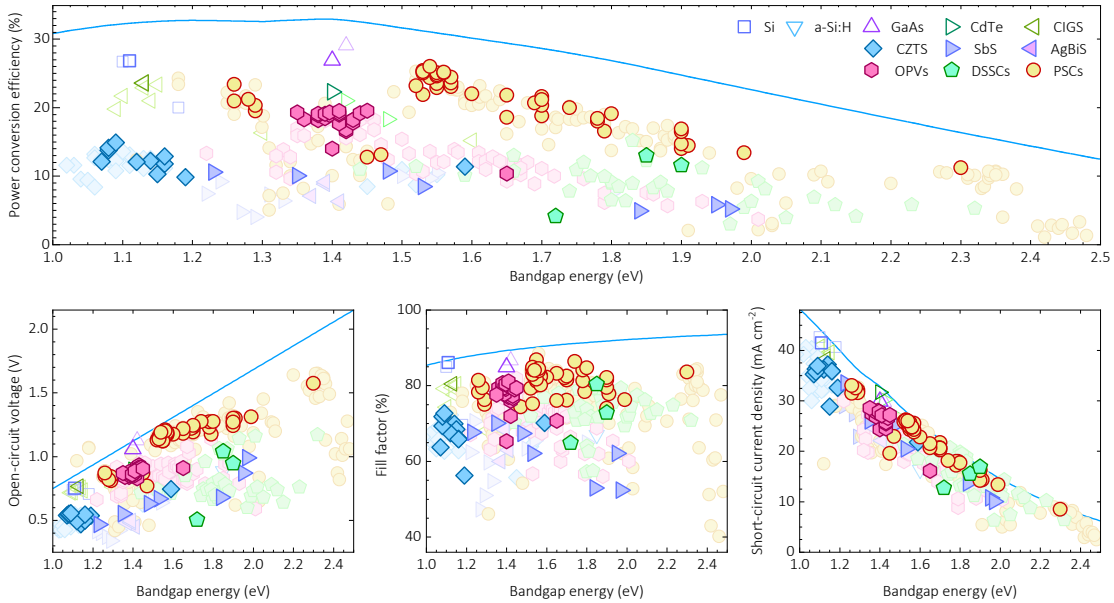

Figure 2. Highest efficiency single junction photovoltaic cells. Performance parameters as a function of effective absorber bandgap for different photovoltaic technologies: *PCE* (top) V_{oc} (bottom left), *FF* (bottom center) and J_{sc} (bottom right). Experimental data are summarized in Section 7.1, with the lighter and more opaque dots corresponding to reports before and after August 2022, respectively. The solid lines indicate the corresponding theoretical detailed-balance efficiency limit.[25]

Analysis of the current state-of-the-art device performance with respect to the DB efficiency limit are illustrated in the top panel of **Figure 3**. In **Figure 3**a one can find the same efficiency data as in **Figure 2**, but framed in terms of the *EDBL* ratio between the experimental value and the theoretical limit for the efficiency, as defined in Equation (4). Among emerging devices, PSCs exhibit the highest degree

of optimization by reaching up to 83% of the DB limit. This level of optimization rivals silicon and is only outperformed by GaAs single-junction cells. Even the wide-bandgap (~2.3 eV) PSCs can achieve 69% of the theoretical limit, while all other e-PV technologies linger below 60%.

Figure 3b shows the updated logarithmic loss analysis[31] for the champion efficiency cells for each technology. The new top-efficiency PSC slightly outperforms the optimized Si device and also shows a nearly uniform distribution of losses between photovoltage, photocurrent and *FF*. Other top devices with approximately even losses include the recent CIGS[6] record and the older best performing a-Si:H cell. The figure also displays the major photovoltage losses (red dashed bars), from higher to lower optimization, for the recently published silicon heterojunction cell[32] and the new records for CdTe,[6] OPV,[33] $Cu_2ZnSn(S,Se)_4$[6] and Sb_2Se_3.[30] Similarly, the older records for dye-sensitized and $AgBiS_2$ solar cells present low V_{oc} values as a main issue with respect to the DB radiative limit. In contrast, the top performance GaAs cell is the only one that presents a nearly fully optimized photovoltage and fill factor values, even if its photocurrent still can be improved.

The time evolution of the device performance presented in **Figure 2** is shown in detail in **Figure 3**c, which also includes the data from NREL's "Best research-cell efficiency chart" (solid lines).[34] Among e-PV technologies, the efficiency progress since 2014 continues even though it appears to be a saturation and/or stagnation for the performance optimization of PSCs, OPV and Sb_2Se_3 solar cells. However, kesterite devices display an apparent upswing with continued improvement in efficiency during the last year.

Dale-Scarpulla's[35] plots, illustrating PCE versus research effort – as measured by the cumulative number of academic publications registered in Clarivate's Web of Science – have also been included (see **Figure 3**d). The corresponding annual distribution of the accounted publications is shown in **Figure 1**. Most of the technologies (e.g., Si, PSCs, CdTe, CIGS, $AgBiS_2$) show a behavior near to $PCE = 6\mathrm{Log}(x)$, where x is the publication count (see grey dotted line in **Figure 3**d). This suggest that an unit percentage progress in device performance requires an exponential increase in research efforts. In contrast, cases in which fewer publications translate to a higher PCE increase, is an indication of several

direct or indirect breakthroughs. For instance, this is the case for GaAs, OPV, DSSC and CZTS devices.

The output power in units of milliwatts corresponding to the data in **Figure 2** is presented in **Figure 3**e as a function of the illuminated area of the reported laboratory cells. In this graph, the efficiency isolines (see dash-dot grey line) form diagonal-like contours. The closer they are to the top-right region of the graph, the higher the output power. Overall, e-PV technologies continue to predominantly report areas around 0.1 cm^2, whereas values >1cm^2 remain rare. Among the latest reports, the best PCE×area achievement was reported for PSCs (24.4%×1.01 cm^2),[6] followed by selenium (5.8%×4 cm^2),[36] OPV(14%×1.1 cm^2)[37] and CZTS (12.1%×1.07 cm^2)[6] cells. In particular, we highlight the work by Li et al.[38] who reported a PSC with 22.9% efficiency over 1 square centimeter. Their findings suggest that they were able to improve the stability of the perovskite black phase, which if not done could induce phase transitions and lattice strain due to daily temperature variations. Specifically, they used the ordered dipolar structure of β-poly(1,1-difluoroethylene) to control perovskite film crystallization and energy alignment.

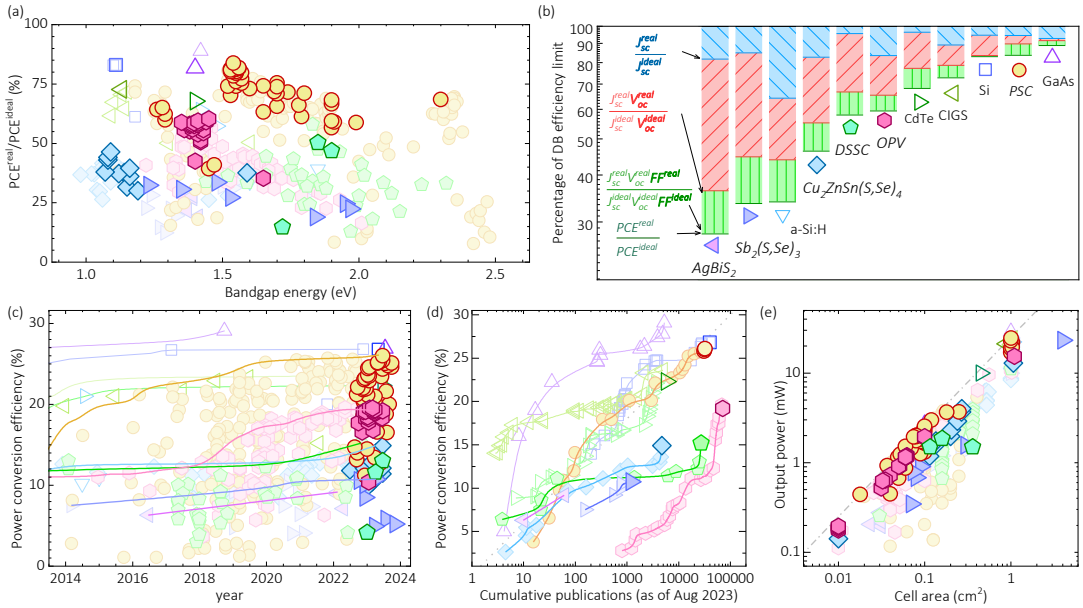

Figure 3. DB efficiency limit on the (a) entire PCE data from **Figure 2** showing the relative efficiencies with respect to the theoretical limit and (b) logarithmic loss analysis[31] for the top efficiency cell of each technology, as defined by Equation (4). The time evolution of PCE is shown in the bottom panel over (c) time, (d) cumulative publication count and (e) as output power with respect to the cell area. The legend is as that of **Figure 2**, where opaque and light symbols indicate reports before and after August 2022, respectively. The solid lines in (c) contain the data from NREL's "Best research-cell efficiency chart.[34] The publication count in (d) was taken from Clarivate's

Web of Science, and the grey dotted line indicates the empirical law $PCE = 6\mathrm{Log}(x)$, where x is the publication count. The dash-dot line in (e) is the efficiency isoline for PCE=25%.

2.2. Multijunction devices (monolithic)

The performance parameters of monolithic/two-terminal multijunction photovoltaic research cells, encompassing up to three junctions, are presented in **Figure 4**. Those values are put into perspective by comparing them to the corresponding optimized bandgap DB efficiency limit, including radiative coupling. Overall, even though gallium-based triple junction cells (InGaP/GaAs/InGaAs and Si/GaInAsP/InGaP) continue to be the top performance devices, silicon-perovskite tandems have shown a consolidated progress with at least 3 reports of over 31% PCE. In terms of photovoltage, triple-junction all-perovskite solar cells are now the second technology in our plots with V_{oc}>3 V, even if top efficiencies still are under 25%. This achievement (V_{oc}=3.23 V) was reported by Wang et al.[39] They utilized a rubidium/cesium mixed-cation perovskite approach for suppressing the light-induced phase segregation that typically hinders the performance of high bandgap perovskites. In terms of photocurrent and large-area demonstration, Si/perovskite tandem devices remains at the forefront, whereas the highest fill factors have been reported for all-perovskite double-junction cells.

The current champion Si/perovskite cell, as recorded in Green's efficiency tables,[6] boast an impressive efficiency of 33.7%. Two other noteworthy advancements for Si/perovskite double-junction solar cells are the studies by Mariotti et al.[40] achieving a PCE value of 32.5%, and Chin et al.[41] reaching 31.25%. In Maroitti's study,[40] the authors combined a triple-halide perovskite with a piperazinium iodide interfacial modification towards the C_{60}-based electron-transporting layer. They suggest that a dipole was created that improved the band alignment, reduced nonradiative recombination losses, and enhanced charge extraction. Conversely, Chin et al.[41] report the uniform deposition of a perovskite top sub-cell on the industrially standardized micro-pyramids of crystalline silicon cells. Additionally, they utilize phosphonic acids as both a hole-transport material and as a perovskite additive for better perovskite crystallization and lower interface charge-carrier recombination.

All-perovskite tandem cells have also shown significant progress during the last year with maximum certified PCE values of 29.1% and 28.2% for cells with designated illumination areas of 0.05 cm^2 and 1.04 cm^2, as reported by Green et al.[6] where no material information is available. Among the reports within academic articles, he highest PCE value has been published by Lin et al.[42] with 28.4% (certified 28.0%). In Lin's work, a hybrid evaporation–solution-processing method was optimized for suppressing interfacial non-radiative recombination and improving charge extraction at the interfaces between the perovskite and the electron-transport layer (ETL). Moreover, the interface between the narrow-bandgap perovskite and the ETL was further improved by introducing a thin interlayer of full-lead wide-bandgap perovskite. Notably, the latter approach was also proven to report a remarkable *PCE* value of 23.4% for single junction Sn-Pb devices.

A new record has also been reported for tandem organic solar cells, with 20.6% (20.3% certified) efficiency, as detailed in a study by Wang et al.[43] They used devices with PFBCPZ:AITC and PBDB-TCl:AITC:BTP-eC9 as top and bottom sub-cell absorber blends, respectively. Remarkably, the cell achieved a V_{oc}=2.02 V and an estimated 50 mV reduction of photovoltage losses (with respect to the non-optimized reference cell). This was attributed to the introduction of AITC which is an asymmetric small molecule acceptor. They posit that this approach reinforces the molecular packing and tune the domain size in a way that suppresses charge carrier recombination, expedites hole transfer, and narrows down the energetic disorder and the electronic density of states in the active layer. Remarkably, the fact that the double-junction organic device outperforms the top-efficiency single-junction OPVs is an indicator of the technological maturity of the research field, a trait that can also be observed among PSCs and established PVs.

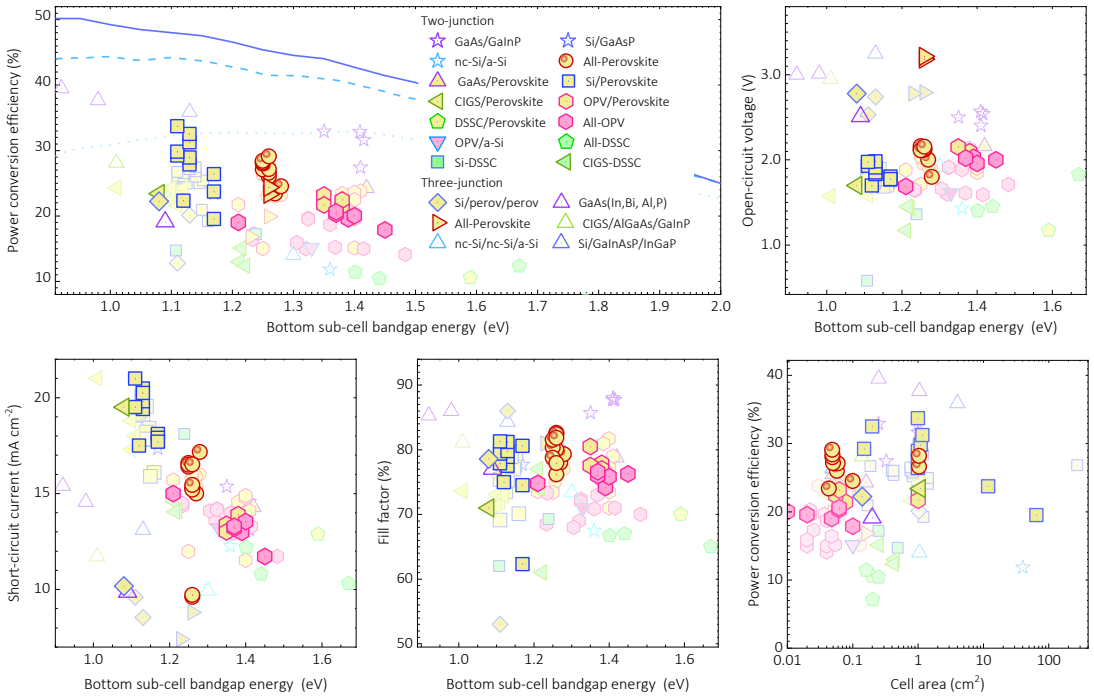

Figure 4. Highest efficiency for monolithic/two-terminal multijunction photovoltaic research cells including up to three junctions. Performance parameters as a function of the absorber bandgap energy of the bottom sub-cell for various photovoltaic technologies: power conversion efficiency (top-left), open-circuit voltage (top-right), short-circuit current density (bottom-left), fill factor (bottom-center) and corresponding area (bottom-right). The dotted, dashed and solid lines in the efficiency graph indicate the single junction, the top-sub-cell-optimized and top- and middle-sub-cell-optimized DB efficiency limits for one junction, double junction and triple junction photovoltaic cells, respectively.[8, 21] Light and opaque symbols indicate the reports published before and after August 2022, respectively.

3. Flexible photovoltaic cells

The research on flexible PVs during the last year has shown significant progress for PSCs, both in terms of the number of reports and PCE values, as summarized in **Figure 5**. Further studies with efficiencies below previous records have also been published on OPV, CZTS, and Sb_2S_3 e-PV flexible cells. Additionally, CdTe and CIGS flexible devices have similarly been reported.

The latest efficiency champion flexible PSC has been reported by Gao et al.[44] with a PCE of 23.68% (23.35% certified), which lost 9% of its initial PCE after 5,000 cycles of mechanical bending at a radius of 4 mm. The authors remarked that their high-performance PSCs (deposited on a PEN/ITO substrate) were possible because the use of the pentyl ammonium acetate (PenAAc) molecule as an interface layer between the 700 nm-thick perovskite and the PTAA hole-

transport material. Their density functional theory modeling suggests that the $PenA^+$ cations and Ac^- anions have strong chemical binding with both acceptor and donor defects of surface-terminating ends on perovskite films, which ultimately reduces trap-state densities and suppresses non-radiative charge-carrier recombination losses. Their resulting devices outperformed every other new report on flexible devices regarding both photovoltage and fill factor, and it showed a significantly optimized photocurrent with respect to the DB limit. Additionally, a 1 square centimeter flexible cell was reported with 21.33% efficiency for a top flexible e-PV output power of 21.33 mW.

Notably, Zheng et al.[45] reported OPV devices with ultra-thin silver transparent electrode on 125 μm-thick polyimide substrates with 0.052 cm^2 and 1.00 cm^2 active areas exhibiting PCEs of 17.4% and 17.17%, respectively. The devices endured the bending test with a radius of 2 mm for 5000 cycles, without any degradation. Moreover, they also fabricated samples on 1.3 μm-thick polyimide substrates demonstrating a PCE of 17.32% for a 0.052 cm^2 active area. These cells showed 97% PCE retention after 5000 compression-stretching cycles with 30% compression. Additionally, a remarkable power-to-weight ratio of 39.7 W g^{-1} was also reported for these samples.

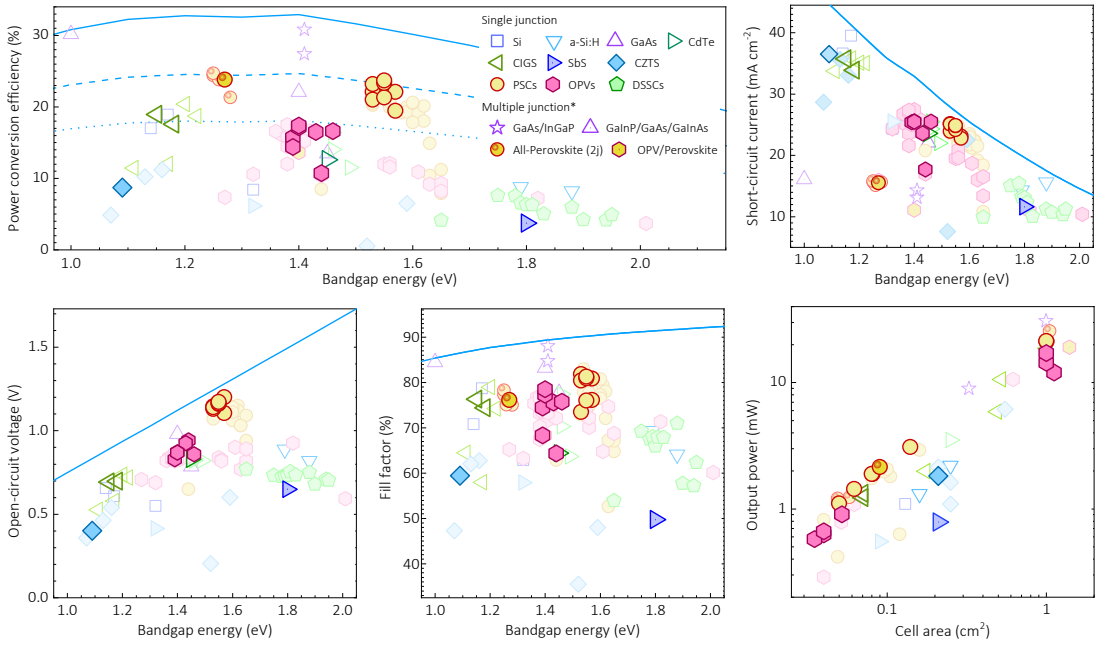

Figure 5. Flexible PVs and their performance parameters as a function of absorber (or bottom junction absorber in case of multijunction devices) bandgap energy for various photovoltaic technologies: power conversion efficiency (top-left), short-circuit current

density (top-right), open-circuit voltage (bottom-left), fill factor (bottom-center) and output power versus area (bottom-right). Experimental data are summarized in Section 7.2 and the solid, dashed and dotted lines indicate 100%, 75% and 55% of the theoretical single junction DB efficiency limit,[25] respectively. The lighter and opaque symbols are reports before and after August 2022, respectively.

4. Transparent and semitransparent photovoltaic cells

The inconspicuous progress in transparent and semitransparent PV devices during the last year is evidenced in **Figure 6**, which continues the trend already identified in the previous e-PV report.[3] Among solar cells, no absolute records regarding light utilization efficiency (LUE) and no significant novel absorber materials for single-junction devices have been reported during the last year; most of the reports on transparent cells focus on the optimization of the absorber layer thickness and on transparent electrodes of otherwise top-performing opaque devices. Notably, Ritzer et al.[46] reported the first micro-patterned translucent two-terminal all-perovskite tandem solar cells with PCEs as high as 15.0% at average visible transmittance (*AVT*) of 12% and 9.3% at 31% *AVT*, for LUE values of 1.8% and 2.9%, respectively. Nevertheless, the latest transparent OPV continue to outperform most transparent PSCs in terms of LUE.

Remarkably, Li et al.[47] reported a transparent luminescent solar concentrator (TLSC) based on organosilane-grafted carbon dots (Si-CDs) with an average visible transmittance (*AVT)* of 89% and a *PCE* of 2.09% for a *LUE* of 1.86%, which is currently the highest *LUE* value for *AVT*>75% in our lists. The authors proposed a hydrothermal method using anhydrous citric acid, ethanolamine and KH-792 as the reaction precursors to prevent the aggregation-induced fluorescence quenching effect in solid-state carbon dots, which would otherwise significantly limit their application in TLSCs. The obtained Si-CDs (average particle size of about 4.35 nm) were uniformly dispersed in the polyvinyl alcohol (PVA) matrix through a dehydration condensation reaction and hydrogen bonding between the silicon hydroxyl group of Si-CDs and the hydroxyl group of PVA. Furthermore, they also presented evidence of the UV shielding properties of the Si-CDs after interacting with PVA, and good optical and device performance properties were maintained even after 12 weeks of storage under natural conditions.

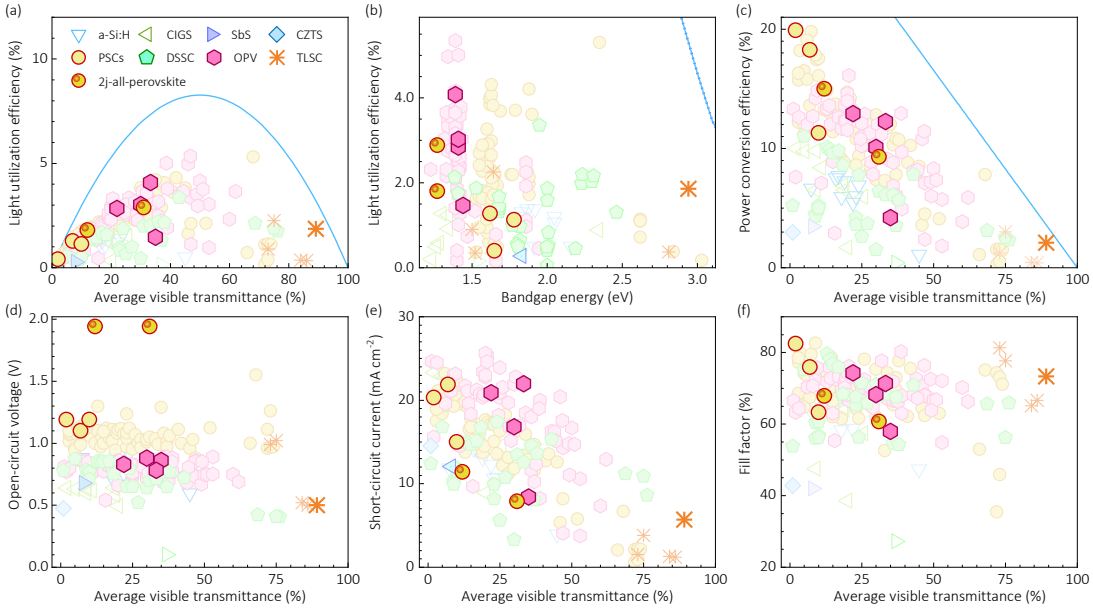

Figure 6. Best performing transparent and semitransparent PVs: *LUE* versus (a) *AVT* and (b) E_g; and (c) *PCE*, (d) V_{oc}, (e) J_{sc} and (f) *FF* as a function of *AVT*. The experimental data are summarized in Section 7.3. The blue solid lines indicate the corresponding theoretical detailed balance efficiency limit for non-wavelength selective PVs. In (b), the multi-junction cells are potted as a function of the bandgap energy of the absorber material in the bottom sub-cell. The lighter and more opaque symbols are reports before and after August 2022, respectively.

5. Operational stability in emerging research solar cells

The stability of e-PVs is paramount not only for their potential industrial deployment but also for ensuring reproducibility and validation of reported research progress. For instance, **Figure 1**b illustrates the proportion of academic publications listed in Clarivate's Web of Science that addresses the stability and/or degradation of three key e-PV technologies. From 2015 onwards, PSCs and OPV have showed an increased emphasis on the subject, with 10% and 5% of their publications, respectively, addressing it. In contrast, DSSCs have dedicated a much lower fraction of their annual research effort towards stability issues. Of significant concern is an emerging trend that could have adverse negative long-term effects: most of the stability analyses either focus on dark storage or do not properly describe their stability measurements. Such ambiguities make it challenging to reproduce and compare result with similar approaches in the literature. We strongly recommend reporting the initial PCE values before the stability test, as well providing explicit details about the illumination, humidity, and temperature conditions.

According to our inclusion criteria (see section 1.1), **Figure 7** summarizes the latest reports from in-situ stability tests conducted over 200 h and/or 1000 h under continuous 1-sun illumination. Overall, most of the new studies continue to focus on PSCs whose as-fabricated PCE (initial) are proved to be state-of-the-art. This produces a cluster-like behavior for the energy yield for bandgap energies around 1.5-1.6 eV, similar to that shown in **Figure 2**. Another consolidated behavior arises when comparing the final PCE and the degradation rates after 200 h and 1000 h of operational stability testing as a function of the initial PCE. Most PSCs show higher instability over the first 200 h, and may even see an increase in the PCE over that time, whereas a performance decrease generally is reported after 1000 h. This behavior is still valid even for silicon/perovskite tandem devices.

A new champion energy yield PSC after 1000 h of operational stability test (and overall champion among single junction e-PVs) has been reported by Li et al.[48] They report an E_{1000h}=23.3 Wh·cm^{-2} and a degradation rate of DR_{1000h}=+0.09 %/week. Notably, this cell did not only exhibit remarkable stability over 1000 h; it also consistently maintained a PCE of approximately 23.4% trough 3500 h of testing. The operational test was conducted under continuous AM1.5G illumination at room temperature (~40°C w/o cooling) and the bias voltage of the cell was set by MPP tracking. Interestingly, unlike the above-mentioned general trend, this cell stabilizes its performance after the first 200 h PCE increase, instead of the more often found subsequent decrease. This was attributed to the introduction of a 1,3-bis(diphenylphosphino)propane (DPPP) treatment that passivates, binds, and bridges interfaces and grain boundaries in the perovskite. The choice of DPPP was suggested by density functional theory calculations which found diphosphine Lewis base molecules to have one of the strongest binding energies for approaching the issue of uncoordinated lead atoms in the perovskite.

An inorganic wide-bandgap device reported by Li et al.[49] is, nonetheless, the new champion PSC in terms of degradation rate after 1000 h of operational stability test with a value of DR_{1000h}=+0.05 %/week. For this, the authors introduced a 4-(Trifluoromethyl) phenethylammonium (CF3-PEA) passivating dipole layer between the perovskite ($CsPbBr_xI_{3-x}$) and the ETL (C_{60}/BCP). This strategy is believed to reduce the energetic mismatch and increase the charge extraction at the ETL. Subsequently, the same approach was considered for the fabrication of all-

perovskite tandem devices that produced the highest operational stability among all e-PV multijunction solar cells with E_{1000h}=23.7 Wh·cm^{-2} and a degradation rate of DR_{1000h}=−0.16 %/week.

The new top performance stability OPV cells have been reported by Fu et al.[50] and Sun et al.[51] with unprecedented E_{1000h}=15.7 Wh·cm^{-2} and E_{1000h}=15.5 Wh·cm^{-2}, respectively (see **Figure 7**d). Notably, these are the first OPV stability studies in our list with PCE>8%, and the DR_{1000h}=−0.5 %/week value from the work by Sun et al.[51] is second only to the wide-bandgap PSC from Li et al.[49] among all e-PV cells in the range 10%<PCE<20% (see **Figure 7**f). This significant improvement was attributed to the introduction of a chlorinated P_A PY-2Cl polymer into a PM6:PY-1S1Se host binary blend for a ternary all-polymer system. This strategy optimizes phase separation with fibrillar morphology, produces a broader light-harvesting spectrum, improves the exciton dissociation, increases the charge-carrier generation, and hinders the non-radiative charge-carrier recombination. On the other hand, the strategy by Fu et al.[50] utilized 1,3,5-trichlorobenzene as crystallization regulator for avoiding the excessive aggregation of the non-fullerene acceptor in PM6:BTP-eC9 blends.

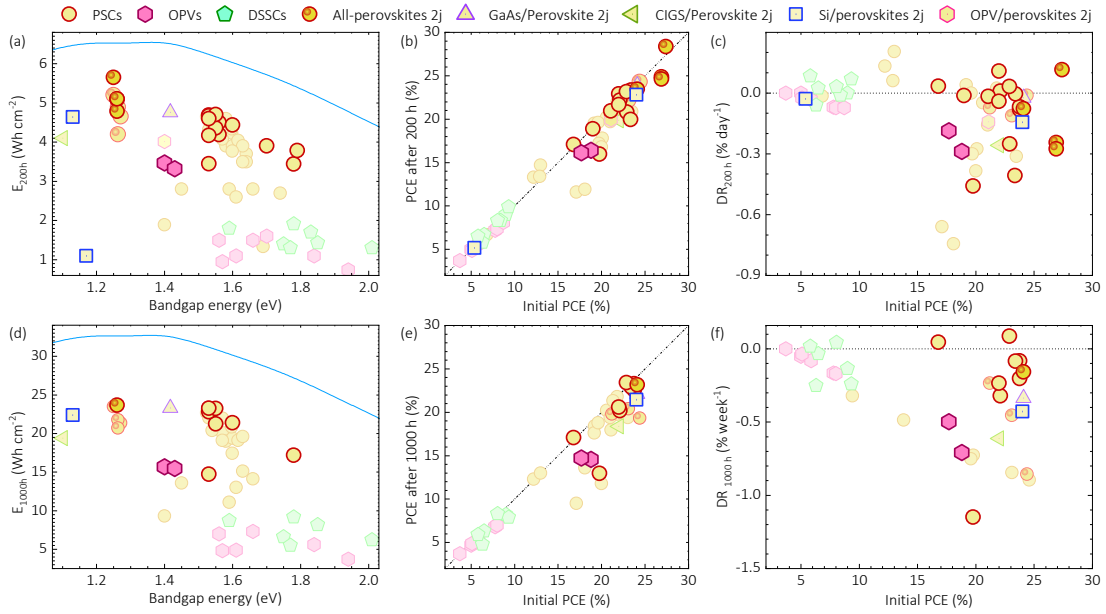

Figure 7. Operationally most stable emerging PVs for each technology during 200 h (a-c) and 1000 h (d-f) of testing: stability test energy yield (Equation (8)) as a function of bandgap energy (a, d), final power conversion efficiency as a function of the initial value (d, e), and overall degradation rate (Equation (9)) as a function of initial power conversion efficiency (s, f). The experimental data are summarized in Section 7.4 and the solid blue lines in the STEY panel (left) are the corresponding DB theoretical limits. The diagonal dot-dot-dashed lines in the middle panel indicate where the final

efficiencies equal the initial values. The positive values above the horizontal dotted lines in the degradation rate panel (right) indicates that *PCE* increases with respect to the initial values.

6. Conclusions

In summary, in this fourth installment of the emerging PV reports, we provide a substantial update on data for record devices and on the advancements in PV research landscape. Among the most significant and positive trends, we have demonstrated: (i) a marked progress in Si-perovskite tandem solar cells evident by both new *PCE* records and an increased number of publications; (ii) a continuous progress of the perovskite-based single junction solar cells , especially with regards to stability, and (iii) the consolidated reproducibility of the PCE>19% values among the OPVs. Moreover, we have noted that the efficiency of OPV tandem cells now has exceeded OPV single junction cells—an indication of maturity for a technology, which other technologies like perovskites have achieved. Further, new record performance reports have been reported for kesterite and Sb_2S_3 inorganic solar cells, as well as for flexible e-PV solar cells and for transparent luminescent solar concentrators.

However, no significant recent progress has been made in the field of transparent and semitransparent solar cells. Similarly, but reinforcing a previously trend, the studies on performance stability continue to be scarce and/or poorly described, which hinders the analysis and comparison of the results within the literature. With respect to the latter, we one again encourage the PV research community to use dimensional parameters (e.g., initial PCE, $DR_{\Delta\tau}$, $E_{\Delta\tau}$) rather than, or in addition to, relative percentages in degradation and optimization studies. Moreover, while the interest on stability from the device performance point of view has arguably been primarily focused on the reproducibility side of research, it also reflects the interest on industrial compatibility that should receive more consideration. Additionally, other relevant aspects such as fabrication method and material suitability for upscaling should also gain attention during the following years.

7. Tables

The tables below list the reports on the best achievements in most of the established and emerging PV technologies as a function of the device bandgap E_g. Unless otherwise noted, E_g values were estimated by fitting the absorption threshold region of the corresponding *EQE* spectra to Equation (2). Note that, for some absorber materials this definitition may result in a value slightly larger (typically on the order of the thermal energy) than that of the optical bandgap.[6] The new reports, from articles published since August 2022, are highlighted in bold. The older reports, from articles published before August 2022, which were already included in our previous surveys are referenced to the corresponding e-PVr. In contrast, each older report that was missed in the corresponding previous e-PVr, is now included with its corresponding individual citation. All the citations, further data, and visualization tools can be found on the emerging-pv.org website.[5] This website and database is the main and recommended data collection path for the e-PVr and an useful instrument that complements the below tables.

In the case of *PCE* reports of PSCs showing hysteresis behavior in the *J-V* characteristic, while sweeping voltage in different directions and/or scan rates, the lower *PCE* value has been considered in each case. This is discussed in details in section S1.1 of the supporting information.

The *FF* values have been automatically corrected to match the reported values of the *PCE*, J_{sc} and V_{oc} under standard 100 mW cm^{-2} illumination of AM1.5G spectrum. Some reports have introduced up to ±0.5% discrepancies between the values in our tables and those reported in the original publications owing to differences in the rounding digits and/or typos in the original manuscripts. Cells with mismatches of >0.5% may have been discarded (see section S1.5 in the supporting information).

For the transparent/semitransparent cells, note that the *AVT* values may differ from those reported in the original manuscripts when a definition different from that of Equation (5) was used in the original published article.

For GaAs-based and related III-V semiconductor-based devices, the performance parameters are listed either among tables for established technologies or in independent tables. This is a notable exception to the PV emergence definition

in **Table 1** since the high fabrication costs of these devices hinder the classification as either established or emerging PVs.

7.1. Highest efficiency research solar cells tables

Table 4. Single-junction **perovskite** research solar cells with the highest efficiency: performance parameters as a function of device absorber bandgap energy (from the EQE spectrum).

E_g [eV]	PCE [%]	V_{oc} [mV]	J_{sc} [mA cm^{-2}]	FF [%]	Absorber perovskite	Ref.
1.12	12.4	967	17.5	72.9	$MAPb_{0.5}Sn_{0.5}Br_3:Bi^{3+}:BA_2MA_4Sn_5I_{16}$	[3]
1.18	24.3	1070	29.1	78.0	$FA_{0.7}MA_{0.3}Pb_{0.7}Sn_{0.3}I_3$/BTBTI:PCBM	[3]
1.18	23.4	1067	28.9	75.8	$FA_{0.7}MA_{0.3}Pb_{0.7}Sn_{0.3}I_3$/BTBTI:PCBM	[3]a)
1.25	20.7	843	30.6	80.2	$FA_{0.6}MA_{0.4}Pb_{0.4}Sn_{0.6}I_3$	[2]
1.25	22.2	841	33.0	80.0	$FA_{0.7}MA_{0.3}Pb_{0.5}Sn_{0.5}I_3$	[3]
1.26	**23.4**	**871**	**33.0**	**81.4**	**$FA_{0.7}MA_{0.3}Pb_{0.5}Sn_{0.5}I_3$**	**[42]**
1.26	**21.0**	**850**	**31.5**	**79.11**	**$Cs_{0.1}FA_{0.6}MA_{0.3}Pb_{0.5}Sn_{0.5}I_3$**	**[52]**
1.26	20.4	834	30.5	80.2	GuaSCN:$FA_{0.6}$ $MA_{0.4}Sn_{0.6}Pb_{0.4}I_3$	[2]
1.27	20.9	827	31.4	80.5	$FA_{0.7}MA_{0.3}Pb_{0.5}Sn_{0.5}I_3$	[2]
1.28	20.6	842	30.6	80.1	FSA: $FA_{0.7}MA_{0.3}Pb_{0.5}Sn_{0.5}I_3$	[2] a)
1.28	21.7	850	31.6	80.8	FSA: $FA_{0.7}MA_{0.3}Pb_{0.5}Sn_{0.5}I_3$	[2]
1.28	**21.2**	**820**	**32.5**	**79.3**	**$Cs_{0.2}FA_{0.8}Pb_{0.5}Sn_{0.5}I_3$**	**[53]**
1.29	23.3	880	32.8	80.8	$Cs_{0.025}FA_{0.475}MA_{0.5}Pb_{0.5}Sn_{0.5}Br_{0.075}I_{2.925}$	[3]
1.29	**20.3**	**842**	**31.6**	**76.3**	**$Cs_{0.17}FA_{0.83}Pb_{0.5}Sn_{0.5}I_3$**	**[54]**
1.29	**19.5**	**810**	**32.1**	**75.0**	**$Cs_{0.25}FA_{0.75}Pb_{0.5}Sn_{0.5}I_3$**	**[55]**
1.30	18.8	820	29.6	77.3	$FA_{0.6}MA_{0.4}Pb_{0.4}Sn_{0.6}I_3$	[2]
1.30	17.1	840	27.9	73.0	$Cs_{0.05}FA_{0.8}MA_{0.15}Pb_{0.5}Sn_{0.5}I_3$	[2]
1.31	5.0	420	23.8	50.3	$CsSnI_3$	[2] b)
1.31	7.1	486	22.9	64.0	$MASnI_3$	[2] b)
1.31	14.1	740	26.7	71.4	$Cs_{0.25}FA_{0.75}Pb_{0.5}$ $Sn_{0.5}I_3$	[2]
1.32	11.6	720	23.4	68.9	$MAPb_{0.4}Sn_{0.6}$ $Br_{0.2}I_{2.8}$	[2]
1.33	7.5	450	24.9	67.0	$CsSnI_3$:MBAA	[2]
1.34	10.0	767	20.5	63.6	$MAPb_{0.4}Sn_{0.6}I_3$	[2]
1.34	12.1	780	20.7	75.1	$MAPb_{0.4}Sn_{0.6}Br_{0.4}I_{2.6}$	[2]
1.35	16.3	780	26.5	79.0	$FAPb_{0.7}Sn_{0.3}I_3$	[2]
1.36	8.2	630	19.7	66.1	$CsSnI_3$	[2]
1.37	14.7	737	27.1	73.6	$FA_{0.3}MA_{0.7}Pb_{0.7}Sn_{0.3}I_3$	[2]
1.38	17.3	810	28.2	75.4	$FAPb_{0.75}Sn_{0.25}I_3$	[2]
1.38	15.2	800	26.2	72.5	$MAPb_{0.75}Sn_{0.25}I_3$	[2]
1.39	20.6	1020	26.6	76.0	$FA_{0.7}MA_{0.3}Pb_{0.7}Sn_{0.3}I_3$	[2]
1.40	8.2	745	17.8	61.8	$MAPb_{0.6}Sn_{0.4}I_3$	[2]
1.40	10.1	655	22.1	69.6	$FASnI_3$ + DipI + $NaBH_4$	[3]
1.41	5.9	487	20.0	60.6	$FA_{1-x}Rb_xSnI_3$	[2]
1.42	14.3	920	20.4	76.2	$FASnI_3$	[3]
1.42	14.4	820	22.4	78.0	$MAPb_{0.75}Sn_{0.25}I_3$	[2]

1.42	13.2	840	20.3	78.0	$EA_{0.098}EDA_{0.01}FA_{0.882}SnI_3$	[2]
1.43	12.4	949	17.4	74.9	$FA_{0.85}PEA_{0.15}SnI_3$:NH_4SCN	[2] a)
1.44	12.3	750	21.7	75.3	$EA_{0.098}EDA_{0.01}FA_{0.882}SnI_3$	[3]
1.44	10.1	642	22.2	70.8	$Cs_{0.2}FA_{0.8}SnI_3$	[2] a)
1.44	10.2	638	22.0	72.5	$FASnI_3$:FOEI	[2] a)
1.45	13.6	840	22.9	70.8	$FASnI_3$	[3]
1.45	**12.8**	**869**	**19.6**	**74.5**	**$FARbSn(Br,Cl,I)_3$**	**[56]**
1.47	**13.1**	**770**	**22.9**	**74.4**	**$Cs_{0.05}FA_{0.95}SnI_3$**	**[57]**
1.48	6.0	460	23.9	53.9	$CsSnI_3$	[2]
1.49	22.3	1090	26.3	78.0	$FA_{0.6}MA_{0.4}PbI_3$ (sc)	[2]
1.51	19.3	1047	23.8	77.5	$FA_{0.6}MA_{0.4}PbI_3$	[2]
1.52	**23.2**	**1130**	**25.9**	**79.3**	**$FAMAPbCl_xI_{3-x}$**	**[58]**
1.52	25.3	1150	26.2	83.9	$Cs_{0.05}FA_{0.85}MA_{0.05}Rb_{0.05}PbBr_{0.15}I_{2.85}$	[3]
1.52	24.1	1161	25.4	81.4	$Cs_{0.05}FA_{0.85}MA_{0.05}Rb_{0.05}PbBr_{0.15}I_{2.85}$	[3] a)
1.53	**21.9**	**1142**	**25.5**	**75.2**	**$CsFAMARbPb(Cl,I)_3$**	**[59] b)**
1.53	**25.1**	**1157**	**26.1**	**83.0**	**$Cs_{0.015}FA_{0.985}PbI_3$**	**[60]**
1.53	**25.4**	**1150**	**26.2**	**82.0**	**$Cs_{0.05}MA_{0.05}FA_{0.9}PbI_3$**	**[26]**
1.53	25.2	1174	26.2	81.8	α-$FAPbI_3$	[2] a)
1.53	25.4	1174	26.4	81.9	$FAPbI_3$	[3]
1.53	25.5	1189	25.7	83.2	a, c)	[2]
1.54	**24.4**	**1159**	**25.6**	**82.1**	**a, c)**	**[6]**
1.54	**26.0**	**1190**	**26.0**	**84.0**	**a, c)**	**[6]**
1.54	24.6	1181	26.2	79.6	$FAPbI_3$	[2] a)
1.54	25.6	1182	26.2	82.6	$FAPbI_3$: $(PbI_2)_2RbCl$	[3] a)
1.54	**25.2**	**1138**	**26.1**	**84.9**	**$Cs_{0.05}FA_{0.9}MA_{0.05}PbI_3$**	**[61]**
1.54	24.3	1141	25.7	82.6	$Cs_{0.03}FA_{0.97}Pb\ Br_{0.09}I_{2.91}$	[3]
1.54	25.7	1179	25.8	84.5	a, c)	[3]
1.55	**22.9**	**1176**	**24.3**	**80.1**	**$Cs_{0.05}FA_{0.931}MA_{0.19}PbBr_{0.06}I_{2.94}$**	**[38] d)**
1.55	**24.6**	**1177**	**24.8**	**84.3**	**$Cs_{0.05}FA_{0.931}MA_{0.19}PbBr_{0.06}I_{2.94}$**	**[38]**
1.55	**24.6**	**1121**	**25.7**	**85.5**	**$CsPbBr_3$:$FAPbI_3$**	**[62] a)**
1.55	**24.8**	**1190**	**25.5**	**81.6**	**$FAPbI_3$**	**[63]**
1.55	**25.1**	**1123**	**25.7**	**86.9**	**$CsPbBr_3$:$FAPbI_3$**	**[62]**
1.55	24.1	1158	25.3	82.3	$FA_{0.95}MA_{0.05}PbBr_{0.15}I_{2.85}$	[3]
1.56	**25.2**	**1201**	**24.8**	**84.5**	**$Cs_{0.05}FA_{0.9025}MA_{0.0475}PbBr_{0.15}I_{2.85}$**	**[27]**
1.56	**25.1**	**1209**	**24.7**	**83.9**	**$Cs_{0.05}FA_{0.9025}MA_{0.0475}PbBr_{0.15}I_{2.85}$**	**[27] a)**
1.56	25.1	1195	24.9	84.4	$FA_{0.995}MA_{0.005}PbBr_{0.015}I_{0.985}$	[3]
1.56	25.2	1180	24.1	84.8	a, c)	[2]
1.56	25.2	1181	25.1	84.8	$FAMAPb(I,Br,Cl)_3$	[2] a)
1.56	25.3	1193	25.1	84.6	$FAMAPb(I,Br,Cl)_3$	[2]
1.57	**24.4**	**1190**	**25.6**	**80.2**	**$FAPb(I,Cl)_3$**	**[64]**
1.57	**23.6**	**1179**	**24.3**	**82.4**	**$FAPb(I,Cl)_3$**	**[64] a)**
1.57	**23.1**	**1170**	**23.8**	**82.7**	**$Cs_{0.05}\ FA_{0.9025}MA_{0.475}PbBr_{0.15}I_{2.85}$**	**[65]**
1.57	23.0	1170	24.1	81.6	$Cs_{0.05}FA_{0.88}MA_{0.07}PbBr_{0.24}I_{2.76}$	[2]
1.57	23.0	1147	25.1	79.9	$FA_{0.95}MA_{0.05}PbBr_{0.15}I_{2.85}$	[3] a)
1.57	23.4	1153	25.2	80.6	$Cs_{0.05}FA_{0.75}MA_{0.15}Rb_{0.05}PbBr_{0.15}I_{2.85}$	[3]

1.58	22.9	1173	23.4	80.0	$Cs_{0.05}FA_{0.9}MA_{0.05}PbBr_{0.26}I_{2.74}$	[3]
1.58	22.6	1186	24.2	78.6	$FA_{0.92}MA_{0.08}PbBr_{0.24}I_{2.76}$	[2] a)
1.58	22.6	1178	22.73	84.4	a, c)	[2]
1.59	**22.1**	**1160**	**23.1**	**82.4**	**$Cs_{0.05}FA_{0.8}MA_{0.15}PbBr_{0.3}I_{2.7}$**	**[66]**
1.59	21.1	1086	24.0	81.0	$MACu_{0.05}Pb_{0.9}Sn_{0.05}Br_{0.1}I_{2.9}$	[2]
1.59	21.0	1140	23.7	77.7	$FA_{0.85}MA_{0.15}PbBr_{0.45}I_{2.55}$	[2] a)
1.60	**22.0**	**1175**	**22.8**	**82.2**	**$Cs_{0.05}FA_{0.874}MA_{0.076}PbBr_{0.18}I_{2.76}$**	**[67]**
1.60	21.9	1192	22.8	80.6	$GA(MA)_5Pb_5I_{16}$	[3]
1.60	21.9	1131	23.1	83.7	$CsMAFAPbI_3$:PPP	[2]
1.60	20.3	1130	23.2	77.4	$MAPbI_{3-x}Cl_x$	[2] a)
1.61	21.4	1120	23.1	82.9	$MAPbI_3$	[2] b)
1.61	21.5	1192	21.6	83.6	$Cs_{0.05}FA_{0.88}MA_{0.07}PbBr_{0.44}I_{2.56}$	[2] a)
1.61	23.2	1240	22.1	84.5	$Cs_{0.05}FA_{0.88}MA_{0.07}PbBr_{0.44}I_{2.56}$	[2]
1.61	22.6	1200	24.0	78.5	$Cs_{0.07}FA_{0.765}MA_{0.135}Rb_{0.03}PbBr_{0.45}I_{2.55}$	[2]
1.62	21.7	1180	22.5	81.7	$MAPbI_3$-DAP	[2]
1.63	20.3	1130	23.4	76.8	$Cs_{0.05}FA_{0.76}MA_{0.19}PbBr_{0.6}I_{2.4}$	[2]
1.64	22.4	1130	23.7	83.8	$Cs_{0.05}MA_{0.1425}FA_{0.8075}PbBr_{0.45}I_{2.55}$	[3]
1.64	20.4	1140	23.6	75.8	$Cs_{0.05}FA_{0.79}MA_{0.16}PbBr_{0.51}I_{2.49}$	[2]
1.65	**21.8**	**1218**	**21.5**	**83.2**	**$Cs_{0.15}FA_{0.8}MA_{0.05}PbBr_{0.54}I_{2.46}$**	**[68]**
1.65	**18.6**	**1181**	**20.7**	**76.0**	**$Cs_{0.15}FA_{0.8}MA_{0.05}PbBr_{0.54}I_{2.46}$**	**[68] b)**
1.65	21.9	1230	21.2	84.0	$Cs_{0.1}FA_{0.2}MA_{0.7}PbBr_{0.45}I_{0.2.55}$	[3]
1.65	16.2	1109	19.6	74.2	$MAPbBr_xI_{1-x}$	[2] a)
1.66	10.4	904	16.3	70.4	$MAPbBr_{0.39}I_{2.51}$	[2]
1.67	17.9	1190	18.4	81.9	$(PEA)_2(MA)_3Pb_4I_{13}$:$NH_4I_{0.2}Cl_{0.8}$	[2]
1.68	20.7	1220	21.3	79.7	$Cs_{0.05}MA_{0.15}FA_{0.8}PbBr_{0.75}I_{2.25}$	[2]
1.69	**20.7**	**1220**	**20.6**	**82.1**	**$CsPbI_3$**	**[69]**
1.70	**21.6**	**1220**	**21.7**	**81.5**	**$CsPbI_3$**	**[70]**
1.70	**18.8**	**1193**	**20.7**	**76.2**	**$CsPbI_3$**	**[70] b)**
1.70	**21.2**	**1244**	**20.6**	**82.5**	**$CsPbI_3$**	**[71]**
1.70	**20.3**	**1230**	**20.3**	**81.5**	**$CsPbI_3$**	**[72]**
1.70	20.2	1176	20.8	82.5	$CsPbI_3$	[3]
1.70	16.9	1170	20.2	71.5	$Cs_{0.2}FA_{0.8}PbBr_{0.75}I_{2.25}$	[2]
1.71	14.6	1056	17.5	79.0	$CsPbI_3$	[2]
1.72	18.6	1244	19.2	77.9	$Cs_{0.83}FA_{0.17}PbBr_{0.8}I_{2.2}$	[2]
1.72	18.3	1350	17.6	77.0	$MAPbBr_{0.6}I_{2.4}$	[2]
1.72	17.1	1200	19.4	73.5	$Cs_{0.17}FA_{0.83}PbBr_{1.2}I_{1.8}$	[2]
1.74	18.3	1269	18.9	76.3	$Cs_{0.095}MA_{0.1425}FA_{0.7125}Rb_{0.05}PbBrI_2$	[2]
1.74	**20.0**	**1274**	**18.2**	**86.3**	**$Cs_{0.16}FA_{0.80}MA_{0.04}PbBr_{0.96}I_{2.04}$**	**[73]**
1.74	20.2	1210	19.3	86.5	$Cs_{0.2}FA_{0.8}PbBr_{0.9}I_{2.1}$	[3]
1.75	19.8	1310	19.4	78.0	$Cs_{0.17}FA_{0.83}PbBr_{1.2}I_{1.8}$	[2]
1.76	18.5	1210	20.0	76.4	$Cs_{0.05}FA_{0.79}MA_{0.16}PbBr_{1.2}I_{1.8}$	[2]
1.77	18.6	1234	18.3	82.5	$CsPbBr_xI_{3-x}$	[2]
1.78	**18.4**	**1272**	**17.6**	**82.0**	**$FA_{0.8}Cs_{0.2}PbBr_{1.14}I_{1.86}$**	**[42]**
1.78	**18.0**	**1230**	**18.0**	**81.4**	**$CsPbBr_xI_{3-x}$**	**[49]**
1.79	**19.3**	**1330**	**17.3**	**83.9**	**$Cs_{0.2}FA_{0.8}PbBr_{1.2}I_{1.8}$**	**[74] a)**

1.79	19.0	1250	19.0	80.0	$Cs_{0.12}FA_{0.83}MA_{0.05}PbBr_{1.2}I_{1.8}$	[2]
1.79	17.7	1255	17.4	81.1	$Cs_{0.4}DMA_{0.1}FA_{0.5}PbBr_{0.71}Cl_{0.15}I_{2.14}$	[3]
1.79	**16.9**	**1270**	**16.2**	**82.3**	**$Cs_{0.15}FA_{0.85}PbBr_{1.2}I_{1.8}$**	**[75]**
1.79	**16.6**	**1175**	**18.0**	**78.4**	**$Cs_{0.2}FA_{0.8}PbBr_{1.2}I_{1.8}$**	**[76]**
1.79	17.6	1230	18.0	79.5	$Cs_{0.3}FA_{0.7}PbBr_{1.2}I_{1.8}$	[77] a)
1.80	**19.1**	**1274**	**17.7**	**84.5**	**$Cs_{0.2}FA_{0.8}PbBr_{1.2}I_{1.8}$**	**[78]**
1.81	16.3	1220	17.0	78.6	$Cs_{0.4}FA_{0.6}PbBr_{1.05}I_{1.95}$	[2]
1.82	17.2	1266	16.8	80.9	$Cs_{0.35}FA_{0.65}PbBr_{1.2}I_{1.8}$	[3]
1.83	16.9	1240	16.9	80.7	$FA_{0.6}MA_{0.4}PbBr_{1.2}I_{1.8}$	[3]
1.84	15.2	1260	15.6	77.3	$Cs_{0.2}FA_{0.8}PbBr_{1.2}I_{1.8}$-DAP	[2]
1.85	15.0	1296	15.6	74.2	$Cs_{0.17}FA_{0.83}PbBr_{1.5}I_{1.5}$	[2]
1.86	17.0	1340	15.9	79.8	$CsPbBr_{0.75}I_{2.25}$-0.5FAOAc	[2]
1.87	14.0	1280	14.0	78.1	$CsBa_{0.2}Pb_{0.8}BrI_2$	[2]
1.87	13.7	1220	14.6	76.8	$CsEu_{0.05}Pb_{0.95}BrI_2$	[2]
1.88	17.4	1420	15.0	81.4	$CsPbBrI_2$	[3]
1.88	15.9	1300	15.5	79.1	$CsPbBrI_2$	[2]
1.88	15.3	1250	15.4	79.0	$CsPbBrI_2$	[2]
1.89	16.0	1310	15.8	77.5	$CsPbBrI_2$	[2]
1.89	15.6	1300	15.3	78.3	$CsPbBr(Ac)_xI_{2-x}$	[2]
1.90	15.0	1240	16.0	75.6	$InCl_3$:$CsPbI_2Br$	[2] a)
1.90	**16.5**	**1242**	**16.3**	**81.3**	**$CsPbBrI_2$**	**[79]**
1.90	16.1	1320	15.3	79.7	$CsPbBrI_2$	[2]
1.90	14.5	1300	14.3	78.1	$CsPbBrI_2$	[80]
1.90	**14.7**	**1302**	**14.2**	**79.6**	**$CsPbBrI_2$**	**[81]**
1.90	**14.0**	**1269**	**14.9**	**73.8**	**$CsPbBrI_2$**	**[82]**
1.91	**14.5**	**1300**	**14.3**	**77.8**	**$CsPbBrI_2$**	**[83]**
1.91	14.4	1312	15.6	70.1	$Cs_{0.83}FA_{0.17}PbBr_{1.8}I_{1.2}$	[2]
1.91	14.2	1160	15.7	77.9	$CsPbBrI_2$	[2]
1.91	2.0	620	5.4	60.8	$MA_3Sb_2I_9$+HI	[2] b)
1.94	13.4	1240	14.2	76.0	$CsPbBr_{1.2}I_{1.8}$	[3]
1.98	8.3	1080	12.3	62.0	$CsPbBr_2I$	[2]
1.99	**13.4**	**1312**	**13.4**	**76.3**	**$Cs_{0.85}Rb_{0.15}PbBr_{1.25}I_{1.75}$**	**[39]**
2.00	9.6	1185	11.2	72.3	$Cs_{0.15}FA_{0.85}PbBr_{2.1}I_{0.9}$	[2]
2.03	2.8	836	6.4	52.7	$MAPbBr_{1.77}I_{1.23}$	[2]
2.04	10.3	1340	9.7	79.2	$MAPb(I_{0.3}Br_{0.7})_xCl_{3-x}$	[2]
2.05	6.1	1450	5.4	77.1	$MAPbBr_2I$	[2]
2.09	10.2	1270	11.5	69.4	$CsPbBr_2I$	[2]
2.10	10.7	1261	11.8	72.0	$CsPbBr_2I$	[2]
2.11	9.2	1200	10.2	74.6	GAI-DEE-$CsPbBr_2I$	[2]
2.20	8.9	1639	7.7	70.6	$FAPbBr_3$	[3]
2.27	10.6	1552	8.9	76.5	$FAPbBr_3$	[2]
2.28	10.5	1520	8.3	83.0	$CsPbBr_3$	[3]
2.29	10.2	1650	8.7	71.1	$MAPbBr_3$	[3]
2.30	**11.2**	**1574**	**8.5**	**83.7**	**$CsPbBr_3$**	**[84]**
2.31	9.7	1458	8.1	81.9	$CsPbBr_3$	[2]

2.32	10.1	1653	7.7	79.1	$MAPbBr_3$	[2]
2.33	8.5	1580	6.6	82.0	$CsPbBr_3$	[2]
2.33	8.2	1470	7.3	76.1	$CsPbBr_3$	[2]
2.34	10.7	1635	7.8	84.1	$CsPbBr_3$	[3]
2.34	10.1	1602	7.9	80.0	$CsPbBr_3$	[2]
2.34	9.7	1584	7.4	82.8	$CsPbBr_3$	[2]
2.35	10.7	1622	7.9	83.5	$CsPbBr_3$	[2]
2.35	10.6	1610	7.8	84.4	$CsSnBr_3$	[2]
2.35	10.2	1611	7.8	81.0	$CsPbBr_3$	[3]
2.36	10.3	1570	8.2	79.6	$CsPb_{0.97}Tb_{0.03}Br_3$	[3]
2.36	4.0	1130	5.5	63.6	$CsPbBr_{2.9}I_{0.1}$	[2]
2.37	2.2	690	5.0	63.5	$MA_3Sb_2Cl_xI_{9-x}$	[2]
2.38	8.1	1490	6.9	78.8	$CsPbBr_3$	[2]
2.41	2.7	1020	5.2	51.2	$Cs_2AgBiBr_6$	[2]
2.42	1.1	870	2.9	43.0	$BdAPbI_4$	[2]
2.43	2.8	820	5.7	60.3	$CsPb_2Br_5$	[2]
2.44	2.4	1140	3.4	60.9	$FAPbBr_{2.1}Cl_{0.9}$	[2]
2.45	2.9	1010	4.1	70.9	$Cs_2AgBiBr_6$	[2]
2.46	1.7	1060	3.9	40.2	$Cs_2AgBiBr_6$	[2]
2.47	3.3	1278	3.3	77.5	$Cs_2AgBiBr_6$	[3]
2.48	1.4	1060	2.5	52.0	$FAPbBr_2Cl$	[2]

[a] Certified power conversion efficiency; [b] Notable exception included as a material and/or large area highlight; [c] Notable exception included as a *PCE* highlight without the absorber information; [d] PCE from *J-V* with significant hysteresis and MPP tracking closer to the listed value; sc, single crystal.

Table 5. Single-junction **organic** research solar cells with the highest efficiency: performance parameters as a function of device absorber bandgap energy (from the EQE spectrum).

E_g [eV]	PCE [%]	V_{oc} [mV]	J_{sc} [mA cm^{-2}]	FF [%]	Absorber blend	Ref.
1.22	13.4	663	30.0	67.1	BTB7-Th:ATT-9	[3]
1.32	13.0	916	20.2	70.1	BTR:Y6:bis$PC_{71}BM$	[3]
1.32	10.6	690	24.3	63.2	PTB7-Th:IEICO-4F	[2]
1.33	13.9	865	22.4	71.4	BTR:MeIC:Y11	[3]
1.34	12.8	712	27.3	65.9	PTB7-Th:IEICO-4F	[2]
1.35	**19.3**	**870**	**28.6**	**77.9**	**PM6:BTP-eC9:L8-BO**	**[85]**
1.35	17.0	804	27.2	76.4	PM6:mBzS-4F	[2]
1.35	15.9	820	26.3	73.4	PM6:Y6	[2]
1.36	15.9	846	25.4	74.1	PM6:Y11	[2]a)
1.36	**18.3**	**840**	**27.4**	**79.4**	**D18:NFAs**	**[86]**
1.37	18.3	856	26.9	79.4	PM6:BTP-eC9:$PC_{71}BM$	[2]
1.38	**18.9**	**880**	**26.9**	**79.8**	**PBDB-TCl:AITC:BTP-eC9**	**[43] a)**

1.38	**19.1**	**880**	**26.9**	**80.7**	**PBDB-TCl:AITC:BTP-eC9**	**[43]**
1.38	**19.1**	**853**	**27.8**	**80.5**	**PM6:BTP-eC9**	**[87]**
1.38	**18.2**	**840**	**27.5**	**78.6**	**PM6:eC9**	**[88]**
1.38	18.2	857	27.4	77.6	PM6:BTP-T-3Cl:BTP-4Cl-BO	[3]
1.38	18.8	861	27.5	79.4	PM6:BTP-eC9:BTP-S9	[3]
1.38	18.7	853	27.4	80.0	PM6:BTP-eC9:L8-BO-F	[3]
1.38	18.2	847	27.3	78.8	PM6:BTP-eC9:L8-BO-F	[3] a)
1.38	18.7	862	27.4	79.3	PM6:BTP-eC9:BTP-S9	[3] a)
1.39	**19.1**	**858**	**28.0**	**79.5**	**PM6:BTP-eC9:LA23**	**[89]**
1.39	**18.5**	**858**	**27.6**	**77.8**	**PM6-T:BTPeC9**	**[90]**
1.39	18.1	848	27.5	77.5	PM6:Y6-1O:BO-4Cl	[3] a)
1.39	18.2	859	27.7	76.6	D18:Y6	[2] a)
1.39	18.2	863	27.1	77.9	PM6:BTP-eC9:ZY-4Cl	[3] a)
1.39	18.5	855	27.5	78.9	PM6:Y6-1O:BO-4Cl	[3]
1.39	18.7	863	27.4	79.0	PM6:BTP-eC9:ZY-4Cl	[3]
1.40	**19.3**	**861**	**27.9**	**80.4**	**PM6:BTP-eC9**	**[50]**
1.40	**18.9**	**859**	**27.9**	**79.2**	**PM6:BTP-eC9**	**[50] a)**
1.40	19.1	869	27.5	79.9	PBDB-TF:L8-BO:BTP-eC9	[3] a)
1.40	19.4	863	27.6	81.2	PBDB-TF:L8-BO:BTP-eC9	[3]
1.40	18.4	871	26.8	79.1	PM6:AC9	[3]
1.40	**14.0**	**880**	**24.4**	**65.3**	**PBNT-TzTz:Y6-BO**	**[37] b)**
1.40	18.3	845	27.5	78.8	PTzBI-dF:BTP-TBr	[3]
1.41	**19.5**	**886**	**27.2**	**81.1**	**PBQx-TCl:PBDB-TF:eC9-2Cl**	**[33]**
1.41	**19.2**	**879**	**27.2**	**80.3**	**PBQx-TF:eC9-2Cl**	**[28]**
1.41	**19.0**	**877**	**27.1**	**79.8**	**PBQx-TF:eC9-2Cl**	**[28] a)**
1.41	17.6	871	26.4	76.8	D18-Cl:PM6:Y6	[2]
1.41	18.1	860	26.5	79.4	PM6:PB2F:BTP-eC9	[3]
1.41	19.0	879	26.7	81.0	PBQx-TF:eC9-2Cl:F-BTA3	[3]
1.41	18.7	878	26.8	79.4	PBQx-TF:eC9-2Cl:F-BTA3	[3] a)
1.41	**17.7**	**859**	**26.8**	**76.8**	**PM6:Y6/PBB-TSD**	**[91]**
1.42	**16.8**	**830**	**26.6**	**76.1**	**PM6:Y6**	**[85]**
1.42	**16.6**	**919**	**25.1**	**72.0**	**PBDB-T:PTz-BO:PTz-C11**	**[92]**
1.42	15.6	838	25.0	74.4	a, c)	[2]
1.43	18.2	880	25.9	80.1	PM6:BTP-4F-P2EH	[3]
1.43	**18.2**	**914**	**25.7**	**77.4**	**PM6:PY-1S1Se:PY-2Cl**	**[51] a)**
1.43	**18.2**	**914**	**25.7**	**77.2**	**PM6:PY-1S1Se:PY-2Cl**	**[51]**
1.43	**18.2**	**931**	**24.5**	**79.8**	**PBQx-TF:PBDB-TF:PY-IT**	**[93]**
1.44	**19.2**	**914**	**26.6**	**79.0**	**a, b)**	**[6]**
1.44	16.1	955	22.7	74.3	PM6:PY-IT:BN-T	[2]
1.44	18.6	893	26.0	80.0	PM6:L8-BO	[3]
1.44	18.2	883	26.1	79.0	PM6:L8-BO	[3] a)
1.45	**19.5**	**905**	**27.2**	**79.6**	**PBTz-F:PM6:L8-BO**	**[94]**
1.45	19.6	896	26.7	81.9	PM6:D18:L8-BO	[3]
1.45	19.1	918	26.9	77.3	D18:L8-BO	[3]
1.45	19.2	891	26.7	80.7	PM6:D18:L8-BO	[3] a)

1.46	18.2	897	25.7	78.9	[c]	[2] a)
1.46	16.8	949	23.7	74.4	PM6:PY-DT	[3]
1.47	14.6	882	23.1	71.7	PBDB-T-2Cl:BP-4F:MF1	[2]
1.48	12.4	880	20.8	67.7	PBDB-T:IDT-EDOT:$PC_{71}BM$	[2]
1.50	15.4	920	22.6	74.1	PM6:DTTC-4Cl	[2]
1.51	13.3	780	22.9	75.0	PM6:SeTIC4Cl-DIO	[2]
1.52	10.4	850	18.0	68.0	PBDB-T:IDT-EDOT:$PC_{71}BM$	[2]
1.53	10.7	850	22.2	56.7	PM6:SeTIC4Cl	[2]
1.54	13.6	940	19.5	73.8	BTR:NITI:$PC_{71}BM$	[2]
1.55	12.0	840	19.5	73.3	PM6:IT-4F	[2]
1.56	12.1	826	20.9	70.1	PM6:IT-4F	[2]
1.58	13.9	950	21.7	67.4	PM6:DTTC-4F	[2]
1.58	13.5	880	20.6	74.53	PBDB-T-SF:IT-4F	[2]
1.61	13.4	940	20.2	70.5	PM6:DTC-4F	[2]
1.61	12.1	916	18.1	73.0	PBDB-T-2Cl:MF1	[2]
1.62	11.0	793	19.4	71.5	[a, c]	[2]
1.62	12.2	930	17.5	75.0	PTQ10:IDTPC	[2]
1.63	12.8	910	19.1	73.6	PTQ10:IDIC-2F	[2]
1.64	12.9	960	17.4	71.3	PTQ10:IDIC	[2]
1.65	**10.4**	**910**	**16.2**	**70.6**	**PBDB-T:ITIC**	**[95]**
1.66	12.1	815	20.3	73.2	[a, c]	[2]
1.67	11.2	1080	16.3	63.6	PvBDTTAZ:O-IDTBR	[96]
1.67	11.5	791	19.7	73.7	[a, c]	[2]
1.68	12.0	1030	18.5	63.0	PBDTTT-EFT:EHIDTBR	[2]
1.69	8.9	878	13.9	72.9	PBT1-C:NFA	[2]
1.70	11.1	867	17.8	71.9	[a, c]	[2]
1.72	10.0	899	16.8	66.4	[a, c]	[2]
1.76	9.6	786	17.0	72.0	PPDT2FBT:$PC_{70}BM$	[2]
1.79	7.5	1140	10.6	62.1	BDT-ffBX-DT:PDI4	[2]
1.79	6.2	1230	8.9	56.6	BDT-ffBX-DT:SFPDI	[2]
1.85	9.0	900	13.8	72.9	BTR:$PC_{71}BM$	[2]
1.85	7.6	830	13.3	69.1	PBDB-T:$PC_{71}BM$	[2]
1.86	7.4	940	12.7	61.9	PBDB-T:NDP-Se-DIO	[2]
1.88	5.7	950	10.7	55.9	PBDB-T-2Cl:PC61BM	[2]
1.93	6.3	790	12.2	65.3	P3HT:TCBD14	[2]
2.01	3.7	592	10.4	59.2	P3HT:PCBM	[2]

[a] Certified power conversion efficiency; [b] Notable exception included as a large area highlight; [c] Notable exception included as a *PCE* highlight without the absorber information

Table 6. Single-junction dye sensitized research solar cells with the highest efficiency: performance parameters as a function of device absorber bandgap energy (from the *EQE* spectrum).

E_g [eV]	PCE [%]	V_{oc} [mV]	J_{sc} [mA cm^{-2}]	FF [%]	Sensitizing dye	Ref.

1.44	11.0	714	21.9	70.3	a,b)	[2]
1.52	11.4	743	21.3	71.9	a,b)	[2]
1.59	10.1	710	18.5	76.9	TF-tBu_C_3F_7	[2]
1.66	13.0	910	18.1	78.0	SM315	[3]
1.66	10.7	849	16.6	75.9	bJS2	[2]
1.72	**4.2**	**503**	**12.7**	**64.9**	**NP2**	**[97]**
1.74	7.8	694	15.4	72.7	YD2	[2]
1.75	10.9	745	20.7	70.8	YKP-88/YKP-137 (6/4)	[2]
1.76	12.0	960	15.9	79.0	SM371	[3]
1.77	10	740	18.1	74.7	N719	[2]
1.79	9.9	740	19.0	70.5	PI-COF:N719	[3]
1.80	9.1	744	19.0	64.0	N719	[2]
1.80	9.0	790	19.8	57.2	N719	[2]
1.80	6.5	663	13.3	74.5	SK7	[2]
1.81	8.5	700	19.4	62.6	N719	[3]
1.82	6.4	680	13.1	71.8	AN-11	[2]
1.83	15.2	1063	18.0	79.4	SL9 + SL10 /BPHA	[3] a)
1.83	8.9	820	19.0	57.5	N719	[2]
1.85	12.3	1020	15.2	79.1	a, b)	[2]
1.85	**13.4**	**1040**	**15.6**	**80.4**	**a, b)**	**[6]**
1.86	8.3	782	14.8	71.7	N719	[2]
1.87	9.1	1060	11.2	76.7	L351	[2]
1.88	7.8	730	14.3	74.7	TY4	[2]
1.90	**11.6**	**0.946**	**16.9**	**72.9**	**ZL004**	**[98]**
1.93	11.2	1140	13.0	75.6	L350	[2]
1.97	3.0	600	6.3	79.4	AN-14	[2]
1.99	5.4	689	11.3	69.5	SK6	[2]
2.00	6.3	732	12.0	71.7	CW10+SK6	[2]
2.01	9.2	1160	11	72.1	L349	[2]
2.02	8.1	760	14.3	75.0	TY6	[2]
2.05	3.9	680	7.4	77.5	AN-12	[2]
2.09	6.9	780	11.6	76.3	TY3	[2]
2.12	5.8	739	10.8	72.7	CW10	[2]
2.15	4.1	640	8.76	73.6	PS1	[3]
2.23	5.8	760	10.2	74.8	MS3	[2]
2.32	5.3	1170	6.4	70.8	L348	[2]

[a] Certified power conversion efficiency; [b] Notable exception included as a *PCE* highlight without the absorber information

Table 7. Single-junction research solar cells with the highest efficiency: performance parameters as a function of device absorber bandgap energy (from the EQE spectrum) among several **inorganic emerging** technologies.

E_g [eV]	PCE [%]	V_{oc} [mV]	J_{sc} [mA cm^{-2}]	FF [%]	Absorber material/ technology	Ref.
0.98	11.2	430	39.2	66.8	$Cu_2ZnSn(Se,S)_4$	[2]

1.02	11.6	441	39.2	67.4	$Cu_2ZnSnSe_4$	[2]
1.03	11.6	423	40.6	67.3	$Cu_2ZnSnSe_4$	[2] a)
1.04	9.6	425	34.9	64.5	$Cu_2ZnSnSe_4$	[2]
1.05	9.4	457	32.5	63.3	$Cu_2ZnSnSe_4$	[2]
1.06	9.5	460	31.1	66.4	$Cu_2ZnSnSe_4$	[2]
1.06	13.2	477	40.1	69.0	$Cu_2ZnSn(S,Se)_4$	[2]
1.06	12.7	461	40.4	68.3	$Cu_2ZnSn(S,Se)_4$	[2] a)
1.07	12.5	491	37.4	68.2	$Cu_2ZnSnSe_4$	[2] a)
1.07	**12.1**	**538**	**35.3**	**63.7**	**$Cu_2ZnSn(S,Se)_4$**	**[6] a)**
1.08	**13.8**	**546**	**36.3**	**69.4**	**$Cu_2ZnSn(S,Se)_4$**	**[29] a)**
1.08	**14.1**	**551**	**35.7**	**71.8**	**$Cu_2ZnSn(S,Se)_4$**	**[29]**
1.08	12.4	522	33.3	71.3	$Cu_2ZnSn(S,Se)_4$	[2]
1.09	**14.9**	**555**	**36.9**	**72.7**	**$Cu_2ZnSn(S,Se)_4$**	**[6] a)**
1.09	12.2	475	37.2	68.8	$Cu_2ZnSn(S,Se)_4$	[2]
1.09	12.5	540	32.1	72.1	$(Ag,Cu)_2ZnSn(S,Se)_4$	[2]
1.10	13.6	538	36.2	69.9	$Cu_2ZnSn(S,Se)_4$	[3]
1.11	13.1	547	34.3	70.0	$Cu_2ZnSn(S,Se)_4$	[3]
1.11	12.8	526	35.3	68.9	$Cu_2ZnSn(S,Se)_4$	[3] a)
1.12	**12.1**	**494**	**36.2**	**67.5**	**$Cu_2ZnSn(S,Se)_4$**	**[99] a)**
1.12	12.3	527	32.3	72.3	$Cu_2Zn(Sn_{0.78}Ge_{0.22})Se_4$	[2]
1.13	12.6	513	35.2	69.8	$Cu_2ZnSn(S,Se)_4$	[2] a)
1.13	11.1	460	34.5	69.8	$Cu_2ZnSn(S,Se)_4$	[2] a)
1.14	**12.2**	**470**	**37.2**	**69.9**	**$Cu_2ZnSn(S,Se)_4$**	**[100]**
1.14	12.6	541	35.4	65.9	$Cu_2ZnSn(S,Se)_4$	[2] a)
1.15	**10.3**	**522**	**28.9**	**68.5**	**$Cu_2ZnSn(S,Se)_4$**	**[101] a)**
1.16	11.2	539	33.1	62.8	$Cu_2ZnSn(S,Se)_4$	[2]
1.16	**12.9**	**546**	**35.9**	**65.8**	**$Cu_2ZnSn(S,Se)_4$**	**[102] b)**
1.16	**11.8**	**498**	**36.3**	**66.5**	**$Cu_2ZnSn(S,Se)_4$**	**[103] b)**
1.19	**9.8**	**537**	**32.6**	**56.3**	**$Cu_2ZnSn(S,Se)_4$**	**[104]**
1.22	7.5	413	28.9	62.4	Sb_2Se_3	[2]
1.23	**10.6**	**467**	**33.5**	**67.6**	**Sb_2Se_3**	**[105] b)**
1.24	9.2	400	32.6	70.6	Sb_2Se_3	[2]
1.27	4.8	370	27.3	47.3	Sb_2Se_3	[2]
1.29	4.0	340	22.9	51.0	Sb_2Se_3	[2]
1.31	7.3	420	29.2	59.7	Sb_2Se_3	[2]
1.33	8.6	520	27.8	59.8	Sb_2Se_3	[3]
1.35	**10.1**	**551**	**26.0**	**70.1**	**$Sb_2(S,Se)_3$**	**[106]**
1.37	7.1	480	24.7	60.0	$AgBiS_2$	[3]
1.39	8.9	482	26.8	68.5	$AgBiS_2$	[3] a)
1.39	9.2	495	27.1	68.4	$AgBiS_2$	[3]
1.41	6.3	450	22.1	63.0	$AgBiS_2$	[107]
1.48	**10.8**	**631**	**25.3**	**67.4**	**$Sb_2(S,Se)_3$**	**[30]**
1.45	8.5	625	24.4	55.7	$Cu_2ZnGeSe_4$	[3]
1.50	11.0	731	21.7	69.3	Cu_2ZnSnS_4	[2] a)
1.50	10.0	655	24.1	63.3	$Sb_2(S,Se)_3$	[3] a)

1.52	8.7	664	20.6	63.9	$(Cu_{0.99}Ag_{0.01})_{1.85}(Zn_{0.8}Cd_{0.2})_{1.1}SnS_4$	[2]
1.53	**8.5**	**670**	**20.4**	**62.1**	**$Sb_2(S,Se)_3$**	**[108]**
1.54	10.7	673	23.7	66.8	$Sb_2(S,Se)_3$	[3]
1.54	9.7	638	23.2	65.5	$Sb_2(S,Se)_3$	[3]
1.55	10.2	736	21.0	65.8	Cu_2ZnSnS_4	[109]
1.55	10.5	664	23.8	66.3	$Sb_2(S,Se)_3$	[3]
1.59	**11.4**	**746**	**21.8**	**70.1**	**Cu_2ZnSnS_4**	**[6] a)**
1.73	8.0	757	60.5	17.4	Sb_2S_3	[3]
1.80	7.5	711	16.1	65.0	Sb_2S_3	[2]
1.84	**4.9**	**680**	**13.7**	**53.0**	**Sb_2S_3**	**[110]**
1.95	**5.8**	**870**	**10.8**	**62.1**	**Se**	**[36]**
1.97	**5.2**	**991**	**10.0**	**52.4**	**Se**	**[111]**

[a] Certified power conversion efficiency; [b] Notable exception included missing the aperture/mask area information

Table 8. Single-junction research solar cells with the highest efficiency: performance parameters as a function of device absorber bandgap energy (from the EQE spectrum) among **established** technologies.

E_g [eV]	PCE [%]	V_{oc} [mV]	J_{sc} [mA cm^{-2}]	FF [%]	Absorber material/ technology	Ref.
1.09	19.8	716	34.9	79.2	CIGS	[2] a)
1.10	21.7	718	40.7	74.3	CIGS	[2] a)
1.11	**26.7**	**751**	**41.2**	**86.5**	**Si**	**[32] a)**
1.11	26.7	738	42.7	84.9	Si	[2] a)
1.13	22.9	744	38.8	79.5	CIGS	[2] a)
1.13	**23.6**	**767**	**38.3**	**80.5**	**CIGS**	**[6] a)**
1.14	21.0	757	35.7	77.6	CIGS	[2] a)
1.15	23.4	734	39.6	80.4	CIGS	[2] a)
1.18	20.0	706	40.7	69.7	Si	[3]
1.30	16.3	762	31.4	68.1	CIGS	[2]
1.40	**22.3**	**898**	**31.7**	**78.9**	**CdTe**	**[6] a)**
1.42	29.1	1127	29.8	86.7	GaAs	[2] a)
1.42	21.0	876	30.3	79.4	CdTe	[2] a)
1.48	18.3	857	27.0	77.0	CdTe	[2] a)
1.60	15.2	902	23.1	73	CIGS	[2]
1.60	10.2	896	16.4	69.8	Si (amorphous)	[2] a)
1.69	10.6	896	16.1	75.6	Si (amorphous)	[2]
1.85	10.1	886	16.8	67.0	Si (amorphous)	[2] a)

[a] Certified power conversion efficiency

Table 9. Monolithic **multijunction perovskite**-based research solar cells with the highest efficiency: performance parameters as a function of the device bandgap energies (from the EQE spectra) of the sub-cells.

$E_{g,bottom}$ [eV]	$E_{g,middle}$, $E_{g,top}$ [eV]	PCE [%]	V_{oc} [mV]	J_{sc} [mA cm^{-2}]	FF [%]	Bottom absorber material	Middle, top absorber material(s)	Ref.

							Si/perovskite	
1.11	1.63	24.1	1786	19.5	69.1	Si	$Cs_xFA_{1-x}Pb(I,Br)_3$	[2]
1.11	1.66	26.0	1820	19.2	75.4	Si	$Cs_{0.1}MA_{0.9}PbBr_{0.3}I_{2.7}$	[2]
1.11	**1.67**	**33.7**	**1974**	**21.0**	**81.3**	**Si**	**a, b)**	**[6]**
1.11	**1.67**	**29.8**	**1920**	**19.5**	**79.4**	**Si**	**$Cs_{0.209}FA_{0.741}MA_{0.05}PbBr_{0.4275}Cl_{0.15}I_{2.4225}$**	**[40]**
1.11	1.67	26.7	1756	19.2	79.2	Si	$FA_{0.65}MA_{0.2}Cs_{0.15}PbBr_{0.6}I_{2.4}$:PEA($I_{0.25}SCN_{0.75}$)	[2]
1.11	1.68	25.7	1781	19.1	75.4	Si	$Cs_{0.05}FA_{0.8}MA_{0.15}PbBr_{0.75}\ I_{2.25}$	[2] a)
1.11	1.69	29.8	1190	19.5	79.8	Si	a, b)	[3]
1.11	**1.69**	**29.2**	**1929**	**19.5**	**77.6**	**Si**	**$Cs_{0.05}FA_{0.703}MA_{0.247}PbBr_{0.78}I_{2.22}$**	**[112]**
1.12	**1.55**	**22.3**	**1700**	**17.5**	**75.0**	**Si**	**$FAMAPbI_3$**	**[113]**
1.12	1.64	26.0	1760	19.2	76.5	Si	$FA_{0.83}MA_{0.17}PbI_3$	[2]
1.12	1.65	26.5	1760	19.4	77.0	Si	$Cs_{0.05}\ FA_{0.79}MA_{0.16}PbBr_{0.51}\ I_{2.49}$	[2]
1.12	1.68	28.8 (29.2) c)	1895	19.2	78.9	Si	$Cs_{0.05}FA_{0.73}MA_{0.22}PbBr_{0.69}I_{2.31}$	[2]
1.13	**1.69**	**32.5**	**1980**	**20.2**	**81.2**	**Si**	**$Cs_{0.209}FA_{0.741}MA_{0.05}PbBr_{0.4275}Cl_{0.15}I_{2.4225}$**	**[40] a)**
1.13	**1.69**	**31.3**	**1910**	**20.5**	**79.8**	**Si**	**$Cs_{0.18}FA_{0.82}Pb(Br,I)_3$**	**[41] a)**
1.13	1.67	28.3	1776	20.1	79.6	Si	$FAMAPb(Br,Cl,I)_3$	[3]a)
1.13	1.65	24.9	1735	19.5	73.5	Si	$CsFAPb(Br,I)_3$	[2]
1.13	1.67	27.1	1886	19.1	75.3	Si	$CsFAMAPb(Br,Cl,I)_3$	[2]
1.13	**1.68**	**28.9**	**1850**	**19.8**	**78.9**	**Si**	**$CsFAPb(Br,I)_3$:$MA(Cl_{0.5}SCN_{0.5})_{28.9}$**	**[114]**
1.13	**1.68**	**27.9**	**1833**	**19.4**	**77.5**	**Si**	**$CsFAPb(Br,I)_3$:$MA(Cl_{0.5}SCN_{0.5})_{28.9}$**	**[114] a)**
1.13	1.69	29.5	1884	20.3	77.3	Si	a, b)	[2]

1.14	1.68	27.5	1779	19.6	78.9	Si	$Cs_{0.22}FA_{0.78}PbBr_{0.45}Cl_{0.09}I_{2.55}$	[3]
1.14	1.69	26.8	1891	17.8	79.4	Si	a, b)	[3]
1.14	1.69	26.0	1780	18.2	80.2	Si	$Cs_{0.15}FA_{0.7055}MA_{0.1445}PbBr_{0.6}I_{2.4}$	[3]
1.15	1.62	20.9	1690	15.9	77.6	Si	$MAPbI_3$	[2]
1.15	1.68	25.4	1800	17.8	79.4	Si	$Cs_{0.15}FA_{0.71}MA_{0.14}PbBr_{0.6}I_{2.4}$	[2]
1.15	1.68	25.0	1770	18.4	77.0	Si	$Cs_{0.25}FA_{0.75}PbBr_{0.6}I_{2.4}$	[2]
1.16	1.62	19.2	1701	16.1	70.1	Si	$MAPbI_3$	[2]
1.17	**1.63**	**26.4**	**1804**	**18.1**	**80.6**	**Si**	**$FA_{0.83}MA_{0.17}PbBr_{0.51}I_{2.49}$**	**[115]**
1.17	**1.63**	**23.7**	**1770**	**17.9**	**74.5**	**Si**	**$FA_{0.83}MA_{0.17}PbBr_{0.51}I_{2.49}$**	**[115] b)**
1.17	**1.63**	**19.5**	**1772**	**17.7**	**62.3**	**Si**	**$FA_{0.83}MA_{0.17}PbBr_{0.51}I_{2.49}$**	**[115] b)**
						GaAs/perovskite		
1.42	1.85	24.3	2160	14.3	78.8	GaAs	$Cs_{0.16}FA_{0.80}MA_{0.04}PbBr_{1.50}I_{1.50}$	[2]
						CIGS/perovskite		
1.01	1.61	24.3	1570	21.0	73.6	$CuInSe_2$	$Cs_{0.05}FA_{0.85}MA_{0.1}PbI_{2.7}Br_{0.3}$	[3]
1.01	1.61	23.5	1590	19.4	75.5	$CuInSe_2$	$Cs_{0.05}FA_{0.85}MA_{0.1}PbI_{2.7}Br_{0.3}$	[3] a)
1.08	**1.64**	**23.5**	**1700**	**19.5**	**71.0**	**$Cu(In,Ga)Se_2$**	**$Cs_{0.05}FA_{0.7885}MA_{0.1615}PbBr_{0.51}I_{2.49}$**	**[116]**
1.10	1.65	22.4	1774	17.3	73.1	$Cu(In,Ga)Se_2$	$Cs_{0.09}FA_{0.77}MA_{0.14}PbBr_{0.42}I_{2.58}$	[2] a)
1.11	1.64	21.6	1580	18.0	76.0	$Cu(In,Ga)Se_2$	$Cs_{0.05}FA_{0.7885}MA_{0.1615}PbBr_{0.51}I_{2.49}$	[2]
1.11	1.65	23.3	1680	19.2	71.9	$Cu(In,Ga)Se_2$	$Cs_{0.05}FA_{0.7885}MA_{0.1615}PbBr_{0.51}I_{2.49}$	[2]
1.11	1.68	24.2	1770	18.8	71.2	$Cu(In,Ga)Se_2$	$Cs_{0.05}FA_{0.7315}MA_{0.2185}PbBr_{0.69}I_{2.31}$	[3]
1.12	1.68	24.2	1768	19.2	72.9	$Cu(In,Ga)Se_2$	a, b)	[2]
						Perovskite/perovskite		

1.25	**1.78**	**27.1**	**2200**	**15.3**	**80.8**	**$FA_{0.6}MA_{0.4}Pb_{0.4}Sn_{0.6}I_3$**	**$Cs_{0.3}DMA_{0.1}FA_{0.6}PbBr_{0.9}I_{2.1}$**	**[117]**
1.25	**1.80**	**28.4**	**2111**	**16.5**	**81.5**	**$FA_{0.7}MA_{0.3}Pb_{0.5}Sn_{0.5}I_3$**	**$Cs_{0.2}FA_{0.8}PbBr_{1.14}I_{1.86}$**	**[42]**
1.25	**1.80**	**28.0**	**2125**	**16.4**	**80.3**	**$FA_{0.7}MA_{0.3}Pb_{0.5}Sn_{0.5}I_3$**	**$Cs_{0.2}FA_{0.8}PbBr_{1.14}I_{1.86}$**	**[42] a)**
1.25	**1.80**	**28.2**	**2159**	**16.6**	**78.9**	**a, b)**	**a, b)**	**[6]**
1.25	1.80	26.3 (26.4) c)	2044	16.5	78.1	$Cs_{0.2}FA_{0.8}PbBr_{1.14}I_{1.86}$	$FA_{0.7}MA_{0.3}Pb_{0.5}Sn_{0.5}I_3$	[3] a) d)
1.26	1.79	23.1	1950	15.8	75.0	$FA_{0.66}MA_{0.34}Pb_{0.5}Sn_{0.5}I_3$	$Cs_{0.05}(FAMA_{0.95})K_{0.05}Pb(BrI)_3$	[3]
1.26	**1.80**	**29.1**	**2952**	**16.5**	**81.7**	**a, b)**	**a, b)**	**[6]**
1.26	**1.80**	**27.1**	**2132**	**15.5**	**82.4**	**$Cs_{0.1}FA_{0.6}MA_{0.3}Pb_{0.5}Sn_{0.5}I_3$**	**$Cs_{0.2}FA_{0.8}PbI_{1.8}Br_{1.2}$**	**[118]**
1.26	**1.80**	**26.0**	**2123**	**15.3**	**80.0**	**$Cs_{0.1}FA_{0.6}MA_{0.3}Pb_{0.5}Sn_{0.5}I_3$**	**$Cs_{0.2}FA_{0.8}PbI_{1.8}Br_{1.2}$**	**[118] a)**
1.26	1.80	26.2	2040	16	80.1	$FA_{0.7}MA_{0.3}Pb_{0.5}Sn_{0.5}I_3$	$Cs_{0.4}DMA_{0.1}FA_{0.5}PbBr_{0.71}Cl_{0.15}I_{2.14}$	[3]
1.26	**1.80**	**25.6**	**2000**	**16.1**	**79.6**	**$FA_{0.7}MA_{0.3}Pb_{0.5}Sn_{0.5}I_3$**	**$CsPbBr_xI_{3-x}$**	**[49]**
1.26	**1.82**	**26.3**	**2130**	**15.2**	**81.0**	**$Cs_{0.05}FA_{0.7}MA_{0.25}Pb_{0.5}Sn_{0.5}I_3$**	**$Cs_{0.2}FA_{0.8}PbBr_{1.2}I_{1.8}$**	**[74] a)**
1.26	1.82	24.0	1986	15.8	76.6	FSA:$FA_{0.7}MA_{0.3}Pb_{0.5}Sn_{0.5}I_3$	$Cs_{0.2}FA_{0.8}PbBr_{1.2}I_{1.8}$	[2] a)
1.26	1.82	25.5	2009	15.9	79.8	FSA:$FA_{0.7}MA_{0.3}Pb_{0.5}Sn_{0.5}I_3$	$Cs_{0.2}FA_{0.8}PbBr_{1.2}I_{1.8}$	[2]
1.26	**1.84**	**26.6**	**2119**	**15.2**	**82.4**	**$FA_{0.6}MA_{0.3}Cs_{0.1}Sn_{0.5}Pb_{0.5}I_3$**	**$FA_{0.8}Cs_{0.2}PbBr_{1.2}I_{1.8}$**	**[52] a, b)**
1.27	1.72	22.9	1915	15.0	79.8	$FA_{0.6}MA_{0.4}Pb_{0.4}Sn_{0.6}I_3$	$Cs_{0.05}FA_{0.8}MA_{0.15}PbBr_{0.45}I_{2.55}$	[2]
1.27	**1.81**	**25.1**	**2021**	**15.6**	**79.5**	**$FA_{0.7}MA_{0.3}Pb_{0.5}Sn_{0.5}I_3$**	**$Cs_{0.2}FA_{0.8}PbBr_{1.2}I_{1.8}$**	**[78]**
1.27	1.81	24.3	2030	15.2	78.8	$Cs_{0.05}FA_{0.5}MA_{0.45}Pb_{0.5}Sn_{0.5}I_3$	$Cs_{0.4}FA_{0.6}PbBr_{1.05}I_{1.95}$	[2]
1.27	1.81	24.5	1927	15.9	80.0	$FA_{0.7}MA_{0.3}Pb_{0.5}Sn_{0.5}I_3$	$Cs_{0.2}FA_{0.8}PbBr_{1.2}I_{1.8}$	[2] a)
1.27	1.82	23.2	1890	15.4	79.8	$Cs_{0.2}FA_{0.8}Pb_{0.5}Sn_{0.5}I_3$	$Cs_{0.2}FA_{0.8}PbBr_{1.2}I_{1.8}$	[3]
1.27	**1.85**	**23.4**	**2000**	**15.0**	**77.8**	**$Cs_{0.17}FA_{0.83}Pb_{0.5}Sn_{0.5}I_3$**	**$Cs_{0.05}FA_{0.57}MA_{0.38}PbBr_{1.2}I_{1.8}$**	**[119]**
1.28	1.73	23.1	1880	16.0	77.0	$Cs_{0.25}FA_{0.75}Pb_{0.5}Sn_{0.5}I_3$	$Cs_{0.3}DMA_{0.1}FA_{0.6}PbBr_{0.6}I_{2.4}$	[2]

1.28	**1.79**	**24.5**	**1.8**	**17.16**	**79.3188 3**	**$Cs_{0.025}FA_{0.475}MA_{0.5}Sn_{0.5}Pb_{0.5}Br_{0.075}I_{2.925}$**	**$FA_{0.8}Cs_{0.2}PbI_{1.8}Br_{1.2}$**	**[76]**
						OPV/perovskite		
1.21	1.83	21.7	1880	15.7	73.5	PTB7-Th:BTPV-4Cl-eC9	$FA_{0.6}MA_{0.4}PbBr_{1.2}I_{1.8}$	[3]
1.25	1.91	15.0	1710	12.0	73.4	PTB7-Th:COi8DFIC:$PC_{71}BM$	$CsPbBrI_2$	[2]
1.35	**1.91**	**23.2**	**2150**	**13.4**	**80.3**	**D18-Cl:N3:$PC_{61}BM$**	**$CsPbBr_{1.1}I_{1.9}$**	**[120]**
1.35	**1.91**	**21.7**	**2150**	**13.0**	**77.5**	**D18-Cl:N3:$PC_{61}BM$**	**$CsPbBr_{1.1}I_{1.9}$**	**[120] b)**
1.38	1.91	21.1	1960	13.3	80.9	PM6:Y6-BO	$CsPbBrI_2$	[2]
1.38	1.88	23.4	2136	14.6	75.2	a, b)	a, b)	[3]
1.38	**1.88**	**21.4**	**2078**	**13.2**	**77.9**	**PM6:CH1007**	**$CsPbBr_{1.2}I_{1.8}$**	**[121] a)**
1.38	**1.88**	**22.4**	**2095**	**13.9**	**77.0**	**PM6:CH1007**	**$CsPbBr_{1.2}I_{1.8}$**	**[121]**
1.40	1.81	23.6	2063	14.8	77.2	PM6:Y6:$P_{71}CBM$	$Cs_{0.25}FA_{0.75}PbBr_{1.2}I_{1.8}$	[77]
1.40	1.81	22.5	2058	14.9	73.5	PM6:Y6:$P_{71}CBM$	$Cs_{0.25}FA_{0.75}PbBr_{1.2}I_{1.8}$	[77] a)
1.40	1.83	15.1	1850	11.5	71.0	PBDB-T:SN6IC-4F	$Cs_{0.1}FA_{0.54}MA_{0.36}PbBr_{1.4}I_{1.8}$	[2]
1.40	1.82	19.5	1925	13.1	77.2	PBDBT-2F:Y6:$PC_{71}BM$	$Cs_{0.18}FA_{0.8}MA_{0.02}PbBr_{1.2}I_{1.8}$	[2] a)
1.40	1.82	20.4	1902	13.1	81.5	PBDBT-2F:Y6:$PC_{71}BM$	$Cs_{0.18}FA_{0.8}MA_{0.02}PbBr_{1.2}I_{1.8}$	[2]
1.41	1.86	23.8	2140	14.1	79.0	PM6:Y6:$PC_{61}BM$	$FA_{0.8}Cs_{0.2}PbBr_{1.5}I_{1.5}$	[122]
						DSSC/perovskite		
1.59	1.93	10.5	1170	12.9	70.0	$FA_{0.85}MA_{0.15}PbBr_{0.45}I_{2.49}$	N719	[2]
						Triple-junction		
1.08	**1.53, 1.89**	**22.2**	**2780**	**10.2**	**78.6**	**Si**	**$Cs_{0.1}FA_{0.85}MA_{0.05}PbI_3$, $MAPbBr_{1.05}Cl_{0.45}I_{1.5}$**	**[123]**
1.13	1.54, 1.91	20.1	2740	8.5	86.0	Si	$Cs_{0.1}FA_{0.9}PbI_3$, $Cs_{0.2}FA_{0.8}PbBr_{1.65}I_{1.35}$	[3]

1.23	1.57, 1.78	16.8	2780	7.4	81	$FA_{0.66}MA_{0.34}Pb_{0.5}Sn_{0.5}I_3$	$FA_{0.66}MA_{0.34}PbBr_{0.15}I_{2.85}$, $Cs_{0.1}FA_{0.594}MA_{0.306}PbBrI_2$	[3]
1.26	1.65, 2.06	19.9	2793	8.8	80.7	$FA_{0.7}MA_{0.3}Pb_{0.5}Sn_{0.5}I_3$	$Cs_{0.05}FA_{0.95}PbBr_{0.45}I_{2.55}$, $Cs_{0.2}FA_{0.8}PbBr_{2.1}I_{0.9}$	[3]
1.26	**1.6, 1.99**	**23.3**	**3181**	**9.61**	**76.2**	**$Cs_{0.05}FA_{0.7}MA_{0.25}Pb_{0.5}Sn_{0.5}I_{3-0.05}SnF$**	**$Cs_{0.05}FA_{0.9}MA_{0.05}PbBr_{0.3}I_{2.7}$, $Cs_{0.85}Rb_{0.15}PbBr_{1.25}I_{1.75}$**	**[39] a)**
1.26	**1.6, 1.99**	**24.3**	**3215**	**9.71**	**77.9**	**$Cs_{0.05}FA_{0.7}MA_{0.25}Pb_{0.5}Sn_{0.5}I_{3-0.05}SnF$**	**$Cs_{0.05}FA_{0.9}MA_{0.05}PbBr_{0.3}I_{2.7}$, $Cs_{0.85}Rb_{0.15}PbBr_{1.25}I_{1.75}$**	**[39]**

[a] Certified power conversion efficiency; [b] Notable exception included as a large area highlight, or a *PCE* highlight without the absorber material information; [c] in parentheses, the certified efficiency from MPP tracking.

Table 10. Monolithic **multijunction organic-** and **dye sensitized-**based research solar cells with the highest efficiency: performance parameters as a function of the device bandgap energies (from the EQE spectra) of the sub-cells.

$E_{g,bottom}$ [eV]	$E_{g,top}$ [eV]	PCE [%]	V_{oc} [mV]	J_{sc} [mA cm^{-2}]	FF [%]	Bottom absorber	Top absorber	Ref.
						OPV/OPV		
1.21	**1.58**	**19.0**	**1690**	**15.0**	**74.8**	**PTB7-Th:BTPSeV-4F**	**PM6:O1-Br**	**[124]**
1.23	1.66	16.4	1650	14.5	68.5	PTB7-Th:BTPV-4F:$PC_{71}BM$	PM6:m-DTC-2F	[2]
1.24	1.72	17.3	1640	14.4	73.3	PTB7-Th:O6T-4F:$PC_{71}BM$	PBDB-T:F-M	[2]
1.31	1.64	15.9	1660	14.1	68.0	PM6:SFT8-4F	PCE-10:BT-CIC:BEIT-4F	[2]
1.32	1.65	15.0	1600	13.6	69.0	PTB7-Th:PCDTBT:IEICO-4F	PBDB-T-2F:TfIF-4FIC	[2]
1.32	1.74	19.6	1910	14.2	72.4	PBDB-TF:ITCC	PBDB-TF:BTP-eC11	[2]
1.32	1.74	19.5	1912	14.2	72.0	PBDB-TF:ITCC	PBDB-TF:BTP-eC11	[2]
1.36	1.73	18.7	1883	14.0	70.9	PM6:CH1007:PC_{71}BM	D18:F-ThBr	[3]
1.37	1.73	15.2	1610	12.9	73.0	PM6:Y6	PV2000:PCBM	[2]
1.37	**1.77**	**20.3**	**2020**	**13.2**	**76.0**	**BTP-eC9:AITC:PBDB-TCI**	**AITC:PFBCPZ**	**[43]**

1.37	**1.77**	**20.6**	**2020**	**13.3**	**76.6**	**BTP-eC9:AITC:PBDB-TCl**	**AITC:PFBCPZ**	**[43]**
1.38	1.80	20.3	2010	13.1	76.8	PBDB-TF:GS-ISO	PBDM-TF:BTp-eC9	[3]
1.38	1.80	20.3	2010	13.1	76.8	PBDB-TF:GS-ISO	PBDM-TF:BTp-eC9	[3]
1.39	**1.78**	**19.6**	**2030**	**13.0**	**74.2**	**PBDB-TF:HDO-4Cl:BTP-eC9**	**PB2:GS-ISO**	**[125]**
1.40	**1.71**	**20.0**	**1960**	**13.5**	**75.9**	**PB4:FTCC-Br**	**PBQx-TCl:PBDB-TF:eC9-2Cl**	**[33]**
1.42	1.79	15.0	1590	13.3	71.0	PCE-10:BTCIC	DTDCPB:C_{70}	[2]
1.45	**1.76**	**17.9**	**2000**	**11.7**	**76.3**	**PM6:PY-IT**	**PM7:PIDT**	**[126]**
1.48	1.74	14.1	1710	11.7	70.0	PTB7-Th: NOBDT	PBDB-T: F-M	[2]
						OPV/a-Si		
1.33	1.78	15.1	1610	13.2	71.0	PTB7-Th:IEICO-4F	a-Si	[2]
						Si/DSSC		
1.11	1.84	14.7	580	40.9	62.0	Si	N719	[2]
1.24	1.67	17.2	1360	18.1	69.3	Si	SGT-021	[2]
						CIGS/DSSC		
1.21	1.82	13.0	1170	14.6	77.0	CIGS	N719	[2]
1.22	1.90	12.4	1435	14.1	61.0	CIGS	N719	[2]
1.22	1.82	15.1	1450	14.1	74.0	CIGS	N719	[2]
						DSSC/DSSC		
1.40	1.98	11.4	1400	12.2	66.7	DX1	N719	[2]
1.44	1.95	10.4	1450	10.8	67	N719	Black dye	[2]
1.67	1.98	12.3	1825	10.3	65	SGT-121/HC-A1	SGT-021/HC-A4	[3]

1.78	2.37	7.1	1420	7.2	69	N719	D131	[2]

Table 11. Monolithic **multijunction** research solar cells with the highest efficiency: performance parameters as a function of the device bandgap energies (from the EQE spectra) of the sub-cells among other **established technologies**.

$E_{g,bottom}$ [eV]	$E_{g,middle}$, $E_{g,top}$, [eV]	PCE [%]	V_{oc} [mV]	J_{sc} [mA cm^{-2}]	FF [%]	Bottom absorber	Middle, top absorber(s)	Ref.
						GaAs/GaInP		
1.35	1.90	32.9	2500	15.4	85.7	GaAs	GaInP	[2]
1.41	1.88	32.8	2568	14.66	87.7	GaAs	GaInP	[2]
1.41	1.92	27.4	2400	13.1	88.0	GaAs	GaInP	[2]
1.42	1.85	31.6	2538	14.2	87.7	GaAs	GaInP	[2]
						Si/GaAsP		
1.17	1.90	23.4	1732	17.34	77.7	Si	GaAsP	[2]
						nc-Si/a-Si		
1.36	1.93	11.8	1428	12.27	67.5	nc-Si	a-Si	[2]
						Triple-junction cells		
0.92	1.33,1.88	39.5	3000	15.4	85.3	InGaAs	GaAs, InGaP	[3]
0.98	1.41, 1.89	37.7	3014	14.6	86.0	InGaAs	GaAs, InGaP	[3]
1.09	**1.42, 1.92**	**19.1**	**2510**	**9.9**	**77.0**	**GaAsBi**	**GaAs, AlGaAs**	**[127]**
1.13	1.48, 1.93	35.9	3248	13.1	84.3	Si	GaInAsP, InGaP	[3]
1.01	1.50, 1.92	28.1	2952	11.7	81.1	CIGS	AlGaAs/GaInP	[3]
1.30	1.27, 2.03	14.0	1922	9.9	73.4	nc-Si	nc-Si, a-Si	[3]

7.2. Best performing flexible research solar cells tables

Table 12. Flexible perovskite single-junction research solar cells with the highest efficiency: performance parameters as a function of photovoltaic bandgap energy (from the *EQE* spectrum).

E_g [eV]	PCE [%]	V_{oc} [mV]	J_{sc} [mA cm^{-2}]	FF [%]	Absorber perovskite	Ref.
1.44	8.5	650	20.8	62.9	$FAGe_{0.1}Sn_{0.9}I_3$	[3]
1.53	**23.2**	**1145**	**25.2**	**80.5**	**$FAPbI_3$**	**[128]**
1.53	**21.0**	**1140**	**25.1**	**73.5**	**$FAPbI_3$**	**[128] a)**
1.53	**22.1**	**1130**	**23.9**	**81.8**	**$FAMAPbI_3$**	**[129]**
1.53	20.5	1070	23.6	81.2	$FAMAPbI_3$	[3]
1.53	20.2	1123	24.7	72.9	$FA_{0.87}MA_{0.13}Pb(Cl,I)_3$	[2]
1.54	22.4	1151	23.4	82.9	$FAMAPbI_3$	[3]
1.54	22.4	1170	24.6	77.8	$Cs_{0.1}FA_{0.9}PbI_3$	[3]
1.55	**23.4**	**1164**	**24.8**	**80.9**	**$Cs_{0.05}FA_{0.931}MA_{0.019}PbBr_{0.06}I_{2.94}$**	**[44] a)**
1.55	**23.7**	**1172**	**24.9**	**81.3**	**$Cs_{0.05}FA_{0.931}MA_{0.019}PbBr_{0.06}I_{2.94}$**	**[44]**
1.55	**21.3**	**1160**	**24.2**	**76.0**	**$Cs_{0.05}FA_{0.931}MA_{0.019}PbBr_{0.06}I_{2.94}$**	**[44] b)**
1.56	21.7	1127	24.8	77.7	$Cs_{0.05}FA_{0.931}MA_{0.019}PbBr_{0.06}I_{2.94}$/PM6:CH1007:PCBM	[3]
1.56	20.8	1190	21.9	79.6	$FA_{0.95}MA_{0.05}PbBr_{0.15}I_{2.85}$	[2]
1.56	20.3	1160	23.4	74.8	$FA_{0.95}MA_{0.05}PbBr_{0.15}I_{2.85}$	[2]
1.56	19.9	1109	23.2	77.3	$Cs_{0.05}$ $FA_{0.747}MA_{0.153}Rb_{0.05}PbBr_{0.15}I_{2.85}$	[2] a)
1.56	19.9	1192	21.9	76.3	$FA_{0.95}MA_{0.05}PbBr_{0.15}I_{2.85}$	[2] a)
1.57	**22.1**	**1200**	**22.8**	**80.9**	**$Cs_{0.05}FA_{0.90}MA_{0.05}PbBr_{0.15}I_{2.85}$**	**[130]**
1.57	19.5	1110	23.1	76.0	$Cs_{0.03}FA_{0.945}MA_{0.025}PbBr_{0.075}I_{2.925}$	[2]
1.57	**19.5**	**1105**	**23.1**	**76.1**	**$CsFAMAPb(Br,I)_3$**	**[131]**
1.58	19.2	1120	21.7	78.9	$Cs_{0.08}FA_{0.87}MA_{0.05}PbBr_{0.12}I_{2.88}$	[2]
1.59	19.9	1120	23.0	77.5	$FAMAPb(Br,I)_3$	[2]
1.59	19.3	1090	22.7	78.1	$MAPbI_3$–NH_4Cl	[2]
1.59	20.2	1120	22.2	81.1	FAMAPbBrI	[3]
1.60	20.6	1110	23.0	80.7	CsFAMAPbBrI	[3]
1.60	20.5	1140	23.5	76.5	$Cs_{0.04}FA_{0.86}MA_{0.1}PbBr_{0.29}I_{2.71}$	[3]
1.60	17.8	1060	21.8	77.3	CsFAMAPbBrI	[3] b)
1.61	17.3	1062	21.7	74.9	$Cs_{0.05}FA_{0.81}MA_{0.14}PbBr_{0.45}I_{2.55}$	[2] a)
1.61	19.1	1135	21.2	79.2	$Cs_{0.05}FA_{0.75}K_{0.04}MA_{0.15}Rb_{0.01}PbBr_{0.51}I_{2.49}$	[2]
1.62	20.1	1150	22.4	78.0	$Cs_{0.04}FA_{0.8064}MA_{0.1536}PbBr_{0.48}I_{2.52}$	[2]
1.62	18.0	1120	22.3	72.1	$Cs_{0.06}FA_{0.79}MA_{0.15}PbBr_{0.45}I_{2.55}$	[2]
1.63	14.9	1030	21.5	67.3	$MAPbI_3$	[3]
1.63	10.4	1030	19.2	52.8	$FA_{0.85}MA_{0.15}PbBr_{0.45}I_{2.55}$	[2]
1.65	11.2	940	18.4	64.9	$MAPbI_3$	[2]
1.65	7.9	1090	10.8	70.7	$(\alpha\text{-}FAPbI_3)_{0.5}(MAPbI_2Br)_{0.5}$	[2]

[a] Certified power conversion efficiency; [b] Notable exception included as materials and/or large area highlights.

Table 13. Flexible organic single-junction research solar cells with the highest efficiency: performance parameters as a function of photovoltaic bandgap energy (from the *EQE* spectrum).

E_g [eV]	PCE [%]	V_{oc} [mV]	J_{sc} [mA cm^{-2}]	FF [%]	Absorber blend	Ref.
1.27	7.4	708	15.9	65.2	PTB7-Th:COi 8DFIC:$PC_{71}BM$	[2]
1.32	10.6	690	24.3	63.2	PTB7-Th:IEICO-4F	[2]
1.36	16.6	821	26.8	75.4	PM6:BTP-4Cl-12	[3]
1.37	16.1	840	25.0	76.7	PM6:N3:$PC_{71}BM$	[2]
1.38	12.0	827	21.6	67.4	PM6:BTP-4Cl-12	[3] a)
1.38	17.5	835	27.4	76.7	PM6:BTP-eC9:$PC_{71}BM$	[3]
1.39	16.1	820	25.9	75.8	PM6:BTP-eC9:$PC_{71}BM$	[2]
1.39	15.9	864	25.0	73.5	D-18-Cl:G19:Y6	[3]
1.39	**15.7**	**830**	**25.4**	**74.5**	**PM6:BTP-eC9**	**[132]**
1.39	**14.4**	**830**	**25.4**	**68.3**	**PM6:BTP-eC9**	**[132] b)**
1.40	**17.2**	**870**	**25.5**	**77.3**	**PM6:L8-BO**	**[45] b)**
1.40	**17.4**	**869**	**25.5**	**78.5**	**PM6:L8-BO**	[45]
1.40	16.1	860	25.9	74.7	PM6:Y6	[2]
1.40	15.2	832	25.1	73.0	PM6:Y6	[2]
1.40	17.1	830	27.4	74.9	PM6:BTP-eC9:$PC_{71}BM$	[3]
1.41	15.2	830	25.0	73.3	PM6:Y6	[3]
1.41	15.1	847	24.9	71.6	PM6:Y6:C6	[2]
1.42	16.6	860	25.9	74.7	PM6:Y6	[2]
1.43	**16.5**	**925**	**23.6**	**75.6**	**PBQx-TF:PBDB-TF:PY-IT**	**[93]**
1.44	**10.7**	**943**	**17.7**	**64.3**	**D18:(40)-b-PYIT**	**[133]**
1.44	10.4	848	17.0	72.2	PM6:Y6	[2]
1.45	**16.6**	**860**	**25.5**	**75.8**	**PM6:L8-BO**	**[134]**
1.55	12.0	840	19.5	73.3	PM6:IT-4F	[2]
1.56	11.6	820	19.6	72.2	PM6:IT-4F	[2]
1.56	12.1	826	20.9	70.1	PM6:IT-4F	[2]
1.61	10.9	900	18.7	64.8	PBDB-T:ITIC	[2]
1.63	9.2	770	16.0	74.7	PTB7-Th:$PC_{71}BM$	[2]
1.65	9.3	820	16.5	68.7	J51:ITIC	[2]
1.65	8.2	890	13.4	68.6	PBDB-T:ITIC	[2]
1.82	7.2	925	10.9	71.3	JP02	[2]
2.01	3.7	592	10.4	59.2	P3HT:PCBM	[2]

[a)] Certified power conversion efficiency; [b)] Notable exception included as a material and/or high area cell highlight

Table 14. Flexible dye-sensitized single-junction research solar cells with the highest efficiency: performance parameters as a function of device absorber bandgap energy (from the *EQE* spectrum).

E_g [eV]	PCE [%]	V_{oc} [mV]	J_{sc} [mA cm^{-2}]	FF [%]	Sensitizing dye	Ref.
1.65	4.1	770	9.9	53.9	N719	[2]

1.74	4.6	750	10.5	58.0	N719	[2]
1.75	7.6	732	15.0	69.2	N719	[2] a)
1.78	7.5	725	15.4	67.5	N719	[2]
1.79	6.5	729	13.2	68.0	N719	[2]
1.80	6.3	732	13.1	66.0	N719	[2]
1.81	6.3	754	12.3	67.9	$(JH\text{-}1)_{0.6}(SQ2)_{0.4}$	[2]
183	5.0	735	10.0	67.8	N719	[2]
1.88	6.0	750	11.2	71.0	N719	[2]
1.90	4.2	680	10.7	57.7	N719	[2]
1.94	4.2	710	10.3	57.2	N719	[2]
1.95	4.9	702	11.2	62.3	N719	[2]
2.02	3.9	720	11.9	45.2	N719	[3]
2.12	5.4	680	10.4	76.3	N719	[2]

a) Certified power conversion efficiency

Table 15. Flexible monolithic multijunction research solar cells with the highest efficiency: performance parameters as a function of photovoltaic bandgap energies (from the *EQE* spectrum) of each sub-cell. For triple-junction devices the middle and top sub-cell values are listed with a comma separator.

$E_{g,bottom}$ [eV]	$E_{g,top}$ [eV]	PCE [%]	V_{oc} [mV]	J_{sc} [mA cm^{-2}]	FF [%]	Bottom absorber material	Top absorber material (s)	Ref.
						Double junction cells		
1.25	1.78	24.7	2000	15.8	78.3	$FA_{0.7}MA_{0.3}Pb_{0.5}Sn_{0.5}I_3$	$Cs_{0.2}FA_{0.8}PbBr_{1.05}I_{1.95}$	[3]
1.25	1.78	24.4	2016	15.6	77.3	$FA_{0.7}MA_{0.3}Pb_{0.5}Sn_{0.5}I_3$	$Cs_{0.2}FA_{0.8}PbBr_{1.05}I_{1.95}$	[3] a)
1.26	1.79	23.8	2100	15.1	75.1	$FA_{0.6}MA_{0.4}Pb_{0.4}Sn_{0.6}I_3$	$Cs_{0.12}FA_{0.8}MA_{0.08}PbBr_{1.2}I_{1.8}$	[3]
1.27	**1.81**	**23.8**	**2015**	**15.5**	**76.1**	**$FA_{0.7}MA_{0.3}Pb_{0.5}Sn_{0.5}I_3$**	**$Cs_{0.2}FA_{0.8}PbBr_{1.2}I_{1.8}$**	**[78]**
1.28	1.73	21.3	1820	15.6	75.0	$FA_{0.75}Cs_{0.25}Sn_{0.5}Pb_{0.5}I_3$	$Cs_{0.3}DMA_{0.1}FA_{0.6}PbBr_{0.6}I_{2.4}$	[2]
1.40	1.82	13.6	1800	11.1	68.3	PBDB-T:SN6IC-4F	$Cs_{0.1}FA_{0.54}MA_{0.36}PbBr_{1.2}I_{1.8}$	[2]
1.41	1.86	30.4	2547	14.3	84.7	GaAs	InGaP	[2]
1.41	1.92	27.4	2400	13.1	88.0	GaAs	InGaP	[2]
						Triple junction cells		
1.00	1.41, 1.91	30.2	3043	16.1	84.5	$Ga_{0.73}In_{0.27}As$	GaAs, $Ga_{0.51}In_{0.49}P$	b)

a) Certified power conversion efficiency; b) *J-V* measured under AM0 136.7 mW cm^{-2}

Table 16. **Flexible** single junction research solar cells with the highest efficiency: performance parameters as a function of device absorber bandgap energy (from the EQE spectrum) among **emerging inorganic** technologies.

E_g [eV]	PCE [%]	V_{oc} [mV]	J_{sc} [mA cm^{-2}]	FF [%]	Absorber material	Ref.
1.04	4.4	394	23.9	46.4	$Cu_2Cd_xZn_{1-x}Sn(S,Se)_4$	[3]
1.07	4.9	358	28.7	47.3	$Cu_2ZnSn(S,Se)_4$	[3]
1.09	**8.7**	**401**	**36.5**	**59.4**	**$Cu_2ZnSn(S,Se)_4$**	**[135]**
1.13	10.2	463	35.7	62.0	$Cu_2ZnSn(S,Se)_4$	[3]
1.16	11.2	539	33.1	62.8	$Cu_2ZnSn(S,Se)_4$	[2]
1.32	6.13	415	25.5	57.9	Sb_2Se_3	[2]
1.52	0.6	204	7.6	35.5	Cu_2ZnSnS_4	[2]
1.59	6.5	601	22.6	48.0	CZTSSe	[3]
1.80	**3.8**	**650**	**11.6**	**49.5**	**Sb_2S_3**	**[136]**

Table 17. **Flexible** single-junction research solar cells with the highest efficiency: performance parameters as a function of device absorber bandgap energy (from the *EQE* spectrum) among **established inorganic** technologies.

E_g [eV]	PCE [%]	V_{oc} [mV]	J_{sc} [mA cm^{-2}]	FF [%]	Absorber material/ technology	Ref.
1.11	11.5	526	33.8	64.6	CIGSSe	[3]
1.14	17.0	656	36.6	70.8	Si	[2]
1.15	**18.9**	**693**	**35.8**	**76.3**	**CIGS**	**[137]**
1.17	18.9	608	39.5[3]	63.0	Si	[2]
1.17	12.0	580	35.8	58.4	CIGS	[2]
1.18	**17.6**	**698**	**33.9**	**74.4**	**CIGS**	**[137]**
1.20	20.4	736	35.1	78.9	CIGS	[2] a)
1.22	18.7	720	35.0	74.4	CIGS	[2]
1.32	8.4	550	24.3	63.0	Si	[2]
1.42	22.1	980	27.1	83.4	GaAs	[2]
1.45	13.5	786	22.1	77.7	GaAs	[3]
1.45	**12.6**	**829**	**23.6**	**64.3**	**CdTe**	**[138]**
1.46	14.1	821	24.3	70.3	CdTe	[3] a)
1.46	16.4	831	25.5	77.4	CdTe	[2]
1.49	11.5	821	22.0	63.9	CdTe	[2]

1.79	8.8	888	14.3	70	a-Si:H	[2]
1.88	8.2	820	15.6	64.0	a-Si:H	[2]

a) Certified power conversion efficiency

7.3. Best performing transparent and semitransparent research solar cells tables

Table 18. Transparent/semitransparent perovskite solar cells with the highest efficiency: performance parameters as a function of *AVT* and the photovoltaic bandgap energy (from the *EQE* spectrum). For the tandem cells, the bandgap energies and absorber materials for the bottom and top sub-cells are separated with a comma, in that order.

AVT [%]	E_g [eV]	PCE [%]	V_{oc} [mV]	J_{sc} [mA cm^{-2}]	FF [%]	Absorber	Ref.
2	**1.65**	**19.9**	**1189**	**20.3**	**82.0**	**$Cs_{0.15}FA_{0.8}MA_{0.05}PbBr_{0.54}I_{2.46}$**	**[68]**
3	1.67	16.3	1099	18.9	78.3	$Cs_{0.25}FA_{0.75}PbBr_{0.6}I_{2.4}$	[3]
3	1.64	15.7	1070	19.0	77.2	$Cs_{0.175}FA_{0.75}MA_{0.075}PbBr_{0.375}I_{2.625}$	[2]
3	1.53	12.2	1017	17.5	68.5	$MAPbI_3$	[2]
4	1.63	18.2	1076	21.1	80.0	$CsFAMAPb(BrI)_3$	[2]
5	1.60	19.1	1120	23.2	73.4	$MAPbI_3$	[3]
5	1.60	16.5	1080	20.6	74.2	$MAPbI_3$	[2]
5	1.61	12.0	960	19.2	65.3	$MAPbCl_xI_{3-x}$	[2]
5	1.65	11.2	940	18.4	64.9	$MAPbI_3$	[2]
6	1.60	15.8	1100	19.3	74.4	$MAPbI_3$	[2]
7	**1.62**	**18.3**	**1100**	**21.9**	**75.8**	**$MAPbBr_{0.12}I_{2.88}$**	**[139]**
7	1.55	13.6	988	20.4	67.5	$MAPbI_3$	[2]
8	1.52	19.8	1137	21.9	79.5	$Cs_{0.05}FA_{0.95}PbI_3$	[2]
9	1.63	17.8	1120	19.3	82.7	$Cs_{0.13}FA_{0.87}PbBr_{0.39}I_{2.61}$	[3]
9	1.64	17.4	1083	21.5	75.1	$Cs_{0.175}FA_{0.825}PbBr_{0.375}I_{2.625}$	[2]
10	**1.78**	**11.3**	**1190**	**15.0**	**63.1**	**$CsPbI_3$**	**[140]**
10	1.59	17.5	1070	22.4	73.1	$MAPbI_3$	[2]
10	1.65	16.1	1060	20.4	74.5	$Cs_{0.05}FA_{0.8075}MA_{0.1425}PbBr_{0.45}I_{2.55}$	[2]
12	**1.27, 1.80**	**15.0**	**1940**	**11.4**	**68.0**	**$Cs_x(FA_{0.83}MA_{0.17})_{1-x}Pb_{0.5}Sn_{0.5}I_3$, $Cs_{0.2}FA_{0.8}Br_{1.2}I_{1.8}$**	**[46]**
12	1.60	13.2	1000	19.5	67.8	$MAPbI_3$	[2]
13	1.67	14.9	1100	19.8	68.4	$MAPbBr_{0.5}I_{2.5}$	[2]
13	1.88	13.2	1298	13.8	74.1	$Cs_{0.25}FA_{0.75}PbBr_{1.5}I_{1.5}$	[3]
14	1.64	13.6	1048	16.5	78.6	$Cs_{0.175}FA_{0.825}PbBr_{0.375}I_{2.875}$	[2]
14	1.57	13.0	970	19.1	69.9	$MAPbI_{3-x}Cl_x$	[2]
15	1.64	11.4	1094	16.8	62.0	$Cs_{0.05}FA_{0.775}MA_{0.1615}PbBr_{0.51}I_{2.49}$	[3]
15	1.61	11.9	1000	17.8	66.3	$MAPbI_3$	[2]
16	1.76	13.7	1120	16.7	73.4	$MAPbBrI_2$	[2]
17	1.65	12.8	1040	16.6	74.1	$Cs_{0.05}FA_{0.8075}MA_{0.1425}PbBr_{0.45}I_{2.55}$	[2]
18	1.77	12.2	1110	15.1	72.7	$MAPbBrI_2$	[2]
18	1.53	9.1	1017	14.6	61.5	$MAPbI_3$	[2]

19	1.55	8.8	941	13.7	68.3	$MAPbI_3$	[2]
20	1.63	11.7	1080	14.5	74.6	$MAPbI_3$+ BiPy-I	[2]
20	1.63	14.7	1108	17.6	75.2	$K_xCs_{0.05}FA_{0.8075}MA_{0.1425}PbBr_{0.45}I_{2.55}$	[2]
21	1.63	14.2	1117	17.4	73.2	$K_xCs_{0.05}FA_{0.8075}MA_{0.1425}PbBr_{0.45}I_{2.55}$	[2]
22	1.61	13.2	1073	17.2	71.7	$K_xCs_{0.05}FA_{0.8075}MA_{0.1425}PbBr_{0.45}I_{2.55}$	[2]
23	1.61	12.3	1082	17.1	66.6	$K_xCs_{0.05}FA_{0.8075}MA_{0.1425}PbBr_{0.45}I_{2.55}$	[2]
23	1.62	11.3	1040	15.1	72.3	$MAPbI_3$	[2]
23	1.57	10.8	970	17.3	64.4	$MAPbCl_xI_{3-x}$	[2]
23	1.88	8.6	1236	10.0	69.9	$Cs_{0.25}FA_{0.75}PbBr_{1.5}I_{1.5}$	[3]
24	1.87	9.4	1120	13.6	61.6	$MAPbBr_{1.5}I_{1.5}$	[2]
25	1.55	10.8	950	16.3	69.7	$MAPbI_3$	[2]
26	1.63	10.2	1070	12.2	78.1	$MAPbI_3$	[2]
27	1.60	12.1	1000	18.3	66.2	$MAPbI_3$	[2]
28	1.60	8.5	964	13.1	66.8	$MAPbCl_xI_{3-x}$	[2]
28	1.57	8.1	1030	11.2	70.2	$MAPbCl_xI_{3-x}$	[2]
30	1.62	12.8	1030	16.5	74.9	$MAPbCl_xI_{3-x}$	[2]
30	1.65	7.4	1010	11.8	62.2	$Cs_{0.05}FA_{0.8075}MA_{0.1425}PbBr_{0.45}I_{2.55}$	[2]
31	**1.27, 1.80**	**9.3**	**1940**	**7.9**	**61.0**	**$Cs_x(FA_{0.83}MA_{0.17})_{1-x}Pb_{0.5}Sn_{0.5}I_3$, $Cs_{0.2}FA_{0.8}Br_{1.2}I_{1.8}$**	**[46]**
31	1.69	11.9	1050	16.3	69.4	$MAPbBr_{0.5}I_{2.5}$	[2]
33	1.55	7.3	1037	13.4	52.5	$MAPbI_3$	[2]
34	1.62	11.7	990	15.9	74.6	$MAPbCl_xI_{3-x}$	[2]
35	1.88	12.0	1289	12.9	72.3	$Cs_{0.25}FA_{0.75}PbBr_{1.5}I_{1.5}$	[3]
36	1.79	10.3	1080	14.6	65.5	$MAPbBr\ I_2$	[2]
37	1.62	10.8	1010	14.7	73.1	$MAPbCl_xI_{3-x}$	[2]
37	1.57	7.8	970	11.6	69.6	$MAPbCl_xI_{3-x}$	[2]
38	1.63	10.7	1060	13.0	77.6	$MAPbI_3$	[2]
41	1.90	8.8	1110	12.8	62.2	$MAPbBr_{1.5}I_{1.5}$	[2]
42	1.63	10.3	1000	13.6	75.6	$MAPbCl_xI_{3-x}$	[2]
45	1.64	8.5	960	12.6	73.5	$MAPbCl_xI_{3-x}$	[2]
46	1.57	3.6	1030	5.4	64.4	$MAPbCl_xI_{3-x}$	[2]
47	1.63	4.5	880	8.2	63.0	$MAPbI_3$	[2]
52	1.88	4.1	1125	5.8	63.0	$Cs_{0.25}FA_{0.75}PbBr_{1.5}I_{1.5}$	[3]
66	2.62	1.1	1000	2.1	52.9	$Cs_2AgBiBr_6$	[2]
68	2.35	7.8	1550	6.7	72.0	$FAPbBr_{2.43}Cl_{0.57}$	[2]
72	2.62	1.5	960	2.1	74.3	$Cs_2AgBiBr_6$	[2]
72	3.03	0.2	1110	0.6	35.4	$MAPbCl_3$	[2]
73	2.62	1.6	970	2.2	73.1	$Cs_2AgBiBr_6$	[2]
73	2.84	0.5	1260	0.9	44.9	$MAPbBr_{0.6}Cl_{2.4}$	[2]
74	2.62	1.5	970	2.2	71.1	$Cs_2AgBiBr_6$	[2]

Table 19. Transparent/semitransparent organic research solar cells with the highest efficiency: performance parameters as a function of *AVT* and the photovoltaic bandgap energy (from the *EQE* spectrum).

AVT [%]	E_g [eV]	PCE [%]	V_{oc} [mV]	J_{sc} [mA cm^{-2}]	FF [%]	Active material	Ref.
1	1.40	13.3	810	24.6	66.5	PM6:Y6	[2]
2	1.66	7.6	770	15.6	63.3	PBDTTT-C-T:$PC_{71}BM$	[2]
3	1.40	12.6	800	24.5	64.5	PM6:Y6	[2]
6	1.47	12.0	870	19.6	70.4	PM7/PTTtID-Cl/IT-4F	[2]
8	1.41	12.7	852	21.1	70.4	D18-Cl:Y6:$PC_{71}BM$	[3]
9	1.42	14.2	854	23.0	72.3	PM6:Y6	[2]
10	1.39	14.9	847	23.1	75.8	D18: N3	[141]
11	1.66	7.1	760	14.5	64.4	PBDTTT-C-T:$PC_{71}BM$	[2]
13	1.42	13.3	853	21.7	71.9	PM6:Y6	[2]
14	1.40	13.6	850	21.1	75.8	PM6:Y6	[2]
14	1.41	12.0	844	19.6	72.8	PM6:Y6:C6	[2]
15	1.52	8.9	772	18.3	63.0	PTB7-Th:FNIC1	[2]
16	1.95	2.9	540	9.7	55.4	P3HT-PCBM	[2]
17	1.39	12.6	810	21.2	73.2	PM6:Y6	[2]
18	1.39	11.7	810	20.7	69.6	PM6:Y6	[2]
19	1.42	13.6	830	23.4	70.2	PM6:Y7	[3]
19	1.42	12.4	852	20.4	71.4	PM6:Y6	[2]
20	1.37	14.0	820	23.0	74.3	PM6:Y6:SN3	[3]
20	1.39	14.6	860	22.8	74.7	PM6/ICBA:Y6	[3]
20	1.42	12.3	817	20.6	73.0	PM6:Y6	[2]
20	1.23	11.6	661	25.6	68.2	BTB7-Th:ATT-9	[3]
21	1.39	16.1	859	24.6	76.1	PM6-Ir1:BTP-eC9:$PC_{71}BM$	[3]
21	1.41 [a)]	13.8	820	25.3	66.5	PM6:N3	[2]
22	**1.41**	**12.9**	**831**	**20.9**	**74.3**	**D18:N3**	**[142]**
25	1.34	11.0	750	20.9	70.0	PCE-10:A078	[2]
25	1.39	10.8	830	18.2	71.6	PBT1-C-2Cl : Y6	[143]
25	1.40	10.2	736	20.3	68.3	PTB7-Th:FOIC	[2]
25	1.43	12.1	760	23.9	66.6	PM6:Y6	[3]
26	1.40	12.9	825	21.6	72.4	PM6:Y6	[2]
28	1.39	11.3	816	19.7	70.3	PM6:Y6-BO	[3]
28	1.41 [a)]	8.9	810	16.8	65.1	PM6:N3	[2]
28	1.66	5.6	760	11.9	61.9	PBDTTT-C-T:$PC_{71}BM$	[2]
29	1.41 [a)]	7.8	800	15.2	64. 7	PM6:N3	[2]
30	**1.41**	**10.1**	**880**	**16.8**	**67.8**	**PBOF:eC9:LB-BO**	**[144]**
30	1.35	10.8	718	21.9	68.7	PTB7-Th:IEICO-4F	[2]
31	1.39	12.0	758	22.8	69.5	PCE10-BDT2F-0.8:Y6	[3]
32	1.42	11.2	849	17.0	77.6	PM6:m-BTP-PhC6:BO-Cl	[3]
33	**1.39**	**12.3**	**781**	**22.0**	**71.3**	**PM6:PCE 10-2F:Y6**	**[145]**
34	1.40	9.1	733	18.5	67.1	PTB7-Th:FOIC	[2]
35	**1.44**	**4.2**	**860**	**8.4**	**58.0**	**PBOF:eC9:LB-BO**	**[144]**

36	1.37	8.8	680	18.0	71.9	PCE-10:BT-ClC:TT-FIC	[2]
36	1.86	6.9	890	11.6	66.5	PSEHTT:ICBA	[2]
37	1.86	6.1	890	10.2	66.8	PSEHTT:ICBA	[2]
38	1.33	5.7	700	12.4	66.23	PTB7-Th:IEICO-4F	[2]
39	1.41	13.0	849	19.0	80.3	PBDB-TF:L8-BO:BTP-eC9	[3]
39	1.86	4.9	880	8.3	67.9	PSEHTT:ICBA	[2]
25	1.43	9.7	770	20.0	63.0	PM6:Y6	[3]
43	1.34	8.1	730	16.3	68.1	PCE-10:A078	[2]
44	1.37	8.0	680	16.2	72.6	PCE-10:BT-ClC:TT-FIC	[2]
44	1.39	8.2	806	15.1	67.2	PBT1-C-2Cl:Y6	[143]
46	1.34	10.8	750	20.4	70.6	PCE-10:A078	[2]
47	1.39	11.4	854	18.0	74.5	PM6:BTP-eC9:L8-BO	[3]
47	1.34	7.1	730	14.3	68.0	PCE-10:A078	[2]
47	1.86	2.4	860	4.1	68.2	PSEHTT:ICBA	[2]
49	1.37	7.2	670	14.8	72.6	PCE-10:BT-ClC:TT-FIC	[2]
49	1.41	6.0	851	11.1	63.8	FC-S1:PM6:Y6-BO	[146]
50	1.38	8.3	746	16.7	66.8	PTB7-Th:FOIC:$PC_{71}BM$	[2]
51	1.39	7.4	749	14.7	66.7	PTB7:FOIC:PC71BM	[2]
53	1.86	1.8	890	3.8	54.8	PSEHTT:ICBA	[2]
53	1.32	5.7	750	10.6	69.5	DPP2T:IEICO-4F	[2]
60	1.33	3.9	749	7.34	70.2	DPP2T:IEICO-4F	[2]
62	1.33	5.9	690	12.9	66.0	PTB7-Th:6TIC-4F	[2]

[a] E_g taken from absorbance

Table 20. Semitransparent/transparent dye-sensitized research solar cells with the highest efficiency: performance parameters as a function of *AVT* and the photovoltaic bandgap energy (from the *EQE* spectrum).

AVT [%]	E_g [eV]	PCE [%]	V_{oc} [mV]	J_{sc} [mA cm^{-2}]	FF [%]	Sensitizing dye	Ref.
1	2.00	5.2	780	12.4	53.7	N719	[2]
5	1.80	11.0	871	16.8	75.2	C268+Y1	[3]
9	2.00	4.5	780	10.3	56.0	N719	[2]
9	1.82	4.3	720	9.9	60.0	N719+SDA	[2]
10	2.01	5.2	770	11.9	57.0	N719	[2]
10	2.00	4.9	765	11.4	56.1	N719	[2]
10	1.81	5.0	710	11.7	60.7	N719	[3]
13	1.68	10.1	851	14.9	80.2	SGT-021	[2] a)
14	1.68	9.9	850	14.9	78.5	SGT-021	[2] a)
15	1.68	9.6	850	14.7	77.2	SGT-021	[2] a)
17	1.68	9.8	855	15.1	75.5	SGT-021	[2] a)
18	2.00	8.6	750	16.7	68.4	N719 (EtOH)	[2]
23	1.82	4.2	650	9.9	64.0	N719+SDA	[2]
23	2.01	3.6	650	8.2	68.0	N719	[2]
24	2.00	7.8	794	17.4	56.3	N719 (EtOH)	[2]
25	1.82	2.6	650	5.6	71.0	N719+SDA	[2]

27	1.77	3.7	521	10.7	65.8	NPI	[2]
30	2.19	1.5	640	3.3	70.0	N719	[2]
31	2.23	6.4	698	13.5	67.9	TPA-1 (EtOH)	[2]
33	2.30	6.1	711	12.5	68.3	TPA-2 (EtOH)	[2]
36	2.23	6.1	766	14.5	54.7	TPA-1 (EtOH)	[2]
37	2.46	3.5	648	8.0	67.5	Cz-2	[2]
38	2.31	5.7	769	13.6	54.2	TPA-2 (EtOH)	[2]
43	1.95	7.8	720	15.3	70.8	PdTPBP/BPEA	[2] b)
69	1.39	3.1	422	11.2	65.6	VG20-C_{16}	[2]
75	1.53	2.5	408	10.9	56.2	TB207	[3]
76	1.41	2.3	406	8.6	65.9	VG20-C_{16}	[2]

[a] Selective absorption-like *EQE* spectrum; [b] E_g calculated from the transmittance spectrum.

Table 21. Semitransparent research solar cells with the highest efficiency among emerging inorganic technologies: performance parameters as a function of *AVT* and the photovoltaic bandgap energy (from the *EQE* spectrum).

AVT [%]	E_g [eV]	PCE [%]	V_{oc} [mV]	J_{sc} [mA cm^{-2}]	FF [%]	Absorber/technology	Ref.
1	1.46	3.0	475	14.6	42.8	$Cu_2ZnSn(S,Se)_4$	[2]
8	1.83	3.4	679	12.1	42.0	Sb_2S_3	[2]

Table 22. Semitransparent research solar cells with the highest efficiency among established inorganic technologies: performance parameters as a function of *AVT* and photovoltaic bandgap energy (from the *EQE* spectrum).

AVT [%]	E_g [eV]	PCE [%]	V_{oc} [mV]	J_{sc} [mA cm^{-2}]	FF [%]	Absorber/technology	Ref.
2	1.23	10.0	640	23.3	66.9	CIGS	[2]
5	1.26	9.8	630	22.9	67.6	CIGS	[2]
7	1.92	6.6	881	11.8	63.7	a-Si:H	[2]
9	1.30	9.8	630	20.9	74.1	CIGS	[2]
9	1.28	6.5	597	22.9	46.5	CIGS	[2]
11	1.34	8.4	620	20.4	66.3	CIGS	[2]
16	1.83	7.5	810	14.2	65.3	a-Si:H	[2]
17	1.83	7.7	810	14.1	67.3	a-Si:H	[2]
18	2.05	5.9	720	14.1	58.3	a-SiGe:H	[2]
18	1.50	5.9	710	14.6	57.4	CIGS	[2]
19	1.87	7.3	820	13.1	67.6	a-Si:H	[2]
19	1.30	6.9	640	16.6	64.7	CIGS	[2]
19	1.34	6.5	580	17.5	63.5	CIGS	[2]
20	1.64	1.7	495	8.9	40.8	CIGS	[2]
22	2.05	5.5	760	12.3	58.6	a-Si:H	[2]
23	1.92	6.0	830	10.6	68.2	a-Si:H	[2]
24	1.68[a]	6.9	920	10.7	70.3	a-Si:H	[2]

37	1.54	0.4	101	14.7	27.2	CdTe	[2]
45	2.16	1.1	596	3.9	47.3	a-Si:H	[2]

[a] E_g taken from absorption spectrum

Table 23. Transparent photovoltaic devices with the highest efficiency including research solar cells with transparent luminescent solar concentrators: performance parameters (measured under the standard of Yang et al.)[147, 148] as a function of the average visible transmittance and bandgap energy (from the EQE spectrum).

AVT [%]	E_g [eV]	PCE [%]	V_{oc} [mV]	J_{sc} [mA cm^{-2}]	FF [%]	Luminophore(s)/absorber	Ref.
74	1.50	1.2	990	1.5	81.3	CO_i8DFIC/GaAs	[3]
75	1.64	3.0	1020	3.8	77.7	$Cs_2Mo_6I_8(CF_3CF_2COO)_6$:BODIPY/GaAs	[3]
84	1.11	0.4	520	1.3	65.1	$(TBA)_2Mo_6Cl_{14}$ /Si	[3]
86	1.52	0.4	500	1.2	66.7	Cy7-NHS/Si	[3]
89	2.94	2.1	500	5.7	73.3	Si-CDs/PVA	[47]

7.4. Operational stability tables of emerging research solar cells

Table 24. Most operationally stable perovskite research solar cells in terms of the stability test energy yield for 200 and 1000 hours under simulated 1 sun illumination as a function of the device bandgap energy (from the *EQE* spectrum).

E_g [eV]	0 h PCE [%]	200 h PCE [%]	1000 h PCE [%]	E_{200h} [Wh·cm^{-2}]	E_{1000h} [Wh·cm^{-2}]	Absorber	Comments	Ref.
1.40	9.4	9.4	9.2	1.9	9.3	$FASnI_3$+$NaBH_4$+DipI	MPP, AM1.5G, N_2, 70°C	[3]
1.45	13.8	14.1	13.0	2.8	13.6	$FASnI_3$	MPP, AM1.5G, air	[3]
1.53	**19.8**	**16.0**	**12.9**	**3.5**	**14.7**	**$FAMAPbI_3$**	**MPP, AM1.5G, N_2, 45°C**	**[129]**
1.53	**22.9**	**23.1**	**23.4**	**4.6**	**23.3**	**$Cs_{0.05}FA_{0.95}PbI_3$**	**MPP, AM1.5G, N_2, 40°C**	**[48]**
1.53	**23.8**	**23.1**	**23.3**	**4.7**	**23.2**	**$Cs_{0.05}FA_{0.9}MA_{0.05}PbI_3$**	**MPP, AM1.5G**	**[76]**
1.53	**23.8**	**23.2**	**22.6**	**4.7**	**22.8**	**$Cs_{0.05}MA_{0.05}FA_{0.9}PbI_3$**	**MPP, AM1.5G, air, 30°C**	**[26]**
1.53	**23.4**	**20.0**	**-**	**4.2**	**-**	**$Cs_{0.05}MA_{0.05}FA_{0.9}PbI_3$**	**MPP, AM1.5G, air, 65°C**	**[26]**

1.53	23.5	20.9	--	4.3	--	α-$FAPbI_3$	MPP, w-LED, N_2, 35°C	[3]
1.53	23.1	22.7	20.7	4.6	22.0	$FA_{0.97}MA_{0.03}PbI_{2.91}Br_{0.09}$	MPP, AM1.5G, N_2, 40°C	[3]
1.54	23.0	20.9	19.4	4.3	20.4	$FAPbI_3$/FGCs	MPP, AM1.5G, N_2, 60 °C	[3]
1.55	**23.4**	**23.4**	**22.9**	**4.7**	**23.3**	**$Cs_{0.05}FA_{0.931}MA_{0.019}PbBr_{0.06}I_{2.94}$**	**w-LED**	**[44]**
1.55	**22.0**	**21.6**	**20.6**	**4.4**	**21.2**	**$FAPbI_3$**	**MPP, AM1.5G, air**	**[149]**
1.55	**22.9**	**20.8**	**-**	**4.3**	**-**	**$FAPbI_3$**	**MPP, AM1.5G, N_2**	**[63]**
1.56	**22.0**	**22.9**	**-**	**4.5**	**-**	**$FAPbI_3$**	**MPP, AM1.5G, air, encapsulation**	**[150]**
1.56	**21.1**	**20.9**	**-**	**4.2**	**-**	**$Cs_{0.05}FA_{0.9025}MA_{0.0475}PbBr_{0.15}I_{2.85}$**	**MPP, AM1.5G, air, 30-40% RH, 45°C**	**[27]**
1.57	21.8	22.0	21.8	4.2	22.0	$Cs_{0.05}FA_{0.874}MA_{0.076}PbBr_{0.24}I_{2.76}$	MPP, AM1.5G, N_2, 40°C, UV-f	[3]
1.57	20.6	20.2	20.2	4.1	20.1	$FA_xCs_{1-x}PbI_3$	MPP, w-LED, Ar, 55-60 °C	[3]
1.57	19.8	20.6	17.7	4.1	19.1	$FA_{0.95}MA_{0.05}PbBr_{0.15}I_{2.85}$	MPP, w-LED, air, 55 °C	[3]
1.58	23.1	22.9	-	4.6	-	$Cs_{0.05}FA_{0.9}MA_{0.05}PbBr_{0.26}I_{2.74}$	MPP, N_2	[3]
1.58	23.6	20.2	-	4.4	-	$FA_{0.92}MA_{0.08}PbBr_{0.24}I_{2.76}$	MPP, AM1.5G, air, 50% RH	[3]
1.58	19.2	19.3	18.4	3.9	19.0	$Cs_{0.05}FA_{0.7885}MA_{0.1615}PbBr_{0.3}I_{2.7}$	OC, AM1.5G, encapsulation, 70-75°C	[2]
1.59	17.1	11.6	9.5	2.8	11.1	$Gua_{0.15}MA_{0.85}PbI_3$	MPP, AM1.5G, Ar, 60 °C	[2]
1.60	**22.0**	**22.2**	**20.2**	**4.4**	**21.4**	**$Cs_{0.05}FA_{0.874}MA_{0.076}PbBr_{0.18}I_{2.76}$**	**AM1.5G, encapsulation, 55 °C**	**[67]**
1.60	21.8	21.4	19.8	4.3	20.9	$CsMAFAPbI_3$:PPP	MPP, encapsulation, air, AM1.5G, 75°C	[2]
1.60	21.3	21.1	21.3	4.2	21.2	$CsFAMAPbI_3$:PPP	MPP, encapsulation,	[2]

1.60	19.6	19.6	18.8	3.9	19.4	$Cs_{0.05}FA_{0.81}MA_{0.14}PbBr_{0.45}I_{2.55}$	air, AM1.5G, 45°C MPP-R_L, AM1.5G, encapsulation, 50-70% RH, 65 °C	[2]
1.61	18.1	11.9	13.6	2.6	13.0	$Gua_{0.25}MA_{0.75}PbI_3$	MPP, AM1.5G, Ar, 60 °C	[2]
1.62	21.1	19.9	18.0	4.0	19.1	$Cs_{0.04}FA_{0.8064}MA_{0.1536}PbBr_{0.48}I_{2.52}$	MPP, AM1.5G, N_2, 40°C	[2]
1.63	20.0	16.8	11.8 [a]	3.5	15.1	$Cs_{0.05}FA_{0.79}MA_{0.16}PbBr_{0.51}I_{2.49}$	MPP, AM1.5G, N_2, 25°C	[2]
1.63	21.0	19.7	19.4 [a]	3.9	19.6	$Cs_{0.05}FA_{0.81}MA_{0.14}PbBr_{0.45}I_{2.55}$/FGCs	MPP, AM1.5G, N_2, 60 °C	[2]
1.64	20.1	17.8	-	3.7	-	$Cs_{0.1}FA_{0.747}MA_{0.153}PbBr_{0.51}I_{2.49}$	MPP, w-LED, N_2, 25 °C	[2]
1.64 [b]	19.7	17.2	-	3.5	-	$Cs_{0.5}FA_{0.7885}MA_{0.1615}PbBr_{0.51}I_{2.49}$	MPP, w-LED, N_2, 20 °C	[2]
1.66	13.0	14.7	13.0	2.8	14.1	$Cs_{0.17}FA_{0.83}PbBr_{0.51}I_{2.49}$	MPP, AM1.5G, 40% RH, 35 °C	[2]
1.69	6.8	6.7	-	1.3	-	$CsGe_{0.5}Sn_{0.5}I_3$	MPP†, AM1.5G, N_2, 45 °C	[2]
1.70	**20.1**	**18.8**	**-**	**3.9**	**-**	**$CsPbI_3$**	**MPP, AM1.5G, air, 30% RH**	**[70]**
1.74	12.9	13.4	-	2.7	-	$CsPbI_3$	OC, AM1.5G, N_2, 25°C, UV-f	[2]
1.78	**16.8**	**17.1**	**17.1**	**3.4**	**17.1**	**$CsPbBr_xI_{3-x}$**	**MPP, AM1.5G, air 30-40% RH, 35 °C**	**[49]**
1.79	**19.0**	**18.9**	**-**	**3.8**	**-**	**$Cs_{0.2}FA_{0.8}PbBr_{1.2}I_{1.8}$**	**MPP, AM1.5G, encapsulation**	**[74]**

[a] Extrapolated value; [b] E_g taken from PL peak; abbreviations: MPP, maximum power point (tracking during test); OC, open-circuit (condition during test); UV-f, ultraviolet light filter; w-LED, white light spectrum light emitting diode source; RH, relative humidity; MPP-RL, cell is connected to the load resistance which matches the initial maximum power point.

Table 25. Most operationally **stable organic** research solar cells in terms of the stability test energy yield for 200 and 1000 h under simulated 1 sun illumination as a function of the device bandgap energy (from the *EQE* spectrum).

E_g [eV]	0 h PCE [%]	200 h PCE [%]	1000 h PCE [%]	E_{200h} [Wh·cm^{-2}]	E_{1000h} [Wh·cm^{-2}]	Active material	Comments	Ref.
1.40	**18.8**	**16.4**	**14.6**	**3.4**	**15.6**	**PM6:BTP-eC9**	**MPP, w-LED, air**	**[50]**
1.43	**17.7**	**16.1**	**14.7**	**3.3**	**7.9**	**PM6:PY-1S1Se:PY-2Cl**	**MPP, AM1.5G**	**[51]**
1.56	7.8	7.2	6.8	1.5	7.0	PBDB-T:ITIC-2F	OC, w-LED, N_2, 40°C, UV-f	[2]
1.57	5.0	5.0	4.7	1.0	4.8	P3HT:o-IDTBR	OC, AM1.5G, N_2, UV-f	[2]
1.61	5.1	4.9	4.9	1.1	4.9	Dyad 4	OC, w-LED, N_2, 30°C	[2]
1.66	8.0	7.4	7.0	1.5	7.3	PBDB-T:ITIC-Th	OC, w-LED, N_2, 40°C, UV-f	[2]
1.70	8.7	8.1	-	1.6	-	PBDB-T:IDTBR	OC, AM1.5G, N_2, 35-40 °C	[2]
1.84	5.9	5.6	5.4	1.1	5.6	PBDB-T:PCBM	OC, w-LED, N_2, 40°C, UV-f	[2]
1.94	3.7	3.7	3.7	0.7	3.7	P3HT-PCBM	OC, AM1.5G, air	[2]

Abbreviations: MPP, maximum power point (tracking during test); OC, open-circuit (condition during test); UV-f, ultraviolet light filter; w-LED, white light spectrum light-emitting diode source.

Table 26. Most operationally **stable dye-sensitized** research solar cells in terms of the stability test energy yield for 200 and 1000 h under simulated 1 sun illumination as a function of the device bandgap energy (from the *EQE* spectrum).

E_g [eV]	0 h PCE [%]	200 h PCE [%]	1000 h PCE [%]	E_{200h} [Wh·cm^{-2}]	E_{1000h} [Wh·cm^{-2}]	Sensitizing dye	Comments	Ref.
1.59	9.0	9.0	8.2	1.8	8.7	TF-tBu_C3F7	OC, AM1.5G, 65 °C	[2]
1.75	6.5	6.7	6.3	1.4	6.6	N719	OC, AM1.5G, 35 °C, UV-f	[2]
1.77	6.3	5.8	4.8	1.3	5.5	Z907	OC, w-LED, 20 °C	[2]
1.78	9.3	9.9	7.9	1.9	9.2	N719	OC, AM1.5G, 50 °C	[2]
1.83	8.4	8.3	-	1.7	-	MK2	OC, w-LED	[2]
1.85	8.0	8.3	8.3	1.4	8.1	N719	OC, AM1.5G	[2]
2.07	5.8	6.5	5.9	1.3	6.2	D35	OC, AM1.5G, 60 °C	[2]

Abbreviations: OC, open-circuit (condition during test); UV-f, ultraviolet light filter; w-LED, white light spectrum light emitting diode source.

Table 27. Most operationally **stable multijunction** research solar cells in terms of the stability test energy yield for 200 and 1000 h under simulated/equivalent 1 sun illumination as a function of the device bandgap energies (from the *EQE* spectra) of the absorber materials.

Bottom E_g [eV]	Top E_g [eV]	0 h PCE [%]	200 h PCE [%]	1000 h PCE [%]	E_{200h} [Wh cm^{-2}]	E_{1000h} [Wh cm^{-2}]	Bottom absorber material	Top absorber material	Comments	Ref.
Perovskite/perovskite										
1.25	**1.80**	**27.4**	**28.4**	**-**	**5.6**	**-**	**$FA_{0.7}MA_{0.3}Pb_{0.5}Sn_{0.5}I_3$**	**$Cs_{0.2}FA_{0.8}PbBr_{1.14}I_{1.86}$**	**MPP, AM1.5G, air 30-50% RH, 35 °C**	**[42]**
1.25	1.80	25.6	26.4	17.8	5.2	23.5	$FA_{0.8}Cs_{0.2}Pb(I_{0.62}Br_{0.38})_3$	$FA_{0.7}MA_{0.3}Pb_{0.5}Sn_{0.5}I_3$	MPP, AM1.5G, air 30-50% RH, 35 °C	[3]
1.26	**1.80**	**24.1**	**23.5**	**23.2**	**4.8**	**23.7**	**$FA_{0.7}MA_{0.3}Pb_{0.5}Sn_{0.5}I_3$**	**$CsPbBr_xI_{3-x}$**	**MPP, AM1.5G, air 30-50% RH, 35 °C**	**[49]**
1.26	**1.80**	**26.9**	**24.6**	**-**	**5.1**	**-**	**$Cs_{0.1}FA_{0.6}MA_{0.3}Pb_{0.5}Sn_{0.5}I_3$**	**$Cs_{0.2}FA_{0.8}PbI_{1.8}Br_{1.2}$**	**MPP, AM1.5G, air 25-35 °C**	**[118]**
1.26	1.82	24.4	24.3	19.3[a)]	4.9	21.8[a)]	FSA:$MA_{0.3}FA_{0.7}Pb_{0.5}Sn_{0.5}I_3$	$FA_{0.8}Cs_{0.2}Pb(I_{0.6}Br_{0.4})_3$	MPP, encapsulation, air, 30-50% RH, AM1.5G, no UV-f, 54-60 °C	[2]
1.26	1.82	21.2	20.6	19.8	4.2	20.7	$Cs_{0.05}MA_{0.45}FA_{0.5}Pb_{0.5}Sn_{0.5}I_3$	$Cs_{0.4}FA_{0.6}PbI_{1.95}Br_{1.05}$	MPP-R_L, encapsulation, air, AM1.5G, room T	[2]
1.27	1.72	23.1	22.2	20.4	4.7	21.4	$(FASnI_3)_{0.6}(MAPbI_3)_{0.4}$	$Cs_{0.05}FA_{0.8}MA_{0.15}PbI_{2.55}Br_{0.45}$	MPP, AM1.5G	[2]
GaAs/perovskite										
1.42	1.85	24.1	23.9	22.1[a)]	4.76	23.3[a)]	GaAs	$FA_{0.80}MA_{0.04}Cs_{0.16}Pb(I_{0.50}Br_{0.50})_3$	MPP, air 20-25% RH, AM1.5G, room T, UV-f	[2]
CIGS/perovskite										
1.10	1.65	22.0	19.9	18.4[a)]	4.1	19.4[a)]	CIGS	$Cs_{0.09}FA_{0.77}MA_{0.14}Pb(I_{0.86}Br_{0.14})_3$	MPP, air 20% RH, 30°C	[2]
Si/perovskite										

1.13	1.68	24.0	22.8	21.5	4.6	22.4	Si	$CsFAPb(Br,I)_3$:$MA(Cl_{0.5}SCN_{0.5})$	MPP, w-LED, air, 40% RH, 25°C	[114]
1.17	1.63	5.4	5.2	-	1.1	-	Si	$FA_{0.83}MA_{0.17}PbBr_{0.51}I_{2.49}$	MPP, AM1.5G, 60 ± 20% RH	[115]

[a] Extrapolated value; abbreviations: MPP, maximum power point (tracking during test); UV-f, ultraviolet light filter; RH, relative humidity; MPP-R_L, the cell is connected to the load resistance which matches the initial maximum power point.

Conflicts of interest

R.R.L. is a co-founder, director, and a part owner of Ubiquitous Energy, Inc., a company working to commercialize transparent photovoltaic technologies. All other authors declare no competing financial interest.

Supporting information

Supporting Information is available from the Wiley Online Library or from the author.

Acknowledgements

O. A. acknowledges the Spanish National Research Agency (Agencia Estatal de Investigación) for the Juan de la Cierva 2021 fellowship. C.J.B. gratefully acknowledges the financial support through the "Aufbruch Bayern" initiative of the state of Bavaria (EnCN and SFF), the Bavarian Initiative "Solar Technologies go Hybrid" (SolTech), the DFG - SFB953 (project no. 182849149), and the DFG - INST 90/917-1 FUGG. R. R. L. gratefully acknowledges support from the National Science Foundation under grant CBET-1702591. T.J.J acknowledge the Ministry of Science and Technology in China via the National Key Research and Development Program of China (Grant No. 2021YFF0500501), and Applied Basic Research Projects in Tianjin, (Grant No. 22JCYBJC01530). We also acknowledge Simon Stier for his work as software developer of the emerging-pv.org website and database,[5] and all the contributions to the data updating; particularly the effort by Mostafa Hassan, Anna-Lena Heß, and Wei Yu.

Corresponding Authors

*E-mail: osbel.almora@urv.cat, christoph.brabec@fau.de

Received: ((will be filled in by the editorial staff))
Revised: ((will be filled in by the editorial staff))
Published online: ((will be filled in by the editorial staff))

References

[1] O. Almora, D. Baran, G. C. Bazan, C. Berger, C. I. Cabrera, K. R. Catchpole, S. Erten-Ela, F. Guo, J. Hauch, A. W. Y. Ho-Baillie, T. J. Jacobsson, R. A. J. Janssen, T. Kirchartz, Y. Li, M. A. Loi, R. R. Lunt, X. Mathew, M. D. McGehee, J. Min, D. B. Mitzi, M. K. Nazeeruddin, J. Nelson, A. F. Nogueira, U. W. Paetzold, N.-G. Park, B. P. Rand, U. Rau, H. J. Snaith, E. Unger, L. Vaillant-Roca, H.-L. Yip, C. J. Brabec, *Adv. Energy Mater.* **2021**, *11*, 2002774.

[2] O. Almora, D. Baran, G. C. Bazan, C. Berger, C. I. Cabrera, K. R. Catchpole, S. Erten-Ela, F. Guo, J. Hauch, A. W. Y. Ho-Baillie, T. J. Jacobsson, R. A. J. Janssen, T. Kirchartz, N. Kopidakis, Y. Li, M. A. Loi, R. R. Lunt, X. Mathew, M. D. McGehee, J. Min, D. B. Mitzi, M. K. Nazeeruddin, J. Nelson, A. F. Nogueira, U. W. Paetzold, N.-G. Park, B. P. Rand, U. Rau, H. J. Snaith, E. Unger, L. Vaillant-Roca, H.-L. Yip, C. J. Brabec, *Adv. Energy Mater.* **2021**, *11*, 2102526.

[3] O. Almora, D. Baran, G. C. Bazan, C. I. Cabrera, S. Erten-Ela, K. Forberich, F. Guo, J. Hauch, A. W. Y. Ho-Baillie, T. J. Jacobsson, R. A. J. Janssen, T. Kirchartz, N. Kopidakis, M. A. Loi, R. R. Lunt, X. Mathew, M. D. McGehee, J. Min, D. B. Mitzi, M. K. Nazeeruddin, J. Nelson, A. F. Nogueira, U. W. Paetzold, B. P. Rand, U. Rau, H. J. Snaith, E. Unger, L. Vaillant-Roca, C. Yang, H.-L. Yip, C. J. Brabec, *Adv. Energy Mater.* **2022**, *13*, 2203313.
[4] J. Pastuszak, P. Węgierek, in *Materials*, Vol. 15, 2022.
[5] Emerging PV, https://emerging-pv.org, accessed: 2023.10.23.
[6] M. A. Green, E. D. Dunlop, M. Yoshita, N. Kopidakis, K. Bothe, G. Siefer, X. Hao, *Prog. Photovoltaics* **2023**, *31*, 651.
[7] W. Shockley, H. J. Queisser, *J. Appl. Phys.* **1961**, *32*, 510.
[8] A. S. Brown, M. A. Green, "Radiative coupling as a means to reduce spectral mismatch in monolithic tandem solar cell stacks theoretical considerations", presented at *Conference Record of the Twenty-Ninth IEEE Photovoltaic Specialists Conference, 2002.*, 19-24 May 2002, 2002.
[9] A. S. Brown, M. A. Green, *Phys. Educ.* **2002**, *14*, 96.
[10] M. Saliba, E. Unger, L. Etgar, J. Luo, T. J. Jacobsson, *Nature Communications* **2023**, *14*, 5445.
[11] M. A. Green, *Prog. Photovoltaics* **2001**, *9*, 123.
[12] Pastuszak J, W. P., *Materials (Basel)* **2022**, *15*, 5542.
[13] Muhamad Aamir Iqbal, Maria Malik, Wajeehah shahid, Syed Zaheer Ud Din, Nadia Anwar, Mujtaba Ikram, F. Idrees, in *Thin Films Photovoltaics*, (Eds: B. Zaidi, C. Shekhar), IntechOpen, **2022**.
[14] B. P. Singh, S. K. Goyal, P. Kumar, *Mater. Today Proc.* **2021**, *43*, 2843.
[15] N. Kant, P. Singh, *Mater. Today Proc.* **2022**, *56*, 3460.
[16] R. Chawla, P. Singhal, A. K. Garg, *Transactions on Electrical and Electronic Materials* **2020**, *21*, 456.
[17] S. Bellani, A. Bartolotta, A. Agresti, G. Calogero, G. Grancini, A. Di Carlo, E. Kymakis, F. Bonaccorso, *Chem. Soc. Rev.* **2021**, *50*, 11870.
[18] Jamilu Ya'u Muhammad, Abudharr Bello Waziri, Abubakar Muhammad Shitu, Umar Muhammad Ahmad, Musa Hassan Muhammad, S. o. T. Yusuf Alhaji, Audu Taofeek Olaniyi, Auwal Abdulkadir Bala, *Sci. J. Energy Eng.* **2019**, *7*.
[19] O. Almora, C. I. Cabrera, J. Garcia-Cerrillo, T. Kirchartz, U. Rau, C. J. Brabec, *Adv. Energy Mater.* **2021**, *11*, 2100022.
[20] L. Krückemeier, U. Rau, M. Stolterfoht, T. Kirchartz, *Adv. Energy Mater.* **2020**, *10*, 1902573.
[21] A. S. Brown, M. A. Green, *Phys. E* **2002**, *14*, 96.
[22] J.-F. Guillemoles, T. Kirchartz, D. Cahen, U. Rau, *Nat. Photon.* **2019**, *13*, 501.
[23] C. Yang, D. Liu, M. Bates, M. C. Barr, R. R. Lunt, *Joule* **2019**, *3*, 1803.
[24] C. J. Traverse, R. Pandey, M. C. Barr, R. R. Lunt, *Nature Energy* **2017**, *2*, 849.
[25] S. Rühle, *Solar Energy* **2016**, *130*, 139.
[26] P. Shi, Y. Ding, B. Ding, Q. Xing, T. Kodalle, C. M. Sutter-Fella, I. Yavuz, C. Yao, W. Fan, J. Xu, Y. Tian, D. Gu, K. Zhao, S. Tan, X. Zhang, L. Yao, P. J. Dyson, J. L. Slack, D. Yang, J. Xue, M. K. Nazeeruddin, Y. Yang, R. Wang, *Nature* **2023**, *620*, 323.
[27] S. Zhang, F. Ye, X. Wang, R. Chen, H. Zhang, L. Zhan, X. Jiang, Y. Li, X. Ji, S. Liu, M. Yu, F. Yu, Y. Zhang, R. Wu, Z. Liu, Z. Ning, D. Neher, L. Han, Y.

Lin, H. Tian, W. Chen, M. Stolterfoht, L. Zhang, W.-H. Zhu, Y. Wu, *Science* **2023**, *380*, 404.
[28] J. Wang, Y. Wang, P. Bi, Z. Chen, J. Qiao, J. Li, W. Wang, Z. Zheng, S. Zhang, X. Hao, J. Hou, *Adv. Mater.* **2023**, *35*, 2301583.
[29] J. Zhou, X. Xu, H. Wu, J. Wang, L. Lou, K. Yin, Y. Gong, J. Shi, Y. Luo, D. Li, H. Xin, Q. Meng, *Nature Energy* **2023**, *8*, 526.
[30] X. Chen, B. Che, Y. Zhao, S. Wang, H. Li, J. Gong, G. Chen, T. Chen, X. Xiao, J. Li, *Adv. Energy Mater.* **2023**, *13*, 2300391.
[31] U. Rau, B. Blank, T. C. M. Müller, T. Kirchartz, *Phy. Rev. Appl.* **2017**, *7*, 044016.
[32] H. Lin, M. Yang, X. Ru, G. Wang, S. Yin, F. Peng, C. Hong, M. Qu, J. Lu, L. Fang, C. Han, P. Procel, O. Isabella, P. Gao, Z. Li, X. Xu, *Nat. Energy* **2023**.
[33] P. Bi, J. Wang, Y. Cui, J. Zhang, T. Zhang, Z. Chen, J. Qiao, J. Dai, S. Zhang, X. Hao, Z. Wei, J. Hou, *Adv. Mater.* **2023**, *35*, 2210865.
[34] NREL's Best Research-Cell Efficiency Chart, https://www.nrel.gov/pv/cell-efficiency.html, accessed: 2023.08.30.
[35] P. J. Dale, M. A. Scarpulla, *Sol. Energy Mater. Sol. Cells* **2023**, *251*, 112097.
[36] X. Liu, K. Duan, Z. Ma, X. Tian, F. Li, S. Liang, C. Qin, X. Liu, *Appl. Phys. Lett.* **2023**, *123*.
[37] S. Pang, Z. Chen, J. Li, Y. Chen, Z. Liu, H. Wu, C. Duan, F. Huang, Y. Cao, *Mater. Horiz.* **2023**, *10*, 473.
[38] G. Li, Z. Su, L. Canil, D. Hughes, M. H. Aldamasy, J. Dagar, S. Trofimov, L. Wang, W. Zuo, J. J. Jerónimo-Rendon, M. M. Byranvand, C. Wang, R. Zhu, Z. Zhang, F. Yang, G. Nasti, B. Naydenov, W. C. Tsoi, Z. Li, X. Gao, Z. Wang, Y. Jia, E. Unger, M. Saliba, M. Li, A. Abate, *Science* **2023**, *379*, 399.
[39] Z. Wang, L. Zeng, T. Zhu, H. Chen, B. Chen, D. J. Kubicki, A. Balvanz, C. Li, A. Maxwell, E. Ugur, R. dos Reis, M. Cheng, G. Yang, B. Subedi, D. Luo, J. Hu, J. Wang, S. Teale, S. Mahesh, S. Wang, S. Hu, E. D. Jung, M. Wei, S. M. Park, L. Grater, E. Aydin, Z. Song, N. J. Podraza, Z.-H. Lu, J. Huang, V. P. Dravid, S. De Wolf, Y. Yan, M. Grätzel, M. G. Kanatzidis, E. H. Sargent, *Nature* **2023**, *618*, 74.
[40] S. Mariotti, E. Köhnen, F. Scheler, K. Sveinbjörnsson, L. Zimmermann, M. Piot, F. Yang, B. Li, J. Warby, A. Musiienko, D. Menzel, F. Lang, S. Keßler, I. Levine, D. Mantione, A. Al-Ashouri, M. S. Härtel, K. Xu, A. Cruz, J. Kurpiers, P. Wagner, H. Köbler, J. Li, A. Magomedov, D. Mecerreyes, E. Unger, A. Abate, M. Stolterfoht, B. Stannowski, R. Schlatmann, L. Korte, S. Albrecht, *Science* **2023**, *381*, 63.
[41] X. Y. Chin, D. Turkay, J. A. Steele, S. Tabean, S. Eswara, M. Mensi, P. Fiala, C. M. Wolff, A. Paracchino, K. Artuk, D. Jacobs, Q. Guesnay, F. Sahli, G. Andreatta, M. Boccard, Q. Jeangros, C. Ballif, *Science* **2023**, *381*, 59.
[42] R. Lin, Y. Wang, Q. Lu, B. Tang, J. Li, H. Gao, Y. Gao, H. Li, C. Ding, J. Wen, P. Wu, C. Liu, S. Zhao, K. Xiao, Z. Liu, C. Ma, Y. Deng, L. Li, F. Fan, H. Tan, *Nature* **2023**, *620*, 994.
[43] J. Wang, Z. Zheng, P. Bi, Z. Chen, Y. Wang, X. Liu, S. Zhang, X. Hao, M. Zhang, Y. Li, J. Hou, *Nat. Sci. Rev.* **2023**, *10*, nwad085.
[44] D. Gao, B. Li, Z. Li, X. Wu, S. Zhang, D. Zhao, X. Jiang, C. Zhang, Y. Wang, Z. Li, N. Li, S. Xiao, W. C. H. Choy, A. K. Y. Jen, S. Yang, Z. Zhu, *Adv. Mater.* **2023**, *35*, 2206387.

[45] X. Zheng, L. Zuo, K. Yan, S. Shan, T. Chen, G. Ding, B. Xu, X. Yang, J. Hou, M. Shi, H. Chen, *Energy Environ. Sci.* **2023**, *16*, 2284.
[46] D. B. Ritzer, B. Abdollahi Nejand, M. A. Ruiz-Preciado, S. Gharibzadeh, H. Hu, A. Diercks, T. Feeney, B. S. Richards, T. Abzieher, U. W. Paetzold, *Energy Environ. Sci.* **2023**, *16*, 2212.
[47] J. Li, J. Chen, X. Zhao, A. Vomiero, X. Gong, *Nano Energy* **2023**, *115*, 108674.
[48] C. Li, X. Wang, E. Bi, F. Jiang, S. M. Park, Y. Li, L. Chen, Z. Wang, L. Zeng, H. Chen, Y. Liu, C. R. Grice, A. Abudulimu, J. Chung, Y. Xian, T. Zhu, H. Lai, B. Chen, R. J. Ellingson, F. Fu, D. S. Ginger, Z. Song, E. H. Sargent, Y. Yan, *Science* **2023**, *379*, 690.
[49] T. Li, J. Xu, R. Lin, S. Teale, H. Li, Z. Liu, C. Duan, Q. Zhao, K. Xiao, P. Wu, B. Chen, S. Jiang, S. Xiong, H. Luo, S. Wan, L. Li, Q. Bao, Y. Tian, X. Gao, J. Xie, E. H. Sargent, H. Tan, *Nat. Energy* **2023**, *8*, 610.
[50] J. Fu, P. W. K. Fong, H. Liu, C.-S. Huang, X. Lu, S. Lu, M. Abdelsamie, T. Kodalle, C. M. Sutter-Fella, Y. Yang, G. Li, *Nat. Commun.* **2023**, *14*, 1760.
[51] R. Sun, T. Wang, Q. Fan, M. Wu, X. Yang, X. Wu, Y. Yu, X. Xia, F. Cui, J. Wan, X. Lu, X. Hao, A. K. Y. Jen, E. Spiecker, J. Min, *Joule* **2023**, *7*, 221.
[52] R. He, W. Wang, Z. Yi, F. Lang, C. Chen, J. Luo, J. Zhu, J. Thiesbrummel, S. Shah, K. Wei, Y. Luo, C. Wang, H. Lai, H. Huang, J. Zhou, B. Zou, X. Yin, S. Ren, X. Hao, L. Wu, J. Zhang, J. Zhang, M. Stolterfoht, F. Fu, W. Tang, D. Zhao, *Nature* **2023**, *618*, 80.
[53] J. Wang, Z. Yu, D. D. Astridge, Z. Ni, L. Zhao, B. Chen, M. Wang, Y. Zhou, G. Yang, X. Dai, A. Sellinger, J. Huang, *ACS Energy Lett.* **2022**, *7*, 3353.
[54] F. Yang, R. W. MacQueen, D. Menzel, A. Musiienko, A. Al-Ashouri, J. Thiesbrummel, S. Shah, K. Prashanthan, D. Abou-Ras, L. Korte, M. Stolterfoht, D. Neher, I. Levine, H. Snaith, S. Albrecht, *Adv. Energy Mater.* **2023**, *13*, 2204339.
[55] M. Pitaro, J. S. Alonso, L. Di Mario, D. Garcia Romero, K. Tran, T. Zaharia, M. B. Johansson, E. M. J. Johansson, M. A. Loi, *J. Mater. Chem. A* **2023**, *11*, 11755.
[56] D. B. Khadka, Y. Shirai, M. Yanagida, T. Tadano, K. Miyano, *Chem. Mater.* **2023**, *35*, 4250.
[57] Y. Zhang, J. Zhou, X. Ma, J. Dong, J. Wang, D. Han, Z. Zang, M.-G. Ju, Q. Zhang, N. Wang, *Solar RRL* **2023**, *7*, 2200997.
[58] C. Jiang, J. Zhou, H. Li, L. Tan, M. Li, W. Tress, L. Ding, M. Grätzel, C. Yi, *Nano-Micro Letters* **2022**, *15*, 12.
[59] Q. Wang, W. Tang, Y. Chen, W. Qiu, Y. Wu, Q. Peng, *J. Mater. Chem. A* **2023**, *11*, 1170.
[60] X. Ji, L. Bi, Q. Fu, B. Li, J. Wang, S. Y. Jeong, K. Feng, S. Ma, Q. Liao, F. R. Lin, H. Y. Woo, L. Lu, A. K.-Y. Jen, X. Guo, *Adv. Mater.* **2023**, *n/a*, 2303665.
[61] X. Liu, B. Ding, M. Han, Z. Yang, J. Chen, P. Shi, X. Xue, R. Ghadari, X. Zhang, R. Wang, K. Brooks, L. Tao, S. Kinge, S. Dai, J. Sheng, P. J. Dyson, M. K. Nazeeruddin, Y. Ding, *Angew. Chem. Int. Ed.* **2023**, *62*, e202304350.
[62] X. Li, X. Wu, B. Li, Z. Cen, Y. Shang, W. Lian, R. Cao, L. Jia, Z. Li, D. Gao, X. Jiang, T. Chen, Y. Lu, Z. Zhu, S. Yang, *Energy Environ. Sci.* **2022**, *15*, 4813.
[63] L. Zheng, L. Shen, Z. Fang, P. Song, W. Tian, J. Chen, K. Liu, Y. Luo, P. Xu, J. Yang, C. Tian, L. Xie, Z. Wei, *Adv. Energy Mater.* **2023**, *n/a*, 2301066.

[64] L. Yuan, J. Wang, P. Huang, Q. Yin, S. Zou, L. Wang, Z. Zhang, H. Luo, F. Liu, J. Qiu, J. Xie, L. Ding, K. Yan, *Small Methods* **2023**, *7*, 2201467.
[65] F. Ye, S. Zhang, J. Warby, J. Wu, E. Gutierrez-Partida, F. Lang, S. Shah, E. Saglamkaya, B. Sun, F. Zu, S. Shoaee, H. Wang, B. Stiller, D. Neher, W.-H. Zhu, M. Stolterfoht, Y. Wu, *Nat. Commun.* **2022**, *13*, 7454.
[66] J. Wang, Z. Zhang, J. Liang, Y. Zheng, X. Wu, C. Tian, Y. Huang, Z. Zhou, Y. Yang, A. Sun, Z. Chen, C.-C. Chen, *Small* **2022**, *18*, 2203886.
[67] C. Zhang, X. Shen, M. Chen, Y. Zhao, X. Lin, Z. Qin, Y. Wang, L. Han, *Adv. Energy Mater.* **2023**, *13*, 2203250.
[68] Z. Liu, C. Zhu, H. Luo, W. Kong, X. Luo, J. Wu, C. Ding, Y. Chen, Y. Wang, J. Wen, Y. Gao, H. Tan, *Adv. Energy Mater.* **2023**, *13*, 2203230.
[69] H. Zou, Y. Duan, S. Yang, D. Xu, L. Yang, J. Cui, H. Zhou, M. Wu, J. Wang, X. Lei, N. Zhang, Z. Liu, *Small* **2023**, *19*, 2206205.
[70] S. S. Mali, J. V. Patil, J.-Y. Shao, Y.-W. Zhong, S. R. Rondiya, N. Y. Dzade, C. K. Hong, *Nat. Energy* **2023**, *8*, 989.
[71] J. Wang, Y. Che, Y. Duan, Z. Liu, S. Yang, D. Xu, Z. Fang, X. Lei, Y. Li, S. Liu, *Adv. Mater.* **2023**, *35*, 2210223.
[72] Y. Du, Q. Tian, S. Wang, T. Yang, L. Yin, H. Zhang, W. Cai, Y. Wu, W. Huang, L. Zhang, K. Zhao, S. Liu, *Adv. Mater.* **2023**, *35*, 2206451.
[73] J. Heo, S. W. Lee, J. Yong, H. Park, Y. K. Lee, J. Shin, D. R. Whang, D. W. Chang, H. J. Park, *Chem. Eng. J.* **2023**, *474*, 145632.
[74] H. Chen, A. Maxwell, C. Li, S. Teale, B. Chen, T. Zhu, E. Ugur, G. Harrison, L. Grater, J. Wang, Z. Wang, L. Zeng, S. M. Park, L. Chen, P. Serles, R. A. Awni, B. Subedi, X. Zheng, C. Xiao, N. J. Podraza, T. Filleter, C. Liu, Y. Yang, J. M. Luther, S. De Wolf, M. G. Kanatzidis, Y. Yan, E. H. Sargent, *Nature* **2023**, *613*, 676.
[75] P. Caprioglio, J. A. Smith, R. D. J. Oliver, A. Dasgupta, S. Choudhary, M. D. Farrar, A. J. Ramadan, Y.-H. Lin, M. G. Christoforo, J. M. Ball, J. Diekmann, J. Thiesbrummel, K.-A. Zaininger, X. Shen, M. B. Johnston, D. Neher, M. Stolterfoht, H. J. Snaith, *Nat. Commun.* **2023**, *14*, 932.
[76] H. Bi, Y. Fujiwara, G. Kapil, D. Tavgeniene, Z. Zhang, L. Wang, C. Ding, S. R. Sahamir, A. K. Baranwal, Y. Sanehira, K. Takeshi, G. Shi, T. Bessho, H. Segawa, S. Grigalevicius, Q. Shen, S. Hayase, *Adv. Functional Mater.* **2023**, *33*, 2300089.
[77] W. Chen, Y. Zhu, J. Xiu, G. Chen, H. Liang, S. Liu, H. Xue, E. Birgersson, J. W. Ho, X. Qin, J. Lin, R. Ma, T. Liu, Y. He, A. M.-C. Ng, X. Guo, Z. He, H. Yan, A. B. Djurišić, Y. Hou, *Nat. Energy* **2022**, *7*, 229.
[78] Y. Wang, R. Lin, X. Wang, C. Liu, Y. Ahmed, Z. Huang, Z. Zhang, H. Li, M. Zhang, Y. Gao, H. Luo, P. Wu, H. Gao, X. Zheng, M. Li, Z. Liu, W. Kong, L. Li, K. Liu, M. I. Saidaminov, L. Zhang, H. Tan, *Nat. Commun.* **2023**, *14*, 1819.
[79] X. Pu, Q. Cao, J. Su, J. Yang, T. Wang, Y. Zhang, H. Chen, X. He, X. Chen, X. Li, *Adv. Energy Mater.* **2023**, *n/a*, 2301607.
[80] Z. Yan, D. Wang, Y. Jing, X. Wang, H. Zhang, X. Liu, S. Wang, C. Wang, W. Sun, J. Wu, Z. Lan, *Chem. Eng. J.* **2022**, *433*, 134611.
[81] G. Zhang, J. Zhang, Z. Yang, Z. Pan, H. Rao, X. Zhong, *Adv. Mater.* **2022**, *34*, 2206222.
[82] X. Zhang, D. Zhang, T. Guo, C. Zheng, Y. Zhou, J. Jin, Z. Zhu, Z. Wang, X. Cui, S. Wu, J. Zhang, Q. Tai, *J. Mater. Chem. C* **2022**, *10*, 15573.

[83] X. Qiu, Y. Xu, R. Li, Y. Jing, Z. Yan, F. Liu, L. Wu, Y. Tu, J. Shi, Z. Du, J. Wu, Z. Lan, *Small* **2023**, *19*, 2206245.
[84] R. Guo, J. Xia, H. Gu, X. Chu, Y. Zhao, X. Meng, Z. Wu, J. Li, Y. Duan, Z. Li, Z. Wen, S. Chen, Y. Cai, C. Liang, Y. Shen, G. Xing, W. Zhang, G. Shao, *J. Mater. Chem. A* **2023**, *11*, 408.
[85] B. Deng, H. Lian, B. Xue, R. Song, S. Chen, Z. Wang, T. Xu, H. Dong, S. Wang, *Small* **2023**, *19*, 2207505.
[86] J. Shi, Z. Chen, H. Liu, Y. Qiu, S. Yang, W. Song, Z. Ge, *Adv. Energy Mater.* **2023**, *13*, 2301292.
[87] M. Zhou, C. Liao, Y. Duan, X. Xu, L. Yu, R. Li, Q. Peng, *Adv. Mater.* **2023**, *35*, 2208279.
[88] Q. Gu, J. Wang, R. Peng, W. Song, L. Xie, R. Zhou, Z. Ge, *ACS Appl. Energy Mater.* **2023**, *6*, 1982.
[89] C. Han, J. Wang, S. Zhang, L. Chen, F. Bi, J. Wang, C. Yang, P. Wang, Y. Li, X. Bao, *Adv. Mater.* **2023**, *35*, 2208986.
[90] Y. Zhang, J. Deng, Q. Mao, S. Young Jeong, X. Huang, L. Zhang, B. Lee, B. Huang, H. Young Woo, C. Yang, J. Xu, F. Wu, Q.-Y. Cao, L. Chen, *Chem. Eng. J.* **2023**, *457*, 141343.
[91] J. Wang, S. Wen, J. Hu, J. Han, C. Yang, J. Li, X. Bao, S. Yan, *Chem. Eng. J.* **2023**, *452*, 139462.
[92] X. Li, X. Duan, J. Qiao, S. Li, Y. Cai, J. Zhang, Y. Zhang, X. Hao, Y. Sun, *Adv. Energy Mater.* **2023**, *13*, 2203044.
[93] L. Ma, Y. Cui, J. Zhang, K. Xian, Z. Chen, K. Zhou, T. Zhang, W. Wang, H. Yao, S. Zhang, X. Hao, L. Ye, J. Hou, *Adv. Mater.* **2023**, *35*, 2208926.
[94] B. Pang, C. Liao, X. Xu, L. Yu, R. Li, Q. Peng, *Adv. Mater.* **2023**, *35*, 2300631.
[95] H. Zhao, Z. Yin, P. Gu, Y. Liu, W. Wang, H. Lai, H.-Q. Wang, N. Li, W. Song, *ACS Appl. Energy Mater.* **2023**, *6*, 1595.
[96] S. Chen, Y. Liu, L. Zhang, P. C. Y. Chow, Z. Wang, G. Zhang, W. Ma, H. Yan, *J. Am. Chem. Soc.* **2017**, *139*, 6298.
[97] V. M. Mwalukuku, J. Liotier, A. J. Riquelme, Y. Kervella, Q. Huaulmé, A. Haurez, S. Narbey, J. A. Anta, R. Demadrille, *Adv. Energy Mater.* **2023**, *13*, 2203651.
[98] L. Zhang, J. Zhang, X. Tang, Y. Chen, X. Wang, Z. Deng, C. Wang, X. Yang, B. Sun, *ACS Appl. Energy Mater.* **2023**, *6*, 4229.
[99] X. Zhao, Y. Pan, S. Liu, L. Jiang, Y. Lai, F. Liu, *Sci. China Mater.* **2023**, *66*, 895.
[100] X. Zhang, Z. Zhou, L. Cao, D. Kou, S. Yuan, Z. Zheng, G. Yang, Q. Tian, S. Wu, S. Liu, *Adv. Functional Mater.* **2023**, *33*, 2211315.
[101] Y. Zhou, C. Xiang, Q. Dai, S. Xiang, R. Li, Y. Gong, Q. Zhu, W. Yan, W. Huang, H. Xin, *Adv. Energy Mater.* **2023**, *13*, 2300253.
[102] Z. Yu, C. Li, S. Chen, Z. Zheng, P. Fan, Y. Li, M. Tan, C. Yan, X. Zhang, Z. Su, G. Liang, *Adv. Energy Mater.* **2023**, *13*, 2300521.
[103] N. Ahmad, Y. Zhao, F. Ye, J. Zhao, S. Chen, Z. Zheng, P. Fan, C. Yan, Y. Li, Z. Su, X. Zhang, G. Liang, *Adv. Sci.* **2023**, *n/a*, 2302869.
[104] L. Zhang, J. Zhang, Y. Cui, Y. Lan, J. Yu, *Opt. Mater.* **2023**, *136*, 113444.
[105] Y. Zhao, S. Wang, C. Li, B. Che, X. Chen, H. Chen, R. Tang, X. Wang, G. Chen, T. Wang, J. Gong, T. Chen, X. Xiao, J. Li, *Energy Environ. Sci.* **2022**, *15*, 5118.

[106] J. Dong, H. Liu, Z. Cao, Y. Liu, Y. Bai, M. Chen, B. Liu, L. Wu, J. Luo, Y. Zhang, S. Liu, *Small* **2023**, *19*, 2206175.
[107] M. Bernechea, N. Cates, G. Xercavins, D. So, A. Stavrinadis, G. Konstantatos, *Nat. Photon.* **2016**, *10*, 521.
[108] S. Rijal, A. Adhikari, R. A. Awni, C. Xiao, D.-B. Li, B. Dokken, A. Ellingson, E. Flores, S. S. Bista, D. Pokhrel, S. Neupane, R. E. Irving, A. B. Phillips, K. Jungjohann, C.-S. Jiang, M. Al-Jassim, R. J. Ellingson, Z. Song, Y. Yan, *Solar RRL* **2023**, *7*, 2201009.
[109] X. Cui, K. Sun, J. Huang, J. S. Yun, C.-Y. Lee, C. Yan, H. Sun, Y. Zhang, C. Xue, K. Eder, L. Yang, J. M. Cairney, J. Seidel, N. J. Ekins-Daukes, M. Green, B. Hoex, X. Hao, *Energy Environ. Sci.* **2019**, *12*, 2751.
[110] S. Mandati, N. Juneja, A. Katerski, A. Jegorovė, R. Grzibovskis, A. Vembris, T. Dedova, N. Spalatu, A. Magomedov, S. Karazhanov, V. Getautis, M. Krunks, I. Oja Acik, *ACS Appl. Energy Mater.* **2023**, *6*, 3822.
[111] R. Nielsen, T. H. Youngman, H. Moustafa, S. Levcenco, H. Hempel, A. Crovetto, T. Olsen, O. Hansen, I. Chorkendorff, T. Unold, P. C. K. Vesborg, *J. Mater. Chem. A* **2022**, *10*, 24199.
[112] K. Yamamoto, R. Mishima, H. Uzu, D. Adachi, *Jpn. J. Appl. Phys.* **2023**, *62*, SK1021.
[113] E. Ugur, E. Aydin, M. De Bastiani, G. T. Harrison, B. K. Yildirim, S. Teale, B. Chen, J. Liu, M. Wang, A. Seitkhan, M. Babics, A. S. Subbiah, A. A. Said, R. Azmi, A. u. Rehman, T. G. Allen, P. Schulz, E. H. Sargent, F. Laquai, S. De Wolf, *Matter* **2023**, *6*, 2919.
[114] X. Luo, H. Luo, H. Li, R. Xia, X. Zheng, Z. Huang, Z. Liu, H. Gao, X. Zhang, S. Li, Z. Feng, Y. Chen, H. Tan, *Adv. Mater.* **2023**, *35*, 2207883.
[115] J. Zheng, W. Duan, Y. Guo, Z. C. Zhao, H. Yi, F.-J. Ma, L. Granados Caro, C. Yi, J. Bing, S. Tang, J. Qu, K. C. Fong, X. Cui, Y. Zhu, L. Yang, A. Lambertz, M. Arafat Mahmud, H. Chen, C. Liao, G. Wang, M. Jankovec, C. Xu, A. Uddin, J. M. Cairney, S. Bremner, S. Huang, K. Ding, D. R. McKenzie, A. W. Y. Ho-Baillie, *Energy Environ. Sci.* **2023**, *16*, 1223.
[116] I. Kafedjiska, I. Levine, A. Musiienko, N. Maticiuc, T. Bertram, A. Al-Ashouri, C. A. Kaufmann, S. Albrecht, R. Schlatmann, I. Lauermann, *Adv. Functional Mater.* **2023**, *n/a*, 2302924.
[117] Q. Jiang, J. Tong, R. A. Scheidt, X. Wang, A. E. Louks, Y. Xian, R. Tirawat, A. F. Palmstrom, M. P. Hautzinger, S. P. Harvey, S. Johnston, L. T. Schelhas, B. W. Larson, E. L. Warren, M. C. Beard, J. J. Berry, Y. Yan, K. Zhu, *Science* **2022**, *378*, 1295.
[118] J. Zhu, Y. Luo, R. He, C. Chen, Y. Wang, J. Luo, Z. Yi, J. Thiesbrummel, C. Wang, F. Lang, H. Lai, Y. Xu, J. Wang, Z. Zhang, W. Liang, G. Cui, S. Ren, X. Hao, H. Huang, Y. Wang, F. Yao, Q. Lin, L. Wu, J. Zhang, M. Stolterfoht, F. Fu, D. Zhao, *Nat. Energy* **2023**, *8*, 714.
[119] J. Thiesbrummel, F. Peña-Camargo, K. O. Brinkmann, E. Gutierrez-Partida, F. Yang, J. Warby, S. Albrecht, D. Neher, T. Riedl, H. J. Snaith, M. Stolterfoht, F. Lang, *Adv. Energy Mater.* **2023**, *13*, 2202674.
[120] H. Yang, W. Chen, Y. Yu, Y. Shen, H. Yang, X. Li, B. Zhang, H. Chen, Q. Cheng, Z. Zhang, W. Qin, J.-D. Chen, J.-X. Tang, Y. Li, Y. Li, *Adv. Mater.* **2023**, *35*, 2208604.

[121] Q. Yao, Y.-M. Xie, Y. Zhou, Q. Xue, X. Xu, Y. Gao, T. Niu, L. Chu, Z. Zhou, F. R. Lin, A. K. Y. Jen, T. Shi, H.-L. Yip, Y. Cao, *Adv. Functional Mater.* **2023**, *33*, 2212599.
[122] K. O. Brinkmann, T. Becker, F. Zimmermann, C. Kreusel, T. Gahlmann, M. Theisen, T. Haeger, S. Olthof, C. Tückmantel, M. Günster, T. Maschwitz, F. Göbelsmann, C. Koch, D. Hertel, P. Caprioglio, F. Peña-Camargo, L. Perdigón-Toro, A. Al-Ashouri, L. Merten, A. Hinderhofer, L. Gomell, S. Zhang, F. Schreiber, S. Albrecht, K. Meerholz, D. Neher, M. Stolterfoht, T. Riedl, *Nature* **2022**, *604*, 280.
[123] Y. J. Choi, S. Y. Lim, J. H. Park, S. G. Ji, J. Y. Kim, *ACS Energy Lett.* **2023**, *8*, 3141.
[124] Z. Jia, Q. Ma, Z. Chen, L. Meng, N. Jain, I. Angunawela, S. Qin, X. Kong, X. Li, Y. Yang, H. Zhu, H. Ade, F. Gao, Y. Li, *Nature Commun.* **2023**, *14*, 1236.
[125] Y. Wang, Z. Zheng, J. Wang, X. Liu, J. Ren, C. An, S. Zhang, J. Hou, *Adv. Mater.* **2023**, *35*, 2208305.
[126] Q. Ma, Z. Jia, L. Meng, H. Yang, J. Zhang, W. Lai, J. Guo, X. Jiang, C. Cui, Y. Li, *Adv. Functional Mater.* **2023**, *33*, 2210733.
[127] T. Paulauskas, V. Pačebutas, V. Strazdienė, A. Geižutis, J. Devenson, M. Kamarauskas, M. Skapas, R. Kondrotas, M. Drazdys, M. Rudzikas, B. Šebeka, V. Vretenár, A. Krotkus, *Discover Nano* **2023**, *18*, 86.
[128] Z. Chen, Q. Cheng, H. Chen, Y. Wu, J. Ding, X. Wu, H. Yang, H. Liu, W. Chen, X. Tang, X. Lu, Y. Li, Y. Li, *Adv. Mater.* **2023**, *35*, 2300513.
[129] L. Zhang, C. Fu, S. Wang, M. Wang, R. Wang, S. Xiang, Z. Wang, J. Liu, H. Ma, Y. Wang, Y. Yan, M. Chen, L. Shi, Q. Dong, J. Bian, Y. Shi, *Adv. Functional Mater.* **2023**, *33*, 2213961.
[130] O. Y. Gong, G. S. Han, S. Lee, M. K. Seo, C. Sohn, G. W. Yoon, J. Jang, J. M. Lee, J. H. Choi, D.-K. Lee, S. B. Kang, M. Choi, N.-G. Park, D. H. Kim, H. S. Jung, *ACS Energy Lett.* **2022**, *7*, 2893.
[131] J. Dou, Q. Song, Y. Ma, H. Wang, G. Yuan, X. Wei, X. Niu, S. Ma, X. Yang, J. Dou, S. Liu, H. Zhou, C. Zhu, Y. Chen, Y. Li, Y. Bai, Q. Chen, *J. Energy Chem.* **2023**, *76*, 288.
[132] C. Xie, Y. Liu, W. Wei, Y. Zhou, *Adv. Functional Mater.* **2023**, *33*, 2210675.
[133] Y. Cheng, Q. Mao, C. Zhou, X. Huang, J. Liu, J. Deng, Z. Sun, S. Jeong, Y. Cho, Y. Zhang, B. Huang, F. Wu, C. Yang, L. Chen, *Angew. Chem. Int. Ed.* **2023**, *n/a*, e202308267.
[134] C. Xie, C. Xiao, J. Fang, C. Zhao, W. Li, *Nano Energy* **2023**, *107*, 108153.
[135] B. Lin, Q. Sun, C. Zhang, H. Deng, Y. Li, W. Xie, Y. Li, Q. Zheng, J. Wu, S. Cheng, *ACS Appl. Energy Mater.* **2023**, *6*, 1037.
[136] H. Deng, Y. Cheng, Z. Chen, X. Lin, J. Wu, Q. Zheng, C. Zhang, S. Cheng, *Adv. Functional Mater.* **2023**, *33*, 2212627.
[137] J. Luo, L. Tang, S. Wang, H. Yan, W. Wang, Z. Chi, J. Gong, J. Li, X. Xiao, *Chem. Eng. J.* **2023**, *455*, 140960.
[138] S. S. Bista, D.-B. Li, S. Rijal, S. Neupane, R. A. Awni, C.-S. Jiang, C. Xiao, K. K. Subedi, Z. Song, A. B. Phillips, X. Wen, R. J. Ellingson, M. J. Heben, Y. Yan, *ACS Appl. Energy Mater.* **2023**, *6*, 885.
[139] Z. Yang, Y. Niu, X. Zhang, Z. Zhang, L. Hu, *J. Mater. Chem. A* **2023**, *11*, 3070.

[140] J. Kim, D. Kim, W. Kim, S. Woo, S.-W. Baek, M. J. Ko, Y. Kim, *Chem. Eng. J.* **2023**, *469*, 143824.
[141] C. Xu, K. Jin, Z. Xiao, Z. Zhao, Y. Yan, X. Zhu, X. Li, Z. Zhou, S. Y. Jeong, L. Ding, H. Y. Woo, G. Yuan, F. Zhang, *Solar RRL* **2022**, *6*, 2200308.
[142] C. Xu, K. Jin, Z. Xiao, Z. Zhao, X. Ma, X. Wang, J. Li, W. Xu, S. Zhang, L. Ding, F. Zhang, *Adv. Functional Mater.* **2021**, *31*, 2107934.
[143] Y. Xie, Y. Cai, L. Zhu, R. Xia, L. Ye, X. Feng, H.-L. Yip, F. Liu, G. Lu, S. Tan, Y. Sun, *Adv. Functional Mater.* **2020**, *30*, 2002181.
[144] D. Xie, Y. Zhang, X. Yuan, Y. Li, F. Huang, Y. Cao, C. Duan, *Adv. Funct. Mater.* **2023**, *33*, 2212601.
[145] L. Zhao, X. Huang, Y. Wang, S. Young Jeong, B. Huang, J. Deng, J. Liu, Y. Cheng, H. Young Woo, F. Wu, L. Chen, L. Chen, *Chem. Eng. J.* **2023**, *451*, 139081.
[146] X. Liu, Z. Liu, M. Chen, Q. Wang, F. Pan, H. Liu, L. Zhang, J. Chen, *Macromol. Rapid Commun.* **2022**, *43*, 2200199.
[147] C. Yang, H. A. Atwater, M. A. Baldo, D. Baran, C. J. Barile, M. C. Barr, M. Bates, M. G. Bawendi, M. R. Bergren, B. Borhan, C. J. Brabec, S. Brovelli, V. Bulović, P. Ceroni, M. G. Debije, J.-M. Delgado-Sanchez, W.-J. Dong, P. M. Duxbury, R. C. Evans, S. R. Forrest, D. R. Gamelin, N. C. Giebink, X. Gong, G. Griffini, F. Guo, C. K. Herrera, A. W. Y. Ho-Baillie, R. J. Holmes, S.-K. Hong, T. Kirchartz, B. G. Levine, H. Li, Y. Li, D. Liu, M. A. Loi, C. K. Luscombe, N. S. Makarov, F. Mateen, R. Mazzaro, H. McDaniel, M. D. McGehee, F. Meinardi, A. Menéndez-Velázquez, J. Min, D. B. Mitzi, M. Moemeni, J. H. Moon, A. Nattestad, M. K. Nazeeruddin, A. F. Nogueira, U. W. Paetzold, D. L. Patrick, A. Pucci, B. P. Rand, E. Reichmanis, B. S. Richards, J. Roncali, F. Rosei, T. W. Schmidt, F. So, C.-C. Tu, A. Vahdani, W. G. J. H. M. van Sark, R. Verduzco, A. Vomiero, W. W. H. Wong, K. Wu, H.-L. Yip, X. Zhang, H. Zhao, R. R. Lunt, *Joule* **2022**, *6*, 8.
[148] C. Yang, D. Liu, R. R. Lunt, *Joule* **2019**, *3*, 2871.
[149] T. N. Mandal, J. H. Heo, S. H. Im, W.-S. Kim, *Solar RRL* **2023**, *n/a*, 2300496.
[150] X. Lin, Y. Wang, H. Su, Z. Qin, Z. Zhang, M. Chen, M. Yang, Y. Zhao, X. Liu, X. Shen, L. Han, *Nano-Micro Letters* **2022**, *15*, 10.

Supporting Information:

Device Performance of Emerging Photovoltaic Materials (Version 4)

Osbel Almora*, Carlos I. Cabrera, Sule Erten-Ela, Karen Forberich, Kenjiro Fukuda, Fei Guo, Jens Hauch, Anita W.Y. Ho-Baillie, T. Jesper Jacobsson, Rene A.J. Janssen, Thomas Kirchartz, Maria A. Loi, Xavier Mathew, David B. Mitzi, Mohammad K. Nazeeruddin, Ulrich W. Paetzold, Barry P. Rand, Uwe Rau, Takao Someya, Eva Unger, Lídice Vaillant-Roca, and Christoph J. Brabec*

Dr. O. Almora
Universitat Rovira i Virgili, 43007 Tarragona, Spain
Dr. O. Almora, Prof. C. J. Brabec
Erlangen Graduate School of Advanced Optical Technologies (SAOT), 91052 Erlangen, Germany.
Prof. C.J. Brabec
Zernike Institute for Advanced Materials University of Groningen Groningen 9747, The Netherlands
Prof. C.I. Cabrera
Unidad Académica de Ciencia y Tecnología de la Luz y la Materia, Universidad Autónoma de Zacatecas, Zacatecas, 98160, Mexico
Prof. S. Erten-Ela
Ege University, Solar Energy Institute, Bornova, 35100, Izmir, Turkey
K. Fukuda
Thin-Film Device Laboratory & Center for Emergent Matter Science, RIKEN, Saitama 351-0198, Japan
Prof. F. Guo
Institute of New Energy Technology, College of Information Science and Technology, Jinan University, Guangzhou 510632, China
Prof. C.J. Brabec, Dr. Karen Forberich, Dr. J. Hauch
Forschungszentrum Jülich GmbH, Helmholtz-Institut Erlangen-Nürnberg for Renewable Energy (HI ERN), 91058 Erlangen, Germany
Prof. A.W.Y. Ho-Baillie
School of Physics and The University of Sydney Nano Institute, The University of Sydney, NSW 2006, Australia
Prof. T.J. Jacobsson
Institute of Photoelectronic Thin Film Devices and Technology, Key Laboratory of Photoelectronic Thin Film Devices and Technology of Tianjin, College of Electronic Information and Optical Engineering, Nankai University, Tianjin 300350, China
Prof. R.A.J. Janssen
Molecular Materials and Nanosystems & Institute for Complex Molecular Systems, Eindhoven University of Technology, 5600 MB Eindhoven, The Netherlands; Dutch Institute for Fundamental Energy Research, De Zaale 20, Eindhoven, 5612 AJ, The Netherlands
Prof. T. Kirchartz, Prof. U. Rau,
IEK5-Photovoltaics, Forschungszentrum Jülich, 52425 Jülich, Germany
Prof. T. Kirchartz
Faculty of Engineering and CENIDE, University of Duisburg-Essen, 47057 Duisburg, Germany
Prof. M.A. Loi
Photophysics and OptoElectronics Group, Zernike Institute for Advanced Materials, University of Groningen, Nijenborgh 4, NL-9747 AG Groningen, The Netherlands
Prof. X. Mathew
Instituto de Energías Renovables, Universidad Nacional Autónoma de México, Temixco, Morelos 62580, México
Prof. D.B. Mitzi
Department of Mechanical Engineering and Material Science & Department of Chemistry, Duke University, Durham, North Carolina 27708, United States
Prof. M. K. Nazeeruddin
Group for Molecular Engineering and Functional Materials, Ecole Polytechnique Fédérale de Lausanne, Institut des Sciences et Ingénierie Chimiques, CH-1951 Sion, Switzerland
Prof. J. Nelson
Department of Physics, Imperial College London, London SW7 2BZ, UK
Prof. A.F. Nogueira
Chemistry Institute, University of Campinas, PO Box 6154, 13083-9 70, Campinas, São Paulo, Brazil
Prof. Dr. U.W. Paetzold
Institute of Microstructure Technology (IMT), Karlsruhe Institute of Technology (KIT), 76344, Eggenstein-Leopoldshafen, Germany; Light Technology Institute (LTI), Karlsruhe Institute of Technology (KIT), 76131, Karlsruhe, Germany
Prof. B.P. Rand
Department of Electrical Engineering and Andlinger Center for Energy and the Environment, Princeton University, Princeton, New Jersey 08544, United States
Prof. H. J. Snaith
Clarendon Laboratory, Department of Physics, University of Oxford, Oxford OX1 3PU, UK.
Prof. T. Someya
Electrical and Electronic Engineering and Information Systems, University of Tokyo, Tokyo 113-8656, Japan
Thin-Film Device Laboratory & Center for Emergent Matter Science, RIKEN, Saitama 351-0198, Japan
Prof. Eva Unger
Helmholtz-Zentrum Berlin, Germany
Prof. L. Vaillant-Roca
Photovoltaic Research Laboratory, Institute of Materials Science and Technology – Physics Faculty, University of Havana, 10400, Havana, Cuba

*osbel.almora@urv.cat, christoph.brabec@fau.de

Keywords: emerging photovoltaics, bandgap energy, flexible photovoltaics, transparent and semitransparent solar cells; photovoltaic device operational stability, tandem solar cells

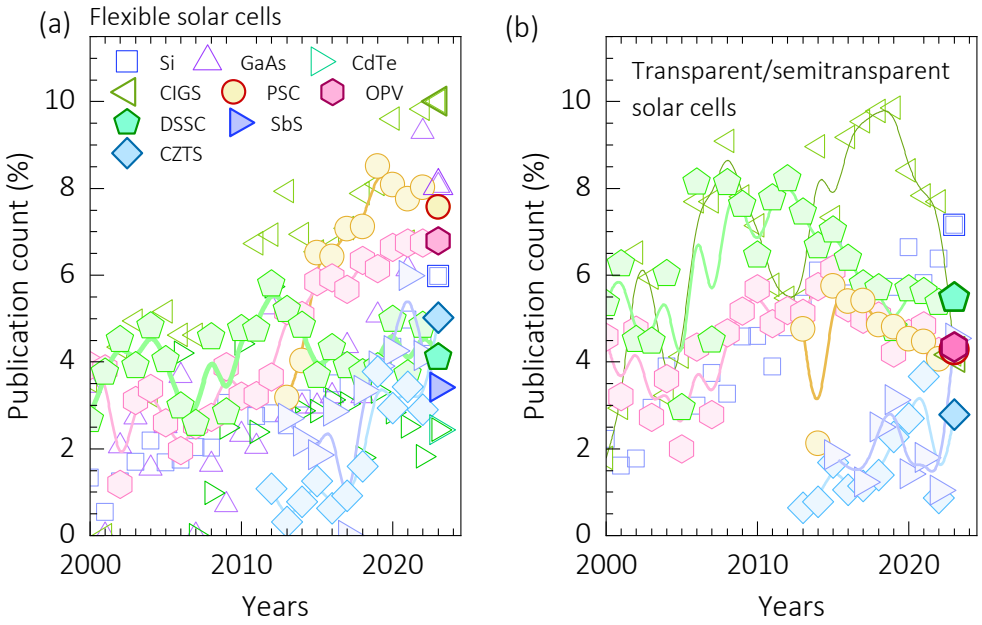

Figure S1. Percentage fraction of annual academic research publications over time (**Figure 1** in the main manuscript) corresponding to (a) flexible and (b) transparent/semitransparent solar cells for several photovoltaic technologies, as indicated. The data corresponds to Clarivate's Web of Science as of August 2023 (see search terms in Table S1).

Table S1. List of key words for the search in Figure 1 (in the main manuscript) and **Figure S1.** Percentage fraction of annual academic research publications over time (**Figure 1** in the main manuscript) corresponding to (a) flexible and (b) transparent/semitransparent solar cells for several photovoltaic technologies, as indicated. The data corresponds to Clarivate's Web of Science as of August 2023 (see search terms in Table S1).**Figure S1**.

PV technology/section	Search filter
Silicon	Silicon solar cell OR Si solar cell
CdTe	CdTe solar cell OR cadmium telluride solar cell
CIGS	CIGS solar cell OR $CuIn_xGa_{1-x}Se_2$ solar cell OR copper indium gallium selenide solar cell
GaAs	GaAs solar cells OR gallium arsenide solar cell
PSC	Perovskite solar cell
OPV	Organic solar cells OR polymer solar cell OR organic photovoltaic cells OR polymer photovoltaics
DSSC	Dye-sensitized solar cell
SbS	$Sb_2(S,Se)_3$ solar cell OR Sb_2S_3 solar cell OR Sb_2Se_3 solar cell OR antimony sulfide-selenide solar cell
AgBiS	$AgBiS_2$ solar cell OR Silver bismuth selenide OR matildite solar cell
CZTS	Kesterite solar cell OR $Cu_2ZnSn(S,Se)_4$ solar cell OR Cu_2ZnSnS_4 solar cell OR $Cu_2ZnSnSe_4$ solar cell OR cupper zinc tin sulfide-selenide solar cell OR cupper zinc tin sulfide solar cell OR cupper zinc tin selenide solar cell
Stability	AND (stability OR degradation)
Flexible	AND (flexible solar cell)
Transparency	AND (transparent solar cell OR semitransparent solar cell)

S1. Inclusion criteria

The main objective of the emerging photovoltaics reports (e-PVr)[1-3] survey series is to provide the photovoltaics (PVs) research community with a resource for the reproduction of best achievements in emerging PVs and the analysis of the current research results and trends. With that motivation, each report must fulfill certain requirements before it can be accepted for inclusion in the graphs and tables in the following sections. These selection criteria may evolve with time, in accord with best practices and tools developed by the research community.

The below text is mostly an adapted reproduction of the corresponding section in the "*Device Performance of Emerging Photovoltaic Materials (Version 1)*"[1] and the subsequent update in the supporting information of the e-PVr previous to this.[3]

S1.1. Highest power conversion efficiency

As a main rule, the reported efficiency should correspond to an original published or already accepted (available DOI) article in a peer-reviewed journal indexed in the ISI-Web-of-Knowledge Journal-Citation-Reports (Clarivate Analytics). The article should include an experimental section with a description of the device structure, fabrication methods and relevant measurement conditions, with enough detail provided to allow the reproduction of the results.

The published/accepted articles must include the current density-voltage ($J-V$) curve validating the *PCE* values and the external quantum efficiency (*EQE)* spectrum,[4-5] sometimes referred to as the incident photon-to-collected-electron conversion efficiency (IPCE). This is true for both PVs and luminescent solar concentrators (LSC). Unpublished certified efficiencies will be considered only in two cases. First, those included in Green's et al. efficiency tables[6] will be incorporated as illustrative references. Otherwise, the authors may provide a digital copy of the certification and the experimental description and validation of the bandgap value (*EQE* spectrum), as would be expected for a publication. The latter information would be incorporated as supporting information if the reported efficiency is ultimately incorporated into the charts. Similarly, the reproduction of results in laboratories different to those of the authors in the original paper will be highlighted upon receipt of the corresponding information.

The current density-voltage ($J-V$) curves should be measured under standard illumination conditions (1 sun = 100 mW·cm^{-2} illumination intensity of AM1.5G spectrum $\Gamma_{AM1.5G}$).[7] The manuscript or its supporting information must explicitly reflect the values for open-circuit voltage (V_{oc}), short-circuit current (J_{sc}), fill factor (FF) and power conversion efficiency (*PCE*) as well as the associated surface area of the device. Regarding the latter, the considered type of area should be clarified (total, aperture or designated as defined in the efficiency tables version 39),[8] and we strongly suggest the use of masks with known aperture. In particular, "active area", which neglects contact and potentially other critical device component areas from consideration, is not a

recommended device area metric. In addition, the type of solar simulator (e.g., AAA, ABA), the corresponding standard (IEC 60904-9,[9] ASTM E 927-05,[10] JIS C 8912-1998),[11] brand and model should be mentioned, as well as the measurement temperature, atmospheric conditions (e.g., air, N_2, A_r), and whether light soaking was included and for how long. We also encourage the reporting of PCE with an maximum power point (MPP) tracking (i.e., "stabilized efficiency" after 5 minutes) measurement, which is specifically important for recording the performance of PSCs, or for related technologies for which device stability and hysteresis[12-13] are known to be issues.

For hysteresis-sensitive devices (e.g. perovskite-based single and multijunction solar cells), the PCE can be reported reliably only by using a method to stabilize the dynamic response of the cell, such as the Asymptotic (or Dynamic) *J-V* and MPP tracking.[14-16] If a stabilized method is used, a brief description of the method and stabilization criteria must be reported. Conventional *J-V*s with a constant preset voltage bias scan rate have been shown to not represent the PCE (and other parameters of the device, such as J_{sc}) accurately.[17] To facilitate comparisons, conventional *J-V* curves will be accepted for reporting *PCE* in the absence of a stabilized PCE. In this case, the voltage scan rate and direction shall be given. Provided the efficiencies for the two voltage scan directions ($PCE_{\rightarrow}$ and $PCE_{\leftarrow}$), only the lowest PCE value shall be considered, i.e. Min[$PCE_{\rightarrow}$, $PCE_{\leftarrow}$]. Exceptionally, the highest efficiency between the two scan directions, i.e. Max[$PCE_{\rightarrow}$, $PCE_{\leftarrow}$], will be taken if (i) the difference is ≤0.1% or (ii) MPP tracking is provided with at least a 1-minute-stable value PCE_{mpp} up to ±0.5% distant from the Max[$PCE_{\rightarrow}$, $PCE_{\leftarrow}$], provided a PCE difference >1% between the two directions.

S1.2. The photovoltaic bandgap energy from the external quantum efficiency

The mandatory *EQE* spectra at short-circuit are typically expressed as a function of the photon wavelength λ, which allows the calculation of the theoretical photocurrent under 1 sun illumination intensity of AM1.5G spectrum ($\Gamma_{AM1.5G}$) according to the integral

$$J_{sc,EQE} = \frac{q}{h\,c}\int EQE(\lambda)\cdot\lambda\cdot\Gamma_{AM1.5G}(\lambda)\,d\lambda \qquad \text{(S1)}$$

where q is the elementary charge, h is the Planck's constant, c the speed of light, and $\Gamma_{AM1.5G}(\lambda)$ is typically in units of $W{\cdot}m^{-2}{\cdot}nm^{-1}$.

The agreement between J_{sc} from the $J-V$ curve and that after Equation (S1) from the *EQE* spectrum (up to 10% of deviation) is a minimal validation required for non-certified *PCE* reports. In addition, the *EQE* is also the essential measurement technique for estimating the bandgap energy value E_g of the device.

The photovoltaic bandgap is here defined as the inflection point of the *EQE* spectra in the region of the absorption threshold,[18-20] typically between 20% and 80% of the maximum *EQE*. This definition is the most appropriate for the evaluation of the Shockley-Queisser (SQ) limit[21-22] and, unlike the optical bandgap, here the aim is to characterize

the complete process from charge charrier generation to current extraction, considering losses in the internal quantum efficiency. Additionally, the *EQE* measurement is relatively simple, the necessary equipment being generally available in the PV laboratories and the data are frequently provided in the literature.

The E_g value (the smallest photoactive bandgap in the system, if there are more than one) would be expected explicitly in the article and endorsed with the *EQE* spectrum analysis. This is expected for both PV and LSC alike. The inflection point can be directly calculated from the data, or a corresponding interpolation, by locating the maximum in the spectra derivative $\partial EQE/\partial E$, or $\partial EQE/\partial \lambda$. Alternatively, our preferred procedure has been the one-step fitting of the EQE spectra in the region around the bandgap wavelength λ_g (inflection point) to the step-like sigmoid function[19]

$$EQE(\lambda) = \frac{A_m}{1 + exp\left[2.63\left(\lambda - \lambda_g\right)/\lambda_s\right]} \quad \text{(S2)}$$

where A_m and λ_s are fitting parameters related with the maximum *EQE* just after the step and the slope during the step, respectively. On the latter, note that λ_s expresses the broadening of the absorption threshold in the *EQE* spectrum, being optimal below 50 nm (like in **Figure S2**) and indicating a graded profile as λ_s approaches and exceeds 100 nm. The device bandgap is defined as

$$E_g = \frac{hc}{\lambda_g} \quad \text{(S3)}$$

and the fitting and λ_g estimation procedures are illustrated in **Figure S2**. Nevertheless, despite reporting an E_g value using a technique different than *EQE* not necessary relates to the corresponding SQ limit, some other methods can be considered additionally, such as the device optical bandgap from typical linear fits for absorption - Tauc plots,[23-24] and Gaussian fits in photoluminescence (PL) and/or electroluminescence (EL) spectra. Importantly, in any case the E_g value must relate to the full device; e.g., one could use optical transmission measurements on thin film cells before the evaporation of the metallic electrodes, but not on the single absorber film without selective layers. In addition, the measurement conditions should be specified, i.e. the equipment model and brand, as well as the temperature and atmosphere for the measurement.

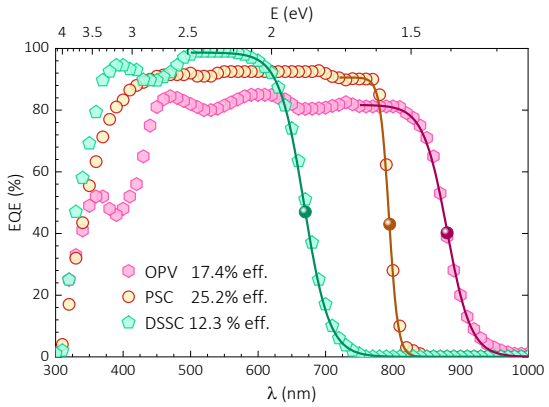

Figure S2. Experimental (data points) external quantum efficiency spectra for certified organic, perovskite and dye sensitized solar cells as reported in Green's et al. tables,[25] copyright 2019, John Wiley & Sons, Ltd. The lines are the fits to Equation (S2) in the regions of the photovoltaic bandgap and the solid circles indicate the λ_g values: 880 nm, 795 nm, and 670 nm for OPV, PSC and DSSC, respectively. Likewise, the corresponding λ_s values are 45 nm, 17 nm, and 49 nm. Reproduced with permission,[1] copyright 2021, Wiley

For each E_g value, the highest published *PCE* value with a bandgap resolution of 10 meV will be taken. For multijunction solar cells, the individual E_g value of the absorber material of each individual junction should be provided along with the respective *EQE* spectrum, with a similar resolution of 10 meV. The labeling convention for the sequence of sub-cells is schemed in **Figure S1** for both the manuscripts and the data submission form in the emerging-pv.org website and database.

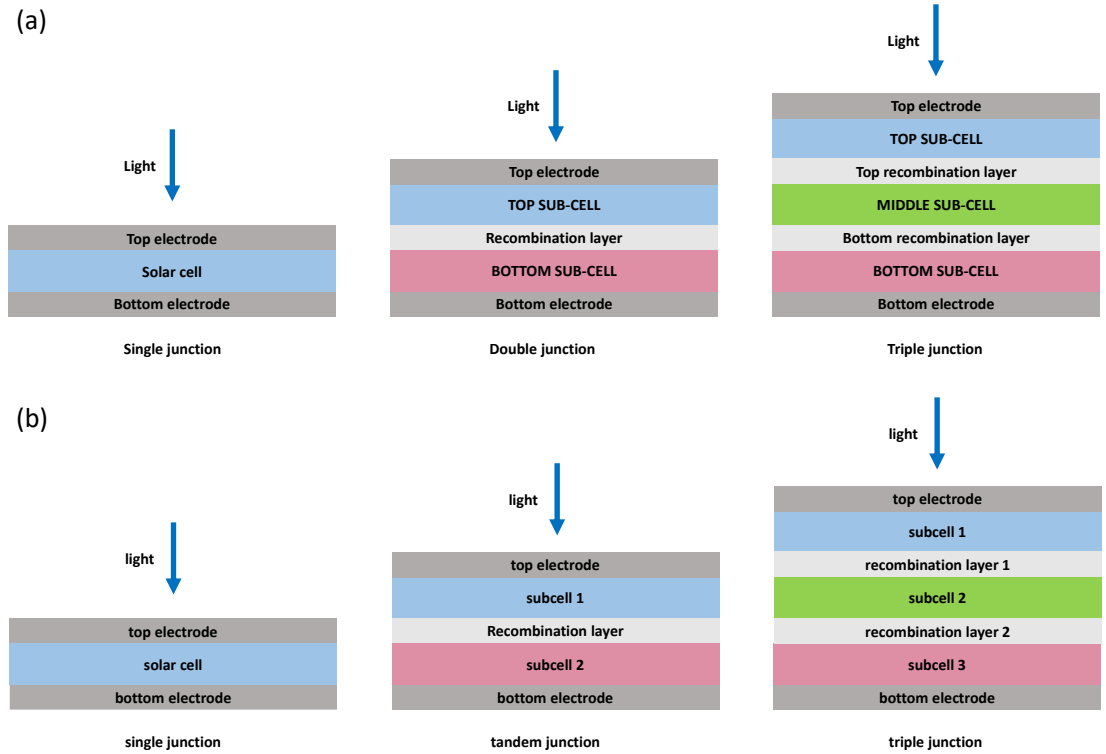

Figure S3. Labeling convention for the multijunction devices in (a) the e-PVr manuscripts and (b) the emerging-pv.org website and database.

For transparent and semitransparent PVs, the corresponding evidence for the average visible transmittance (*AVT*) should be provided by plotting the transmittance curve as a function of wavelength (as measured for the entire device without a reference sample).[26] Reports on flexible substrates should include the thickness and type of the substrate.

S1.3. Special applications: flexible and transparent photovoltaics

Flexible and/or transparent/semitransparent properties should likewise be expressed in the manuscript, or in the supporting information (when relevant), and supported with at least one figure illustrating the transparency/flexibility. The substrate for flexible cells should be thinner than 250 μm, for which a measurement evidence should be presented (e.g. microscopy, profilometry). Additionally, an estimation of the minimum bending radius for which the *PCE* is larger than 5% of that without bending should be provided.

For transparent and semitransparent devices, many of the key protocols for measuring, analyzing, validating, and reporting have recently been outlined.[26-27] When measuring the $J-V$, a black matte background should be placed behind the device to prevent a double pass reflection. The transmittance spectrum $T(\lambda)$ of the device, measured without a reference sample, should be provided to validate the average visible transmittance, defined as[28]

$$AVT = \frac{\int T(\lambda)\, P(\lambda)\ \Gamma_{AM1.5G}(\lambda)\, d\lambda}{\int P(\lambda)\, \Gamma_{AM1.5G}(\lambda)\, d\lambda} \tag{S4}$$

where $P(\lambda)$ is the photopic response of the human eye.[29] Moreover, the aesthetic properties of transparent and semitransparent cells should be reported, including the color rendering index (CRI) and/or the CIELab color coordinates (a^*, b^*). These parameters can be directly obtained using $T(\lambda)$, $\Gamma_{AM1.5G}(\lambda)$ and the reflectance spectrum $R(\lambda)$ (note that a calculator for these metrics is provided in "Data S1" of Ref. [26] and the support section of *emerging-pv.org*) and are directly utilized by various industries including the window industry. Finally, it is necessary to provide a photon balance consistency check (PBCC) to assure that none of the optical measurements ($EQE(\lambda)$ or $T(\lambda)$) are mis-measured or misreported. In units of percentage, the photon balance must satisfy

$$PBCC = EQE(\lambda) + T(\lambda) + R(\lambda) \leq 100\% \tag{S5}$$

where $EQE(\lambda) \leq A(\lambda)$ and becomes equal as the internal quantum efficiency (*IQE*) approaches unity – this substitution is made since the absorbance spectrum $A(\lambda)$ is notoriously difficult to measure directly. We note that a number of articles have reported photon balances with $EQE(\lambda)$ + $T(\lambda)$ > 100%, indicating that either the *EQE* (thus J_{sc}) or *T* (thus *AVT*) are overestimated.

As a summary, Table S2 presents a list of minimal information that should be included in a manuscript, or the corresponding supporting information, to be eligible for incorporation in the below charts. Importantly, independent of possible inclusion, these

guidelines should also be considered important general guidelines for reliable reporting of PV performance metrics.

S1.4. Operational stability

The recommended operational stability test should be 1000 hours under 1 sun AM1.5G illumination, at a temperature of 85 °C, nitrogen atmosphere and MPP-tracking condition. The usage of UV filters, either external or internal ones, their brand, type and cut off wavelength, must be reported together with the brand and type of the light source. Alternative testing conditions may only vary in temperature, time or atmosphere. When testing in conditions other than dry nitrogen, the type of packaging or protection utilized must be denoted. Further information on the bias is essential. Degradation should be done under MPP conditions. In case of other conditions, such as short-circuit (SC), open-circuit (OC) or constant bias voltage, it is important to report that.

The main criteria for presenting the best research cells in terms of overall performance stability would be the stability test energy yield (STEY), resulting from computing the integral

$$E_\tau = \int_0^\tau P_{out}\, dt = \int_0^\tau P_{in}\, PCE\, dt \tag{S6}$$

where P_{in} is the incident light intensity (e.g. 100 mW·cm^{-2}), t is time, τ is the duration of the operational stability test, and the STEY can be taken for 200 h and 1000 h as E_{200h} and E_{1000h}, respectively. An example of the stability test and the energy integration is illustrated in Figure S4 for a 1000 hours test. The best reports for STEY would be presented for each effective device absorption bandgap in two main categories: 200 h and 1000 h stability tests, i.e. E_{200h} and E_{1000h} respectively.

In addition, the *PCE* values before and after 200 h or 1000 h of operational stability testing (measured under standard illumination conditions), as well as *EQE* verification, should be provided. This option of providing only the *PCE* before and after the stability test, rather than the full time-dependent data, can be useful for those PV labs with difficulties in the instrumentation of MPP-tracking algorithms and automatic device performance monitoring during the stability test.

The *PCE* versus time degradation plots should preferably be in efficiency units (not normalized). At a minimum, normalized inline stability plots should be accompanied by the $J-V$ curve under standard 1 sun AM1.5G illumination intensity before the beginning of the degradation test (and after 200 and/or 100 h). This would allow the subsequent calculation of the nonnormalized plots. Besides the calculation of the STEY for 200 h and 100 h, the report of percentage reduction characteristic degradation times is encouraged. Most typically, t95 and t80 indicate the times for which the PCE first reached 95% and 80% of the initial value, respectively. In all cases, the measurement conditions (degradation state, illumination intensity and spectrum, atmosphere,

temperature, details for the instrumentation) should be provided in the manuscript or in the supporting information of the published article.

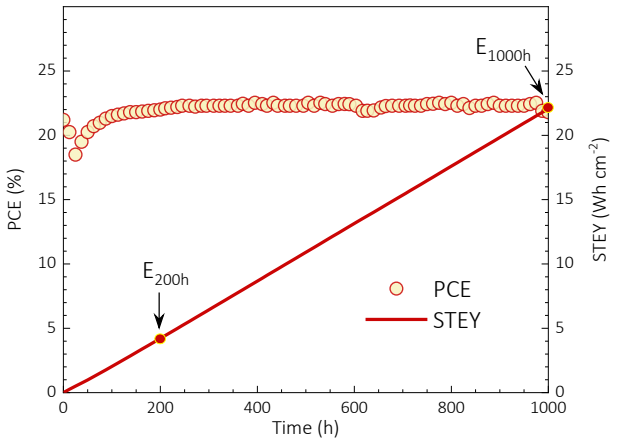

Figure S4. Stability test: efficiency (left axis) and stability test energy yield (right axis) for 1000 hours under 1 sun AM1.5G illumination with MPP tracking. The data resemble that from a PSC reported by Zhen et al.[30] Reproduced with permission,[1] Copyright 2021, Wiley.

Exceptionally, properly described stability tests with duration 500 h< τ<1000 h will be assigned to an extrapolated E_{1000h} value for representation purposes. The extrapolation would be done by using a linear fitting for the PCE data after 200 h of stability test.

The E_g value for each report should be indicated in the manuscript, or supporting information, of the published article, similarly to the procedure outlined in the previous section. To sum up, the last row in **Table S2** comments on the required information to be considered for inclusion in future versions of this survey. Overall, these inclusion criteria encourage the generalization of best practices in the description and reproduction of published academic results.

Table S2. List of items and/or information to include in the manuscripts, or supporting information, for the published article where the achievement in efficiency and/or stability of the research solar cell is first presented. Requirements i-iii are mandatory for all cases and iv.a-c are only required for certain cases.

No.	Information	Figure/data
i	Efficiency under standard test conditions (1 sun AM1.5G illumination, 25ºC): • Performance parameter values from $J-V$ curve (*PCE*, V_{oc}, J_{sc}, and *FF* using Equation $PCE = \frac{V_{oc} \cdot J_{sc} \cdot FF}{P_{in}}$. For perovskite cells (including multijunction) additional stabilized *J-V* parameters are required, see section S1.1. • Area (surface value and type: total, aperture or designated). • Solar simulator (type, standard, model and brand). • Measurement conditions (temperature, air or N_2-atmosphere, whether a black matte background was used).	$J-V$ curve plot
ii	Photovoltaic bandgap: • E_g value(s) (from *EQE* fitting using equation (S2)). • J_{sc} value from *EQE* (using Equation (S1)). • Used instrument for *EQE* (model and brand). • Measurement conditions (voltage bias, temperature, air or N_2-atmosphere, whether a black matte background was used). • Additional methods can also be reported (e.g. Absorption Tauc plot).	$EQE-\lambda$ spectrum
iii	Absorber material: Experimental section: description of structure and fabrication procedure allowing reproduction of the results.	Optional figure/data
iv.a	Photostability test: • *PCE* before and after 200 h and 1000 h (measured as in "i") • Degradation conditions (e.g. MPP, OC, SC). • Illumination spectrum (e.g. AM1.5G, UV filter model & brand). • Illumination intensity (e.g. 100 mW cm^{-2}, provide information on how intensity was tracked). • Measurement conditions: temperature, atmosphere (air with RH or inert N_2/Ar), instrument (model & brand or self-made). • Integrated output energy for 200 h and 1000h under 1 sun illumination (E_{200h} and E_{1000h} using Equation (S6)).	Non-normalized $PCE-t$ degradation record (or normalized one with the initial PCE specified)
iv.b	Transparent and semitransparent PV • *AVT* value (using equation (S4) as determined by the calculator provided in "Data S1" of Ref. [26] and the support section of *emerging-pv.org*) • Aesthetics (e.g. CRI or (a^*, b^*)) • PBCC value (using Equation (S5)) • Used instrument for T and *R* (model and brand) • Measurement conditions (temperature, air or N_2-atmosphere, whether a black matte background was used)	$T-\lambda$ and $R-\lambda$ spectra
iv.c	Flexible PV • Substrate thickness • Minimum radius the solar cell was bent to without reducing <5% performance output • Measurement conditions	Cross section/ bending picture

S1.5. Discarding rules

"Reporting Device Efficiency of Emerging PV Materials" is planned as an open access database following the FAIR principles.[31] This implies that the data must be findable, accessible, inter-operable and reusable. A major concern is of course the quality of the data. We believe that the following principles are sufficient to maintain the highest standard in collecting data on new materials:

First, *PCE* values without explicit description of the $J-V$ measurement conditions (i.e., light intensity, spectrum, suitably-described cell area, measurement instrument) nor *EQE* spectrum must be discarded. Specifically, differences of more than 10 % between short-circuit currents from $J-V$ ($J_{sc,JV}$) and *EQE* ($J_{sc,EQE}$) are considered as a discarding argument. For differences of between 5-10%, the lower efficiency value (i.e., associated with the lower J_{sc} value) shall also be reported. Moreover, the FF value calculated from the reported *PCE*, V_{oc} and J_{sc} should be consistent with the value reported in the original manuscript: mismatches >0.5% may discard the report if it is not the case of a typo in the original manuscript. For transparent and semitransparent devices, *EQE*+*T*>1 would discard the report.

Second, the reports can also be discarded in the absence of evidence for evaluating the photovoltaic bandgap E_g. Similarly, this applies with the values of *AVT*, substrate thickness/bending radius and E_{200h}/E_{1000h} for the transparent, flexible and stability categories, respectively.

Exceptionally, articles lacking some of the mandatory requirements to be included in the e-PVr could be reconsidered, provided an extended/additional supporting information document to be posted in the *emerging-pv.org* website.

Regarding reproducibility, new absorber material cell performance reports can be discarded if: (i) the original publication is addressed in a "comment article" due to reproducibility issues and, (ii) no further evidence of reproduction of the absorber material under examination is found during the subsequent two years after the publication of the original article.

S1.6. Tie rules

Aiming to summarize the best achievements in not-necessarily-certified-*PCE*s for emerging PV technologies, as published in academic articles, this survey focuses on the most efficient photovoltaic materials. Accordingly, there are two main uncertainties, associated with the reports on *PCE* and E_g. The latter would always be considered as ±10 meV by default. Exceptionally, larger E_g uncertainties could be considered for devices with significantly gradual *EQE* absorption onset.

For *PCE* values, the *PCE* uncertainty would always be considered as ±0.5% by default. Then, at the same E_g, only a second uncertified *PCE* record can be included if its average value is within ±0.5% of the best cell at E_g and/or above some *PCE* for the records in the range E_g±10 meV. Analogously, for multijunction solar cells, the highest efficiency is taken for each set of E_g values (corresponding to each individual junction)

with the same resolution. Certified and uncertified records will be considered as separate categories. Thus, up to 4 reports can be included at the same E_g or set of E_g values (2 certified and 2 uncertified) if the above rules are fulfilled.

For the photostability tests, the E_{200h} and E_{1000h} values would follow a ±1Wh·cm^{-2} rule, similar to the *PCE* values, in addition to the E_g±10 meV earlier mentioned. The best semitransparent PVs will be considered as the highest *PCE* at each *AVT* (±1%), and each E_g value (±10 meV). Analogously to the above rules, at both the same *AVT* and E_g, only a second *PCE* record can be included if its average value is within ±0.5% of the best cell at *AVT* and E_g, and/or above some *PCE* for the records in the ranges *AVT*±1% and E_g±10 meV.

Importantly, these would be the tie rules for inclusion in the final tables for each article version. Full data, including all the available records at each E_g, is intended to be accessible in the online database website *emerging-pv.org*, with visualization tools permitting customizable selections. A summary is provided in Table S3.

Table S3. Summary of criteria for discarding, inclusion and/or by-a-tie inclusion

Parameter	Accuracy	Comment
PCE	±0.5%	
E_g	±10 meV	The uncertainty ranges are simultaneously considered in each case
AVT	±1%	
STEY	±0.5 Whcm^{-2}	
$\frac{J_{sc,JV} - J_{sc,EQE}}{J_{sc,JV}}$	±10%	The results will be discarded for larger differences
$PCE_{\rightarrow} - PCE_{\leftarrow}$	±0.1%	When hysteresis, the smaller PCE value between the voltage scan directions will be taken, unless the difference is ≤0.1%
$PCE_{mpp} - \mathrm{Max}[PCE_{\rightarrow} - PCE_{\leftarrow}]$	±0.5%	When hysteresis with PCE difference >1% between the voltage scan directions the highest efficiency from the J-V curves is taken if an MPP tracking is provided with at least a 1-minute-stable PCE value up to ±0.5% distant from the Max[$PCE_{\rightarrow}$, $PCE_{\leftarrow}$].

S1.7. Inclusion methods

The data to be included in the following versions of this survey can be incorporated via several methods. Primarily, we will systematically check in the literature for new developments. On the other hand, we urge the research community to take an active role in the future updates of these reviews, by following one of three approaches. First, the authors can submit data through a template in the online website *emerging-pv.org*. This is a dedicated database collector under development which provides data analysis and visualization functionalities.

Second, the authors can send an email to *report@emerging-pv.org* with the attached data. It is encouraged to use the form provided in the support section of the online website *emerging-pv.org*.

Finally, we also recommend including the above mentioned form as a table/set of tables in the supporting information of the published papers and/or in stable online websites for future automatic digital data collection.

References

[1] O. Almora, D. Baran, G.C. Bazan, C. Berger, C.I. Cabrera, K.R. Catchpole, S. Erten-Ela, F. Guo, J. Hauch, A.W.Y. Ho-Baillie, T.J. Jacobsson, R.A.J. Janssen, T. Kirchartz, Y. Li, M.A. Loi, R.R. Lunt, X. Mathew, M.D. McGehee, J. Min, D.B. Mitzi, M.K. Nazeeruddin, J. Nelson, A.F. Nogueira, U.W. Paetzold, N.-G. Park, B.P. Rand, U. Rau, H.J. Snaith, E. Unger, L. Vaillant-Roca, H.-L. Yip and C.J. Brabec, Device Performance of Emerging Photovoltaic Materials (Version 1), *Adv. Energy Mater.* **2021**, *11*, 2002774. https://doi.org/10.1002/aenm.202002774

[2] O. Almora, D. Baran, G.C. Bazan, C. Berger, C.I. Cabrera, K.R. Catchpole, S. Erten-Ela, F. Guo, J. Hauch, A.W.Y. Ho-Baillie, T.J. Jacobsson, R.A.J. Janssen, T. Kirchartz, N. Kopidakis, Y. Li, M.A. Loi, R.R. Lunt, X. Mathew, M.D. McGehee, J. Min, D.B. Mitzi, M.K. Nazeeruddin, J. Nelson, A.F. Nogueira, U.W. Paetzold, N.-G. Park, B.P. Rand, U. Rau, H.J. Snaith, E. Unger, L. Vaillant-Roca, H.-L. Yip and C.J. Brabec, Device Performance of Emerging Photovoltaic Materials (Version 2), *Adv. Energy Mater.* **2021**, *11*, 2102526. https://doi.org/10.1002/aenm.202102526

[3] O. Almora, D. Baran, G.C. Bazan, C.I. Cabrera, S. Erten-Ela, K. Forberich, F. Guo, J. Hauch, A.W.Y. Ho-Baillie, T.J. Jacobsson, R.A.J. Janssen, T. Kirchartz, N. Kopidakis, M.A. Loi, R.R. Lunt, X. Mathew, M.D. McGehee, J. Min, D.B. Mitzi, M.K. Nazeeruddin, J. Nelson, A.F. Nogueira, U.W. Paetzold, B.P. Rand, U. Rau, H.J. Snaith, E. Unger, L. Vaillant-Roca, C. Yang, H.-L. Yip and C.J. Brabec, Device Performance of Emerging Photovoltaic Materials (Version 3), *Adv. Energy Mater.* **2022**, *13*, 2203313. https://doi.org/10.1002/aenm.202203313

[4] S. Ravishankar, C. Aranda, P.P. Boix, J.A. Anta, J. Bisquert and G. Garcia-Belmonte, Effects of Frequency Dependence of the External Quantum Efficiency of Perovskite Solar Cells, *J. Phys. Chem. Lett.* **2018**, *9*, 3099-3104. https://doi.org/10.1021/acs.jpclett.8b01245

[5] D.J. Wehenkel, K.H. Hendriks, M.M. Wienk and R.A.J. Janssen, The effect of bias light on the spectral responsivity of organic solar cells, *Org. Electron.* **2012**, *13*, 3284-3290. https://doi.org/10.1016/j.orgel.2012.09.040

[6] M.A. Green, E.D. Dunlop, J. Hohl-Ebinger, M. Yoshita, N. Kopidakis and X. Hao, Solar cell efficiency tables (Version 58), *Prog. Photovoltaics Res. Appl.* **2021**, *29*, 657-667. https://doi.org/10.1002/pip.3444

[7] C. Honsberg and S. Bowden, Standard Solar Spectra, https://www.pveducation.org/pvcdrom/appendices/standard-solar-spectra (accessed 30.04.2020)

[8] M.A. Green, K. Emery, Y. Hishikawa, W. Warta and E.D. Dunlop, Solar Cell Efficiency Tables (Version 39), *Prog. Photovoltaics* **2012**, *20*, 12-20. https://doi.org/10.1002/pip.2163

[9] in *IEC 60904-9, International Standard, Photovoltaic devices, Part 9: Solar Simulator performance requirements*, *Vol.* IEC, Geneva, Switzerland, **2007**.

[10] A. International in *ASTM E927 - 05, Standard Specification for Solar Simulation for Terrestrial Photovoltaic Testing*, *Vol.* www.astm.org, West Conshohocken, PA, **2005**.

[11] E. Manke in *Standards For Simulators Can Vary Widely*, *Vol.* Zackin Publications Inc, Newport, **2011**.
[12] E.L. Unger, E.T. Hoke, C.D. Bailie, W.H. Nguyen, A.R. Bowring, T. Heumuller, M.G. Christoforo and M.D. McGehee, Hysteresis and Transient Behavior in Current-Voltage Measurements of Hybrid-Perovskite Absorber Solar Cells, *Energy Environ. Sci.* **2014**, *7*, 3690-3698. https://doi.org/10.1039/C4EE02465F
[13] H.J. Snaith, A. Abate, J.M. Ball, G.E. Eperon, T. Leijtens, N.K. Noel, S.D. Stranks, J.T.-W. Wang, K. Wojciechowski and W. Zhang, Anomalous Hysteresis in Perovskite Solar Cells, *J. Phys. Chem. Lett.* **2014**, *5*, 1511-1515. https://doi.org/10.1021/jz500113x
[14] T. Song, D.J. Friedman and N. Kopidakis, Comprehensive Performance Calibration Guidance for Perovskites and Other Emerging Solar Cells, *Adv. Energy Mater.* **2021**, *11*, 2100728. https://doi.org/10.1002/aenm.202100728
[15] R.B. Dunbar, B.C. Duck, T. Moriarty, K.F. Anderson, Noel W. Duffy, C.J. Fell, J. Kim, A. Ho-Baillie, D. Vak, T. Duong, Y. Wu, K. Weber, A. Pascoe, Y.-B. Cheng, Q. Lin, P.L. Burn, R. Bhattacharjee, H. Wang and G.J. Wilson, How reliable are efficiency measurements of perovskite solar cells? The first inter-comparison, between two accredited and eight non-accredited laboratories, *J. Mater. Chem. A* **2017**, *5*, 22542-22558. https://doi.org/10.1039/C7TA05609E
[16] B. Chen, M. Yang, X. Zheng, C. Wu, W. Li, Y. Yan, J. Bisquert, G. Garcia-Belmonte, K. Zhu and S. Priya, Impact of Capacitive Effect and Ion Migration on the Hysteretic Behavior of Perovskite Solar Cells, *J. Phys. Chem. Lett.* **2015**, *6*, 4693-4700. https://doi.org/10.1021/acs.jpclett.5b02229
[17] T. Song, D.J. Friedman and N. Kopidakis, How Useful are Conventional I–Vs for Performance Calibration of Single- and Two-Junction Perovskite Solar Cells? A Statistical Analysis of Performance Data on ≈200 Cells from 30 Global Sources, *Solar RRL* **2022**, *6*, 2100867. https://doi.org/10.1002/solr.202100867
[18] U. Rau, B. Blank, T.C.M. Müller and T. Kirchartz, Efficiency Potential of Photovoltaic Materials and Devices Unveiled by Detailed-Balance Analysis, *Phys. Rev. Appl.* **2017**, *7*, 044016. https://doi.org/10.1103/PhysRevApplied.7.044016
[19] O. Almora, C.I. Cabrera, J. Garcia-Cerrillo, T. Kirchartz, U. Rau and C.J. Brabec, Quantifying the Absorption Onset in the Quantum Efficiency of Emerging Photovoltaic Devices, *Adv. Energy Mater.* **2021**, *11*, 2100022. https://doi.org/10.1002/aenm.202100022
[20] M.A. Green and A.W.Y. Ho-Baillie, Pushing to the Limit: Radiative Efficiencies of Recent Mainstream and Emerging Solar Cells, *ACS Energy Lett.* **2019**, *4*, 1639-1644. https://doi.org/10.1021/acsenergylett.9b01128
[21] W. Shockley and H.J. Queisser, Detailed Balance Limit of Efficiency of p-n Junction Solar Cells, *J. Appl. Phys.* **1961**, *32*, 510-519. https://doi.org/10.1063/1.1736034
[22] S. Rühle, Tabulated values of the Shockley–Queisser Limit for Single Junction Solar Cells, *Solar Energy* **2016**, *130*, 139-147. https://doi.org/10.1016/j.solener.2016.02.015
[23] J. Tauc, R. Grigorovici and A. Vancu, Optical Properties and Electronic Structure of Amorphous Germanium, *Phys. Status Solidi B* **1966**, *15*, 627-637. https://doi.org/10.1002/pssb.19660150224
[24] B.D. Viezbicke, S. Patel, B.E. Davis and D.P. Birnie Iii, Evaluation of the Tauc method for optical absorption edge determination: ZnO thin films as a model system, *Phys. Status Solidi B* **2015**, *252*, 1700-1710. https://doi.org/10.1002/pssb.201552007
[25] M.A. Green, E.D. Dunlop, J. Hohl-Ebinger, M. Yoshita, N. Kopidakis and A.W.Y. Ho-Baillie, Solar cell efficiency tables (Version 55), *Prog. Photovoltaics* **2020**, *28*, 3-15. https://doi.org/10.1002/pip.3228
[26] C. Yang, D. Liu, M. Bates, M.C. Barr and R.R. Lunt, How to Accurately Report Transparent Solar Cells, *Joule* **2019**, *3*, 1803-1809. https://doi.org/10.1016/j.joule.2019.06.005
[27] C. Yang, D. Liu and R.R. Lunt, How to Accurately Report Transparent Luminescent Solar Concentrators, *Joule* **2019**, *3*, 2871-2876. https://doi.org/10.1016/j.joule.2019.10.009
[28] R.R. Lunt, Theoretical limits for visibly transparent photovoltaics, *A. Phys. Lett.* **2012**, *101*, 043902. https://doi.org/10.1063/1.4738896
[29] E.F. Schubert, *Light-Emitting Diodes*, Cambridge University Press, Cambridge, **2006**, p.
[30] X. Zheng, Y. Hou, C. Bao, J. Yin, F. Yuan, Z. Huang, K. Song, J. Liu, J. Troughton, N. Gasparini, C. Zhou, Y. Lin, D.-J. Xue, B. Chen, A.K. Johnston, N. Wei, M.N. Hedhili, M. Wei, A.Y. Alsalloum, P. Maity, B. Turedi, C. Yang, D. Baran, T.D. Anthopoulos, Y. Han, Z.-H. Lu, O.F. Mohammed, F. Gao, E.H. Sargent and O.M. Bakr, Managing grains and interfaces via ligand anchoring enables 22.3%-efficiency inverted perovskite solar cells, *Nat. Energy* **2020**, *5*, 131-140. https://doi.org/10.1038/s41560-019-0538-4
[31] Fair Principles, https://www.go-fair.org/fair-principles/ (accessed 08.07.2020)